On Continuous Connected Facility Location Problems

A DISSERTATION

SUBMITTED TO THE FACULTY OF THE GRADUATE SCHOOL

OF THE UNIVERSITY OF MINNESOTA

BY

Fan Jia

IN PARTIAL FULFILLMENT OF THE REQUIREMENTS

FOR THE DEGREE OF

DOCTOR OF PHILOSOPHY

Advisor: John Gunnar Carlsson

May, 2015

Acknowledgements

First and foremost, I would like to express my deepest gratitude to my advisor John Gunnar Carlsson for his guidance, support and encouragement during my Ph.D study at the University of Minnesota. His passion for contributing scholarly has always been inspirational for me. He is not only a mentor to me but also a great friend in life. I am truly grateful to have met John and completed my doctoral study under his supervision.

Sincere thanks go to my dissertation committee members Professor Shuzhong Zhang, William Cooper and Ravi Janardan. Their comments and suggests have helped me improve the dissertation greatly.

I would also like to thank my current and former labmates and fellow ISyE students Raghuveer Devulapalli, Ying Li, Mehdi Behroozi and Siyuan Song. Discussions about research and life with them have always been both illuminating and joyful.

Finally, I want to thank my mom and dad for their constant love and support.

Abstract

An important but under-studied problem in location analysis is the so called *connected facility location problem*. In such a problem, each facility is connected with other facilities by a certain network structure and the problem seeks to optimize facility locations so that the total costs including facility connection cost are minimized. Although its applications are seen in a number of network design domains including retail, telecommunication and public transportation, this problem is quite challenging to solve mathematically. In this dissertation, we study the *connected facility location problem* when both the demand set and the feasible set are *continuous*. We first introduce the *continuous connected facility location problem* and perform an asymptotic analysis to the problem. We then introduce a constant factor approximation algorithm for the problem and provide worst case analysis for the algorithm. We extend our analysis to a generalized connected facility location problem where the backbone network takes several different configurations and give an asymptotic analysis and an algorithmic analysis for each configuration. We finally discuss generalizations of our model for alternative cost models and multilevel networks.

Contents

List of Tables **vi**

List of Figures **vii**

1 Introduction **1**

2 Continuous connected facility location problem **4**

2.1 Applications 5

2.2 Related work 6

2.3 Special cases 7

3 Continuous connected facility location problems: algorithmic analysis **10**

3.1 Continuous k-median problem 11

3.1.1 Related Work 11

3.1.2 Preliminaries 12

3.1.3 The algorithm 12

3.1.4 Upper and lower bounds 14

3.1.5 Proof of approximation 24

3.1.6 Running time 25

3.1.7 Simulation results 25

3.2 An approximation algorithm for continuous connected facility location problem . . . 28
3.2.1 Lower bounds on a given convex polygon . . . 29
3.2.2 Upper bounds for Algorithm 4 . . . 34
3.2.3 Approximation algorithm . . . 37
3.2.4 Approximation bounds for Algorithm 4 . . . 39

4 Continuous connected facility location problem: various backbone networks 44
4.1 Introduction . . . 44
4.1.1 Backbone network topologies . . . 45
4.2 Asymptotic analysis . . . 48
4.2.1 Special cases of (4.1) . . . 48
4.2.2 Asymptotic solutions to (4.1) . . . 58
4.3 Algorithmic analysis . . . 67
4.3.1 An algorithmic formulation of (4.1) . . . 67
4.3.2 Proof of approximation bounds . . . 78

5 Extensions to CCFL 83
5.1 Alternative cost models . . . 83
5.2 Multilevel networks . . . 86

6 Conclusions and future directions 92
6.1 Future directions . . . 93

Bibliography 95

Appendix A. Proof of approximation factor for Algorithm 2 101
A.1 The case $k \leq w/\rho h$ . . . 101

A.1.1 Case 1 102
A.1.2 Case 2 102
A.1.3 Case 3 103
A.1.4 Case 4 104
A.1.5 Case 5 104
A.2 The case $k > w/\rho h$ 105
A.2.1 Case 6 105
A.2.2 Case 7 105
A.2.3 Case 8 106

Appendix B. Proof of Theorem 24 **107**

Appendix C. Proof of Theorem 26 **109**

Appendix D. Proof of Theorem 28 **111**

List of Tables

4.1 Summary of the major results from Section 4.2.1 58
4.2 The optimal configurations for various backbone network structures . . 65
4.3 Summary table for Section 4.3 82
5.1 Optimal values to (5.2) 88

List of Figures

2.1 A honeycomb heuristic layout 8

2.2 Optimality of Archimedes spiral 9

3.1 An illustration of Algorithm 2 13

3.2 The optimal regions C^* for increasing values of A 16

3.3 Proof of Lemma 9 18

3.4 Proof of Lemma 13 21

3.5 The approximation ratios of Algorithm 2 when applied to the 50 US states 27

3.6 The output of Algorithm 2 when applied to the state of Minnesota . . . 28

3.7 Proof of Lemma 15 29

3.8 Proof of Theorem 17 33

3.9 Proof of Lemma 18 36

3.10 An illustration of Algorithm 4 38

3.11 Subdomains in proving approximation ratio for Algorithm 4 40

4.1 Backbone network structures considered in Chapter 4 46

4.2 Optimal configurations for the four special instances of (4.1) 51

4.3 A contracted honeycomb configuration 55

4.4 The boundary curves that distinguish different optimal solution configurations for various values of p and q in five of the backbone network structures 66

4.5 The optimal region R that minimizes $\mathrm{FW}(X' \cup Q, R)$ 69
4.6 Surface plots of the approximation ratio 82
5.1 An example of a four-level network 91
5.2 An optimal configuration of a three-level network 91
B.1 The setup for our proof of Theorem 24. 107

Chapter 1

Introduction

The facility location problem is a well-studied optimization problem in the field of operations research and computer science. Although different variations exist with regard to their objective function and constraints, the ultimate goals of these problems are the same: to find the best locations of a set of facilities so that an objective function of interest can be optimized. Depending on characteristics and functionalities of these facilities and the associated resource constraints, a number of subclasses exist under the name of the *facility location problem*. The most classic problem may be the *uncapacitated facility location problem* which forms the basis of many interesting and important problems. For an extensive review of a broad spectrum of facility location problems, readers are referred to the excellent book edited by Eiselt and Marianov [13].

An important but less studied problem related to the classic uncapacitated facility location problem is the so called *connected facility location problem*. In such a problem, each facility is additionally connected with other facilities by a certain network structure and the problem seeks to optimize facility locations so that total costs including facility connection cost are minimized. This problem can arise in a number of settings.

In the retail industry, the connection cost represents the transportation required for replenishing inventory for each store. In public transportation, this connection represents the transportation network between transit terminals. While in telecommunication, the connection, which is often referred to as the *backbone network*, is the part of network infrastructure that interconnects local area networks or subnetworks. In light of the naming convention in telecommunication, we will also refer to the *connected facility location problem* as the *facility location problem with backbone network cost* and use the two terms interchangeably in later chapters.

It is often differentiated in facility location problems by whether the feasible set of candidate locations is discrete or continuous. If the set only consists of a finite number of points, the problem is classified as *discrete*. If on the other hand the feasible set is continuous (e.g. a set of line segments or a continuous region on a plane), the problem is called a *continuous* facility location problem. Another way of categorizing the problem is by whether the demand set is discrete or continuous. However, most of the work on continuous facility location problems only deal with problems that are continuous with regard to the feasible set rather than the demand set.

In this dissertation, we bridge this gap by studying the connected facility location problem when both the demand set and the feasible set are continuous. We introduce the continuous connected facility location problem in chapter 2 and give an asymptotic analysis of the problem. Next, we introduce a constant factor approximation algorithm for the problem and provide a worst case analysis for the algorithm. In chapter 4, we extend our analysis to a generalized connected facility location problem where the backbone network takes several different configurations, we give asymptotic analysis and algorithmic analysis to each configuration. In chapter 5, we further generalize our model for alternative cost models and multilevel networks. We conclude the dissertation and discuss future work in chapter 6.

Aspects of this dissertation have been published as three papers during author's study as a graduate student. Specifically, the approximation algorithm for the continuous k-median problem discussed in chapter 3 has been published in [9]. Asymptotic and algorithmic analysis on the continuous connected facility location problem when the backbone network takes the form of a minimum spanning tree in chapter 2 and chapter 3 has been published in [8]. Analysis on the generalized continuous connected facility location problem where the backbone network is allowed to vary as discussed in chapter 4 and the generalization to multilevel network in chapter 5 has been published in [7].

Chapter 2

Continuous connected facility location problem

In this chapter, we study the continuous connected facility location problem in a convex region. The problem can be stated as follows. Letting $X = \{x_1, \ldots, x_k\}$ denote a set of facilities contained in a convex region R and d be a distance function, the continuous connected facility location problem (CCFL) is given by:

$$\underset{X,k}{\text{minimize}}\ \mathrm{F}(X, R) = \psi \int_{p \in R} d(X, p)dp + \phi\, \mathrm{MST}(X) \tag{2.1}$$

where $d(X, p) = \min_{x \in X} d(x, p)$ is the distance from point p to its nearest facility in X, $\mathrm{MST}(X)$ is the length of the minimum spanning tree of X and ψ and ϕ are positive real numbers. This first term in (2.1) $\int_{p \in R} d(X, p)dp$ denotes the average distance from demand points to facilities and is the objective function used in the continuous *Fermat-Weber* or *k-median* problem when k is given, we refer to this quantity as *Fermat-Weber* value of X and R, and denote it using $\mathrm{FW}(X, R)$. $\mathrm{MST}(X)$ represents the cost of connecting the facilities or the backbone network cost.

2.1 Applications

The continuous connected facility location problem can arise in a couple of settings. As first introduced in [5], the objective function (2.1) can be used to evaluate different location choices for their environmental impact (e.g. carbon emissions) due to activities of a retail firm. In this scenario, the first term in (2.1) models the emissions from customers visiting the stores, while the second term models the emissions generated by the firm from replenishing inventories for its stores. It should be noted that although we are using a minimum spanning tree as the backbone network here, other network topologies, such as traveling salesman tour or star shaped network, are also possible. We will discuss these various backbone network topologies in chapter 4.

Another instance of our problem arises when one considers the problem faced by stores selling items that require delivery or installation, such as appliances or furniture. Large freight trucks distribute products to showrooms, which are then put on display to customers. These customers then schedule a delivery and installation of their desired product. Because of the time sensitivity of such requests and other complications such as the capacities on local delivery vehicles, economies of scale are much harder to leverage at the local store-to-customer level than at the transshipment level. The direct trip cost in our model is therefore justified in this case.

Often times, one might attempt to minimize the actual financial costs incurred by the company in placing its retail stores. In this case, the inclusion of the local transportation costs between stores and customers in (2.1) is not immediately justified because customers generally bear the cost of travel to retail stores rather than vice versa. In such a case, we should use an alternative model for the transportation costs that possesses some kind of spatial demand component (i.e. that customers near a facility are more likely to use it than those farther away), we discuss this in chapter 5.

Another application of our model is in the design of public transportation network

where the facilities represent the transit terminals and the backbone network is for example high speed rail lines.

2.2 Related work

The *connected facility location* problem is, to our knowledge, first introduced in [16] when the authors are analyzing a telecommunication network design problem. In that work, a *discrete* point set is used to represent both the demand and feasible facility locations. The authors formulated the problem using linear programming relaxation and provide a constant factor approximation algorithm adapting the rounding technique of [38]. Several subsequent work provide further improvement on the approximation algorithms ([41], [22], [14]).

There are however much less results on the *continuous* connected facility location problem we are studying. A similar problem has previously been discussed (but not solved) in [24], which gives a taxonomy of six classes that differentiate the various continuous approximation models developed for freight distribution problems. The problem of minimizing objective function (2.1) belongs to class IV, one-to-many distribution with transshipments, which can be readily observed in Figure 2 of that paper. One important distinction between the models of [24] and our own is that we use the expression $\int_{p\in R} \min_{x\in X} d(x,p)dp$ to model the transportation costs, whereas the corresponding models in [24] use traveling salesman tours originating at the facilities. In section 5.1, we will show that the conclusions we derive here are more or less applicable to the approach used therein. Along the same lines, sections 5 and 6 of [28] provide an elegant theoretical justification, using continuum mechanics, for the continuous approximation that this paper employs to describe approximate global optima to the objective functions used herein.

Section 2.3 studies the limiting behavior of the optimal solution to our problem (2.1)

as the *Fermat-Weber* value dominates the backbone network cost. As such, our analysis closely resembles other research on the asymptotic behavior of Euclidean optimization problems, such as the traveling salesman problem ([3], [4], [18]) and general subadditive Euclidean functionals ([35], [40]) as well as the k-center and k-medians problems ([20], [47]). Although our analysis is deterministic (as opposed to the cited works that are probabilistic), the spirit of our contribution is most closely related to the aforementioned results.

2.3 Special cases

In this section, we perform an asymptotical analysis of the model 2.1 when its parameters go to extremes. It is straightforward to see that when $\psi \ll \phi$, the best approach is to minimize $\mathrm{MST}(X)$, thus placing a single facility at the geometric median of R. We devote the rest of the section to the case where $\psi \gg \phi$. We first give a tight lower bound for the popular *honeycomb heuristic*. Then we show that a so called *Archimedean spiral* configuration reduces the objective function value by up to 27%, and it is indeed the asymptotically optimal configuration.

Definition 1 (Voronoi diagram)**.** Let $P := \{p_1, p_2, \ldots, p_n\}$ be a set of n distinct points in the plane and $dist(x, y)$ be a distance function between x and y. The *Voronoi diagram* of P is the subdivision of the plane into n cells, one for each point in P, such that a point q lies in the cell corresponding to p_i if and only if $dist(q, p_i) < dist(q, p_j)$ for each $p_j \in P$ with $j \neq i$.

A *honeycomb heuristic* is a point placement strategy that every cell (except the ones at boundary) of the resulting Voronoi diagram is a hexagon of the same size. It is shown in [31] that this gives an asymptotically optimal solution (i.e. when number of demand points n goes to infinity) when the number of facilities k grows at a rate between $\log n$

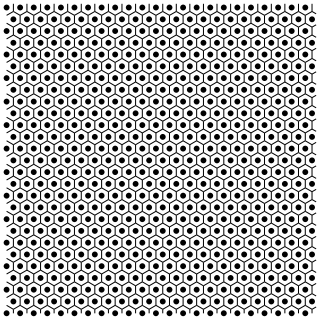

Figure 2.1: A honeycomb heuristic layout

and $n/\log n$. An example of the honeycomb heuristic is shown in Figure 2.1.

The following claim gives a lower bound for using honeycomb heuristic on problem (2.1) when $\psi \gg \phi$.

Claim 2. Let $X = \{x_1, x_2, ...x_k\}$ denote a set of k points placed in a convex polygon C following honeycomb heuristics, $F(X, C) = \mathrm{FW}(X, C) + \phi\,\mathrm{MST}(X)$, $\mathrm{Area}(C) = A$. Then when $\psi \gg \phi$, the following lower bound can be obtained

$$F(X, C) \geq \alpha A\sqrt{\psi\phi}$$

where $\alpha \approx 1.2733$.

Proof. Suppose we use a hexagonal tiling to cover the polygon C. Let X denote the centers of the hexagons inside C and t denote the edge length of each hexagon. It can be calculated that the Fermat-Weber value of any one of the hexagon H is $\mathrm{FW}(H) = \frac{\sqrt{3}(3\ln 3+4)t^3}{8}$. The edge length of the minimum spanning tree of X is $\sqrt{3}t$. For a relatively large k(which is necessarily the case when $\psi \gg \phi$), the Voronoi cells at the boundary negligible and we have $Area(H) = \frac{9t^2}{2\sqrt{3}} \approx \frac{A}{k}$. Then it is straightforward to show that $F(X, C) = \psi k\,\mathrm{FW}(H) + \phi\,\mathrm{MST}(X) \geq 1.2733A\sqrt{\psi\phi}$. Equality holds when $k = 0.3510A\psi/\phi$. □

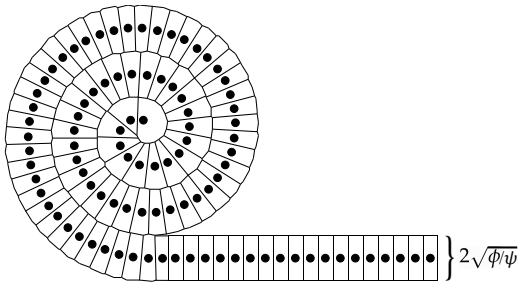

Figure 2.2: Unravelling the spiral (and Voronoi partition) from the Archimedes heuristic while approximately preserving the relevant geometric quantities. As $\psi/\phi \to \infty$ the Voronoi cells of the spiral become increasingly rectangular.

Next, we prove the following result which gives an asymptotically optimal configuration for objective function (2.1).

Theorem 3. *Let $X = \{x_1, x_2, ...x_k\}$ denote a set of k points in a disc C evenly distributed on the Archimedean spiral defined in polar coordinates (r, θ) by equation $r = a + b\theta$, where $a = \sqrt{\phi}$, $b = \frac{\sqrt{\phi}}{\pi}$. $F(X, C) = \psi\,\mathrm{FW}(X, C) + \phi\,\mathrm{MST}(X)$, $\mathrm{Area}(C) = A$. Then when $\psi \gg \phi$,we have $F(X, C) \sim A\sqrt{\psi\phi}$ when $k \to \infty$.*

Proof. First notice that the Voronoi partition of X can be approximated by evenly distribute the points along a straight line in the middle of a skinny rectangle with length $\frac{A}{2\sqrt{\phi/\psi}}$, width $2\sqrt{\phi/\psi}$ (See Figure 2.2). As $\psi/\phi \to \infty$, the Voronoi cells of the spiral become increasingly rectangle. Now we only need to turn our attention to analyzing the following case: a line segment L with length $\frac{A}{2\sqrt{\phi/\psi}}$ and its neighbourhood region $N_\epsilon(L)$ where $\epsilon = \sqrt{\phi}$. Then the Fermat-Weber value is $\mathrm{FW}(L, N_\epsilon(L)) = \frac{A\sqrt{\phi/\psi}}{2} + \frac{2\pi}{3}\phi/\psi^{\frac{3}{2}}$ The minimum spanning tree of L coincides with L. Therefore we have $F(X, C) \sim A\sqrt{\psi\phi}$ □

By winding the points in accordance the shape of the polygon, this result holds for any convex polygon. We will show in Section 3.2.1 that the Archimedes heuristic is indeed an asymptotically optimal configuration

Chapter 3

Continuous connected facility location problems: algorithmic analysis

In this chapter, we turn our attention to algorithmic solutions to the continuous connected facility location problem introduced in Chapter 2. Specifically, we are interested in developing an approximation algorithm with small approximation factor for the problem. Due to a close connection between our problem (2.1) and the continuous k-median problem, it turns out that both problems can be (approximately) solved using the algorithm we will introduce in this chapter with some slight differences. The organization of this chapter is as follows: in section 3.1, we give a fast and simple factor 2.74 approximation algorithm for the continuous k-median problem. In section 3.2, we show how this algorithm can be modified to solve the continuous connected facility location problem with a constant factor.

3.1 Continuous k-median problem

The continuous k-median problem is a natural problem in facility location analysis. Besides the case when the underlining demand distribution is continuous, it is sometimes studied as an approximation to the discrete k-median problem when the problem size is too large (say, more than 1000) to be tractable. The planar continuous k-median problem can be defined as the follows.

Definition 4 (Continuous k-median problem)**.** Given an integer k, a set of points $X = \{x_1, \ldots, x_k\}$ and a region C, the *continuous k-median problem* seeks to find X that solves the following optimization problem:

$$\min_{X:|X|=k} \int_{p \in C} \min_{x \in X} d(x, p) \, \mathrm{d}p$$

where $d(x, y)$ denotes a distance function.

In this section, we give a very simple constant factor approximation algorithm for the continuous k-medians problem in a convex polygon C with n vertices under the L_2 norm. A worst case theoretical analysis shows that our algorithm always produces solutions within a factor of 2.74 of optimality. In addition, simulation results applied to the convex hulls of the 50 states of the United States show that our algorithm generally performs within 10% of optimality in practice.

3.1.1 Related Work

The first exact algorithmic study for the continuous k-median problem was performed in [15], which describes polynomial-time algorithms for various versions of the 1-median (Fermat-Weber) problem under the L_1 norm. The authors also consider the multiple-center version of the L_1 k-median problem, which they prove is NP-hard for large k.

It is also possible to obtain a polynomial-time approximation schemes (PTAS) to this problem by discretizing the region in question into grid cells and then applying one of the PTASes developed for discrete k-median problem (see [2], [27]); however, the running time of such a discretization depends on the fatness of the input shape, because a long and skinny input region will require more grid cells to obtain a sufficiently refined grid approximation. In addition, we are unaware of any implementations of the PTASes for the discrete case of our problem, likely because of their fairly sophisticated nature (and possibly poor practical running time).

3.1.2 Preliminaries

The following are some notational conventions will be used in the rest of the chapter. We define

$$\begin{aligned} \mathrm{FW}(C) &= \min_{x} \int_{p \in C} \|x - p\| \, \mathrm{d}p \\ \mathrm{FW}(C, k) &= \min_{X : |X| = k} \int_{p \in C} \min_{x \in X} \|x - p\| \, \mathrm{d}p \end{aligned}$$

to be the Fermat-Weber objective functions that we seek to minimize, where $\| \cdot \|$ denotes the L_2 (Euclidean) norm. Let $\square C$ denote the *minimum-area bounding box* of C (which can be computed in linear running time [42]), and let $\mathrm{width}(C)$ and $\mathrm{height}(C)$ denote the dimensions of $\square C$. Let $\mathrm{AR}(C)$ denote the *aspect ratio* of C, $\max\left\{\frac{\mathrm{width}(C)}{\mathrm{height}(C)}, \frac{\mathrm{height}(C)}{\mathrm{width}(C)}\right\}$.

3.1.3 The algorithm

We describe our algorithm in this section. The input to our algorithm is a convex polygon C with n vertices and an integer k. We assume without loss of generality that

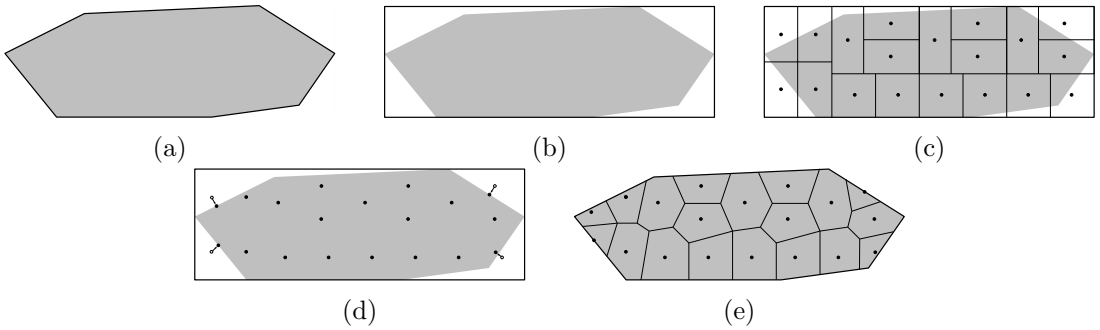

Figure 3.1: The input and output of Algorithm 2. We begin in (3.1a) with a convex polygon C, whose minimum-area bounding rectangle $\square C$ is computed in (3.1b). The bounding box is then partitioned into equal-area pieces in (3.1c) using Algorithm 1. Some of the centers of these pieces are then relocated in (3.1d), and (3.1e) shows the output and Voronoi partition.

C is aligned so that the long side of $\square C$ is aligned with the coordinate x-axis. Note that by construction, it must be the case that $\text{Area}(\square C)/2 \leq \text{Area}(C) \leq \text{Area}(\square C)$. Then, we let $k_1 = \lfloor k/2 \rfloor$ and $k_2 = \lceil k/2 \rceil$ and divide $\square C$ into two pieces of areas $\frac{k_1}{k} \cdot \text{Area}\,(\square C) = \frac{k_1}{k} \cdot wh$ and $\frac{k_2}{k} \cdot \text{Area}\,(\square C) = \frac{k_2}{k} \cdot wh$ respectively, using a vertical line. This is performed recursively (with the option to split using a horizontal line, if the height of an intermediate rectangle exceeds its width) until all regions have area $\text{Area}\,(\square C)\,/k$. This is given in Algorithms 1 and 2 and Figure 3.1.

The following lemma, which is a simplified restatement of a result from [1], states an important property of Algorithm 1.

Lemma 5. *Suppose that $\tilde{R} \subseteq \square C$ is an intermediate rectangle obtained throughout Algorithm 1, which is further subdivided into $\tilde{R}'$ and $\tilde{R}''$. Then:*

1. *If* $\text{AR}(\tilde{R}) > 3$, *then*

$$\text{AR}(\tilde{R}'), \text{AR}(\tilde{R}'') \leq \text{AR}(\tilde{R})\,.$$

2. *If* $\text{AR}(\tilde{R}) \leq 3$, *then*

$$\text{AR}(\tilde{R}'), \text{AR}(\tilde{R}'') \leq 3\,.$$

Proof. Claim 1 is trivial. To prove claim 2 we assume that $\mathrm{AR}(\tilde{R}) \leq 3$. Assume without loss of generality that $\mathrm{width}(\tilde{R}) \geq \mathrm{height}(\tilde{R})$, so that $\mathrm{height}(\tilde{R}') = \mathrm{height}(\tilde{R})$. Since $\tilde{R}$ is always divided into proportions as close as $1/2$ as possible, we have

$$\mathrm{width}(\tilde{R})/3 \leq \mathrm{width}(\tilde{R}') \leq 2\,\mathrm{width}(\tilde{R})/3$$

and, dividing by $\mathrm{height}(\tilde{R})$, we find that

$$\begin{aligned}\mathrm{width}(\tilde{R})/(3\,\mathrm{height}(\tilde{R})) \leq \mathrm{width}(\tilde{R}')/\,\mathrm{height}(\tilde{R}') &= \mathrm{width}(\tilde{R}')/\,\mathrm{height}(\tilde{R}) \\ &\leq 2\,\mathrm{width}(\tilde{R})/(3\,\mathrm{height}(\tilde{R})) \leq 2\end{aligned}$$

so that $\mathrm{width}(\tilde{R}')/\,\mathrm{height}(\tilde{R}') \leq 2$. Taking the reciprocal of this expression and observing that $3 \geq 3\,\mathrm{height}(\tilde{R})/\,\mathrm{width}(\tilde{R})$ since $\mathrm{width}(\tilde{R}) \geq \mathrm{height}(\tilde{R})$, we have

$$\begin{aligned}3 \geq 3\,\mathrm{height}(\tilde{R})/\,\mathrm{width}(\tilde{R}) \geq \mathrm{height}(\tilde{R}')/\,\mathrm{width}(\tilde{R}') &= \mathrm{height}(\tilde{R})/\,\mathrm{width}(\tilde{R}') \\ &\geq 3\,\mathrm{height}(\tilde{R})/(2\,\mathrm{width}(\tilde{R}))\end{aligned}$$

so that $3 \geq \mathrm{height}(\tilde{R}')/\,\mathrm{width}(\tilde{R}')$. This same argument clearly applies to $\tilde{R}''$ as well, which completes claim 2. □

Intuitively, Lemma 5 says that the partition resulted from Algorithm 1 preserves the "fatness" of the input polygon. This property turns out to be very useful in keeping the analysis tractable when proving the approximation factor later in this chapter.

3.1.4 Upper and lower bounds

In this section we establish some upper and lower bounds for the Fermat-Weber value $\mathrm{FW}(C)$ of any convex region C. We begin with some simple lemmas:

Lemma 6. *For a disk D with radius r,*

$$\mathrm{FW}(D) = \frac{2\pi r^3}{3}.$$

Proof. Trivial. □

Remark 7. It is well-known that, for a fixed area, the disk is the region with minimal Fermat-Weber value $\mathrm{FW}(C)$. This gives us an easy lower bound:

$$\mathrm{FW}(C) \geq \frac{2}{3\sqrt{\pi}} A^{3/2}$$

where A is the area of C.

Definition 8. A region C is said to be *star convex at the point p* if the line segment from p to any point $x \in C$ is itself contained in C. Similarly, the *star convex hull* of a region S at the point p is the smallest star-convex region at the point p that contains S (i.e. the union of all segments between points $x \in S$ and p).

Lemma 9. *Let B be a box of dimensions $w \times h$ centered at the origin. The region C^* that solves the infinite-dimensional optimization problem*

$$\begin{aligned} \underset{C}{\text{maximize}}\ \mathrm{FW}(C) \qquad & s.t. \\ C &\subseteq B \\ \mathrm{Area}(C) &= A \\ C &\ni (0,0) \\ C &\text{ is } \text{star convex at } (0,0) \end{aligned} \tag{3.1}$$

is the star convex hull of $B \backslash D$, where D is an appropriately chosen disk centered at the origin, as indicated in Figure 3.2.

Input: An axis-aligned rectangle R and an integer k.
Output: A partition of R into k rectangles, each having area $\text{Area}(R)/k$.
if $k = 1$ **then**
  return R;
else
  Set $k_1 = \lfloor k/2 \rfloor$ and $k_2 = \lceil k/2 \rceil$;
  Let w denote the width of R and h the height;
  if $w \geq h$ **then**
    With a vertical line, divide R into two pieces R_1 and R_2 with area $\frac{k_1}{k} \cdot \text{Area}(R)$ on the right and $\frac{k_2}{k} \cdot \text{Area}(R)$ on the left;
  else
    With a horizontal line, divide R into two pieces R_1 and R_2 with area $\frac{k_1}{k} \cdot \text{Area}(R)$ on the top and $\frac{k_2}{k} \cdot \text{Area}(R)$ on the bottom;
  end
  return $\textit{RectanglePartition}(R_1, k_1) \cup \textit{RectanglePartition}(R_2, k_2)$;
end

Algorithm 1: Algorithm $\text{RectanglePartition}(R, k)$ takes as input an axis-aligned rectangle R and a positive integer k.

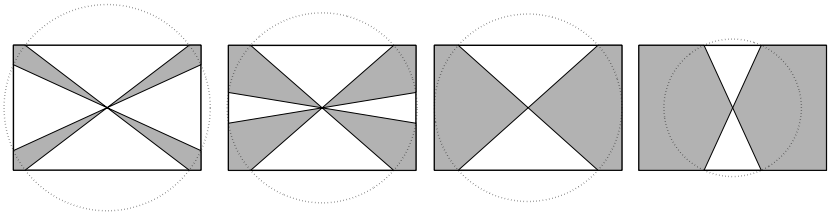

Figure 3.2: The optimal regions C^* in a given box B, for increasing values of A.

Input: A convex polygon C and an integer k.
Output: The locations of k points p_i in C that approximately minimize $\mathrm{FW}(C, k)$ within a factor of 2.74.
Let $\square C$ denote a minimal-area bounding box of C;
Rotate C so that $\square C$ is aligned with the coordinate axes;
Let $R_1, \ldots, R_k = \mathrm{RectanglePartition}(\square C, k)$;
for $i \in \{1, \ldots, k\}$ **do**
    Let c_i denote the center of R_i;
    if $c_i \in C$ **then**
        Set $p_i = c_i$;
    else
        if $R_i \cap C$ *is nonempty* **then**
            Let $R_i^{'}$ be the minimum axis-aligned bounding box of $R_i \cap C$ and let $c_i^{'}$ denote its center;
            Set $p_i = c_i^{'}$;
        else
            Place p_i anywhere in C;
        end
    end
end
return $p_1, \ldots, p_k$;

Algorithm 2: Algorithm $\mathrm{ApproxFW}(R, k)$ takes as input a convex polygon C and an integer k.

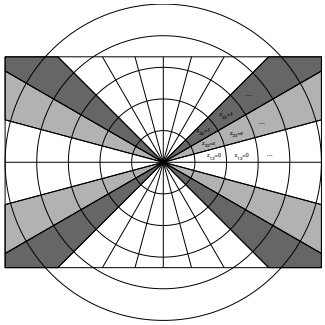

Figure 3.3: In the discretization above, our variables are set up in such a way that the star convexity constraint is equivalent to setting $z_{i(j+1)} \leq z_{ij}$ for all j. By the nature of the constraints it is clear that we may assume that $z^*_{i(j+1)} = z^*_{ij}$ at optimality since the distance from cell ij to the origin increases with j. The diagram above suggests a linear programming formulation, where the lighter regions indicate fractional solutions.

Furthermore for fixed w and h, the function $\Phi(A) = \mathrm{FW}(C^*)$ (i.e. the maximal value of (3.1)) is monotonically increasing and concave.

Proof sketch. This follows from a standard argument where we consider the integer (or linear) program obtained by discretizing problem (3.1) using polar coordinates. See Figure 3.3. Concavity of $\Phi(A)$ follows by observing that we build our optimal solution by adding sectors containing points that are strictly closer than the points in the sector that preceded them. □

Definition 10. Let $\mathbf{x} = (x, y)$ be a point in the plane. We define the $\boxtimes$ and $\boxdot$ norms by

$$\begin{aligned} \|\mathbf{x}\|_{\boxtimes} &= \max\{|x|, |y|\} + \left(\sqrt{2} - 1\right) \min\{|x|, |y|\} \\ \|\mathbf{x}\|_{\boxdot} &= \max\left\{|x|, |y|, \frac{1}{\sqrt{2}}(|x| + |y|)\right\}. \end{aligned}$$

Remark 11. The following identities are easy to verify:

$$\begin{aligned} \|\mathbf{x}\|_{\boxtimes} &\leq \|\mathbf{x}\|_2 \leq \|\mathbf{x}\|_{\boxtimes} \\ \psi\,\|\mathbf{x}\|_{\boxtimes} &\leq \|\mathbf{x}\|_2 \leq \|\mathbf{x}\|_{\boxtimes} \\ \|\mathbf{x}\|_{\boxtimes} &\leq \|\mathbf{x}\|_2 \leq \frac{1}{\psi}\,\|\mathbf{x}\|_{\boxtimes} \end{aligned}$$

where $\psi = \cos(\pi/8) \approx 0.9239$. Both norms have a natural interpretation: $\|\mathbf{x}\|_{\boxtimes}$ is the distance from $(0,0)$ to $\mathbf{x}$ if we are only permitted to move horizontally, vertically, or diagonally (the cardinal and ordinal directions) and $\|\mathbf{x}\|_{\boxtimes}$ is the maximum distance from $(0,0)$ to $\mathbf{x}$ in the horizontal, vertical, or diagonal direction.

Lemma 12. *Let C be a convex region, contained in a box B of dimensions $w \times h$, that contains the center $(0,0)$ of B. If $A = \mathrm{Area}(C)$, then we have*

$$\mathrm{FW}(C) \leq H_1(A,w,h) := \begin{cases} \frac{\sqrt{2}-1}{3}Ah - \frac{\sqrt{2}-1}{12}wh^2 & \\ -\frac{\sqrt{w^2-h^2}}{3}(wh - A) & \\ +\frac{1}{3}w^2h - \frac{1}{12}h^3 & \text{if } A \leq wh - \frac{h}{2}\sqrt{w^2-h^2} \\ \frac{2}{3}Aw + \frac{\sqrt{2}-1}{3}Ah & \\ -\frac{1}{3}\cdot\frac{A^2}{h} - \frac{1}{12}w^2h & \\ -\frac{\sqrt{2}-1}{12}wh^2 & \text{if } wh - \frac{h}{2}\sqrt{w^2-h^2} < A \leq wh - \frac{h^2}{2} \\ \frac{2\sqrt{2}-2}{3}Aw + \frac{1}{3}Ah & \\ +\frac{7-4\sqrt{2}}{12}w^2h + \frac{2-\sqrt{2}}{12}h^3 & \\ -\frac{\sqrt{2}-1}{3}\cdot\frac{A^2}{h} - \frac{7-3\sqrt{2}}{12}wh^2 & \text{otherwise} \end{cases}.$$

If the dimensions w and h are equal, say $2b$, then we have

$$\mathrm{FW}(C) \leq H_2(A, b) := \frac{2\sqrt{2}b}{3}A - \frac{\sqrt{2}-1}{12b}A^2.$$

Proof. We consider the relaxation of the infinite-dimensional optimization problem

$$\begin{aligned} \underset{C}{\text{maximize}}\, \mathrm{FW}\,(C) \qquad & s.t. \\ C &\subseteq B \\ \mathrm{Area}\,(C) &= A \\ C &\ni (0,0) \\ C &\text{ is convex}, \end{aligned}$$

obtained by replacing the convexity constraint with star convexity about the origin. The problem is now equivalent to problem (3.1).

Following lemma 9 we see that the optimal star-convex region C^* takes the form shown in Figure 3.2. If $A \geq wh - \frac{h}{2}\sqrt{w^2-h^2}$, then the optimal solution consists of two components (rather than 4). We evaluate the Fermat-Weber objective value under the $\boxtimes$ norm and we find that

$$\mathrm{FW}_{\boxtimes}(C^*) = \begin{cases} 4\int_0^{h/2}\int_{y/m}^{w/2} x + \left(\sqrt{2}-1\right) y \, dx \, dy & \text{if } wh - \frac{h}{2}\sqrt{w^2-h^2} \leq A \leq wh - h^2 \\ 4\int_0^{h/2}\int_{y/m}^{y} \left(\sqrt{2}-1\right) x + y \, dx & \\ \quad + \int_y^{w/2} x + \left(\sqrt{2}-1\right) y \, dx \, dy & \text{if } A > wh - h^2 \end{cases}$$

where $m = \frac{h^2}{2(wh-A)}$; the formulas are thus found by analytic integration. We find the upper bound for the case $A \leq wh - \frac{h}{2}\sqrt{w^2-h^2}$ simply by using the fact that $\mathrm{FW}_{\boxtimes}(C^*)$ is concave in A, then taking a tangent line at $A = wh - \frac{h}{2}\sqrt{w^2-h^2}$ and extrapolating. $\square$

(a) (b) (c)

Figure 3.4: The region C^* of minimal Fermat-Weber objective value, the rectangles R_1 and R_2, and the hexagon that gives our lower bound.

For the remainder of this chapter we define $\rho = 4.34818$ and $\gamma = 0.11719$.

Lemma 13. *Let C be a convex region with area A, contained in a box B of dimensions $w \times h$, where $w/h \geq \rho$. If $A \geq wh/2$, then*

$$\mathrm{FW}(C) \geq \begin{cases} \frac{\left(16+12\sqrt{2}\right)\gamma(\gamma-1)+\sqrt{2}}{24\left(\sqrt{2}+1\right)^2}h^3 + \frac{8+6\sqrt{2}-\left(28+20\sqrt{2}\right)\gamma}{24\left(\sqrt{2}+1\right)^2}Ah & \\ +\frac{16+11\sqrt{2}}{24\left(\sqrt{2}+1\right)^2}A^2/h & \text{if } A \leq \frac{\left(2\sqrt{2}-2\right)\gamma+1}{\sqrt{2}-1}h^2 \\ \left(\gamma^3/3+\sqrt{2}/6-1/12\right)h^3 - (\gamma/2)\,Ah & \\ +\,(1/4)\,A^2/h & \text{otherwise} \end{cases}.$$

Proof. Refer to Figure 3.4 for this proof. The shape C^* that minimizes $\mathrm{FW}(C)$ in B is the intersection of a disk with a slab of height h. Let R_1 denote the largest rectangle contained in C^* and let R_2 denote the smallest rectangle containing C^*. Clearly, for fixed h, the two rectangles become the same as $\mathrm{Area}(C^*)$ increases. In particular, if $\mathrm{Area}(C^*) \geq wh/2 \geq \rho h^2/2$, then we can verify numerically that the "gap" g between the two (as indicated in Figure 3.4b) is at most γh. Therefore, the hexagon with vertices $(\pm A/2h, 0)$ and $(\pm(A/2h - \gamma h), \pm h/2)$ is contained entirely in C^* whenever $\mathrm{Area}(C^*) \geq \rho h^2/2$. To obtain the desired result, we bound the Fermat-Weber value on

this hexagon under the $\boxtimes$ norm:

$$\mathrm{FW}_{\boxtimes}(C^*) \geq \begin{cases} 4\int_0^{h/2}\int_0^{y/m_1} y\,dx + \frac{1}{\sqrt{2}}\int_{y/m_1}^{y/m_2} x+y\,dx & \\ \quad + \int_{y/m_2}^{-2\gamma y + A/2h} x\,dx\,dy & \text{if } A \leq \frac{(2\sqrt{2}-2)\gamma+1}{\sqrt{2}-1}h^2 \\ 4\int_0^{h/2}\int_0^{y/m_1} y\,dx + \frac{1}{\sqrt{2}}\int_{y/m_1}^{y/m_3} x+y\,dx & \\ \quad + \int_{y/m_3}^{-2\gamma y + A/2h} x\,dx\,dy & \text{otherwise} \end{cases}$$

where $m_1 = \sqrt{2}+1$, $m_2 = \frac{h^2}{A-2\gamma h^2}$, and $m_3 = \sqrt{2}-1$, which gives the desired bounds. $\square$

In summary, we have the following upper and lower bounds for $\mathrm{FW}(C)$ when C is

a convex region of area A contained in a box of dimensions $w \times h$:

$$\mathrm{FW}(C) \leq \begin{cases} \frac{\sqrt{2}-1}{3}Ah - \frac{\sqrt{2}-1}{12}wh^2 & \\ -\frac{\sqrt{w^2-h^2}}{3}(wh-A) & \\ +\frac{1}{3}w^2h - \frac{1}{12}h^3 & \text{if } A \leq wh - \frac{h}{2}\sqrt{w^2-h^2} \\ \frac{2}{3}Aw + \frac{\sqrt{2}-1}{3}Ah - \frac{1}{3}\cdot\frac{A^2}{h} & \\ -\frac{1}{12}w^2h - \frac{\sqrt{2}-1}{12}wh^2 & \text{if } wh - \frac{h}{2}\sqrt{w^2-h^2} < A \leq wh - \frac{h^2}{2} \\ \frac{2\sqrt{2}-2}{3}Aw + \frac{1}{3}Ah + \frac{7-4\sqrt{2}}{12}w^2h & \\ +\frac{2-\sqrt{2}}{12}h^3 - \frac{\sqrt{2}-1}{3}\cdot\frac{A^2}{h} & \\ -\frac{7-3\sqrt{2}}{12}wh^2 & \text{otherwise} \end{cases} \tag{3.2}$$

$$\mathrm{FW}(C) \geq \frac{2}{3\sqrt{\pi}}A^{3/2} \tag{3.3}$$

$$\mathrm{FW}(C) \geq \begin{cases} \frac{\left(16+12\sqrt{2}\right)\gamma(\gamma-1)+\sqrt{2}}{24\left(\sqrt{2}+1\right)^2}h^3 & \\ +\frac{8+6\sqrt{2}-\left(28+20\sqrt{2}\right)\gamma}{24\left(\sqrt{2}+1\right)^2}Ah & \\ +\frac{16+11\sqrt{2}}{24\left(\sqrt{2}+1\right)^2}A^2/h & \text{if } A \leq \frac{\left(2\sqrt{2}-2\right)\gamma+1}{\sqrt{2}-1}h^2 \text{ if } w/h \geq \rho\,. \\ \left(\gamma^3/3 + \sqrt{2}/6 - 1/12\right)h^3 & \\ -\left(\gamma/2\right)Ah + \left(1/4\right)A^2/h & \text{otherwise} \end{cases} \tag{3.4}$$

Notice that both of our lower bounds are convex in A, and one can therefore conclude that (for example)

$$\mathrm{FW}(C,k) \geq k \cdot \left[\frac{2}{3\sqrt{\pi}}(A/k)^{3/2}\right] = \frac{2}{3\sqrt{\pi}} \cdot \frac{A^{3/2}}{\sqrt{k}} \tag{3.5}$$

which simply says that the Fermat-Weber value of k points in a region of area A is at

least that of k balls of area A/k, and similarly

$$\mathrm{FW}\left(C,k\right) \geq \begin{cases} k \cdot \left[\frac{\left(16+12\sqrt{2}\right)\gamma(\gamma-1)+\sqrt{2}}{24\left(\sqrt{2}+1\right)^2} h^3 \right. & \\ \left. + \frac{8+6\sqrt{2}-\left(28+20\sqrt{2}\right)\gamma}{24\left(\sqrt{2}+1\right)^2} \cdot \frac{Ah}{k} \right. & \\ \left. + \frac{16+11\sqrt{2}}{24\left(\sqrt{2}+1\right)^2} \cdot \frac{A^2}{hk^2} \right] & \text{if } A \leq \frac{\left(2\sqrt{2}-2\right)\gamma+1}{\sqrt{2}-1} h^2 \\ k \cdot \left[\left(\gamma^3/3 + \sqrt{2}/6 - 1/12\right) h^3 \right. & \\ \left. - \left(\gamma/2\right) \frac{Ah}{k} + \left(1/4\right) \frac{A^2}{hk^2} \right] & \text{otherwise}. \end{cases} \tag{3.6}$$

provided that $(w/k)/h \geq \rho$. We will not explicitly use these lower bounds for $\mathrm{FW}(C,k)$ in the following section because (3.3) and (3.4) will suffice, but we include them here for the sake of completeness.

3.1.5 Proof of approximation

After performing our algorithm, we have a collection of k rectangles with area wh/k; if $k \geq w/\rho h$, then these rectangles have an aspect ratio not exceeding ρ. If $k < w/\rho h$, then all rectangles are identical and have dimensions $(w/k) \times h$. Since our lower bounds are convex in A and the function $\Phi\left(A\right)$ is concave, we immediately know that the worst possible ratio between the upper and lower bounds for $\mathrm{FW}\left(C,k\right)$ is attained when all rectangles contain the same amount of C in them, i.e. $\mathrm{Area}(R_i \cap C) = A/k$ for all i. Therefore, to find the approximation bounds for this algorithm, it will suffice to consider a single such rectangle with height 1 and width $w_{\mathrm{rect}} \geq 1$, such that $\alpha := \mathrm{Area}(R_i \cap C) = A/k$. The approximation bounds are determined by the value of A and the relationship between k and $w/\rho h$. Note that w represents the width of the bounding box of the input region C (i.e. the diameter of C, by construction) whereas w_{rect} represents the width of one of the rectangles R_i that is output by Algorithm 1. Our general approach is to

reduce the approximation ratio to a function of a single variable, whose upper bound can be easily be verified using standard methods from calculus. Details of the proof can be found in Appendix A.

3.1.6 Running time

This algorithm can be performed with running time $\mathcal{O}(n + k + k \log n)$. This is because Algorithm 1 takes $\mathcal{O}(k)$ operations to partition the rectangle and Algorithm 2 requires $\mathcal{O}(n)$ operations to find a minimum bounding box of C. The last step of Algorithm 2 consists of moving the center points to C when necessary, which takes $\mathcal{O}(k \log n)$ operations using a point-in-polygon algorithm [34].

3.1.7 Simulation results

In order to determine the practical performance of our algorithm (as opposed to the theoretical worst-case bounds), we applied it to a dataset generated by forming the convex hulls of the 50 states of the USA. In order to improve the practical performance of Algorithm 2, we introduce one small modification, which we describe below; we have avoided putting this modification in the description of Algorithm 2 because it is not clear how to incorporate it into the theoretical upper-bounding procedure.

Modification to Algorithm 2

In executing Algorithm 1 as a subroutine in Algorithm 2, it may be the case that a final rectangle R_i lies entirely outside C. If this is the case, we add rectangle R_i to a list `OUT`. It may also be the case that an *intermediate* (not necessarily final) rectangle $\tilde{R}$ lies entirely *inside* C; in this case, we add rectangle $\tilde{R}$ to a list `IN`. We do not add any intermediate rectangles to `IN` if they are themselves contained in a larger intermediate rectangle that is already contained in `IN`. Finally, it may be the case that a final

rectangle R_i is *partially* contained by C; in this case we also add R_i to list `IN`.

After executing Algorithm 1 as a subroutine in Algorithm 2, we now have the lists `OUT` and `IN`. The centers of the rectangles of list `OUT` are clearly not helping us, and we now want to find a reasonable way to move them into C. Let the jth rectangle of list `IN` (which may be an intermediate rectangle) be written as $\tilde{R}_j$, let $\tilde{A}_j$ denote the area of $\tilde{R}_j$, and let N_j denote the number of points that would be assigned to $\tilde{R}_j$, prior to our algorithm modification (which is 1 if $\tilde{R}_j$ is a final rectangle). We then let

$$\tilde{N}_j := k \cdot \left\lfloor \frac{\tilde{A}_j}{\sum_{q=1}^{|\texttt{IN}|} \tilde{A}_q} \right\rfloor \tag{3.7}$$

and we then place $\tilde{N}_j$ points in each rectangle $\tilde{R}_j$ according to Algorithm 2 (i.e. partition $\tilde{R}_j$ into $\tilde{N}_j$ rectangles using Algorithm 1 and place one point at each of their centers). This does not affect our approximation result because $\tilde{N}_j \geq N_j$ and $\sum_j \tilde{N}_j \leq k$. The remaining points are distributed arbitrarily among the rectangles in `IN`, and finally, as prescribed by our original Algorithm 2, we move all points that lie outside C inside C by adjusting (shrinking) their bounding boxes and placing them at the centers of those boxes (this guarantees that all of our output points lie in C, or in the worst case on its boundary).

Results and discussion

Figure 3.5 shows the approximation ratios for $k \leq 1000$ when our algorithm is applied to the convex hulls of the 50 states of the USA; more precisely, we show the ratio between the actual objective function value

$$\int_{p \in C} \min_{x \in X} \|x - p\| \, \mathrm{d}p$$

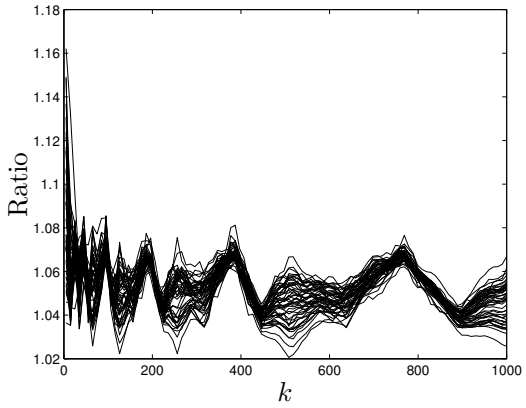

Figure 3.5: The approximation ratios for $k \leq 1000$ applied to the 50 states of the USA.

and the maximum of the two lower bounds (3.5) and (3.6). In order to evaluate the integrals in the expression above we use the *Gaussian cubature method* [25] with tolerance 10^{-5}. As an example, Figure 3.6 shows the output of our algorithm for $k = 100$ applied to the convex hull of the state of Minnesota. The running times of our trials are basically trivial as explained in Section 3.1.6 and we have therefore omitted them.

We first observe that in nearly all of the cases (the exceptions being very low values of k), our algorithm gives a solution that is within 10% of the theoretical lower bound; this suggests both that our algorithm generally performs well and that lower bounds (3.3) and (3.4) are fairly tight. This also suggests that the upper bound (3.2) is the weak point of our worst-case performance bounds. It is also interesting that the approximation ratios in Figure 3.5 seem to exhibit some periodicity; we suspect that this is somehow related to the fact that our algorithm depends on partitioning a rectangle and therefore some pattern persists among the various instances of C.

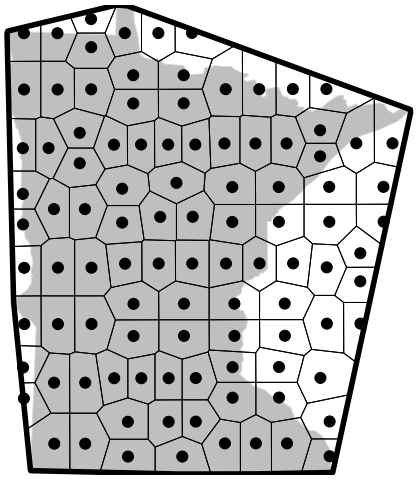

Figure 3.6: The output of our modified algorithm (and the induced Voronoi diagram) for $k = 100$ when applied to the convex hull of the state of Minnesota.

3.2 An approximation algorithm for continuous connected facility location problem

In this section, we extend Algorithm 2 to solve the continuous connected facility location (CCFL) problem (2.1) in a convex polygon under L_2 norm. Recall that CCFL seeks to solve the following optimization problem

$$\underset{X,k}{\text{minimize}}\ \mathrm{F}(X,R) = \mathrm{FW}(X,R) + \phi\,\mathrm{MST}(X)$$

Where $X = \{x_1, \ldots, x_k\}$ denotes a set of facilities in a convex region R, d is a distance function, $d(X,p) = \min_{x \in X} d(x,p)$, $\mathrm{FW}(X,R) = \int_{p \in R} d(X,p)dp$. We give worst case approximation analysis and show that the algorithm is a constant factor approximation algorithm.

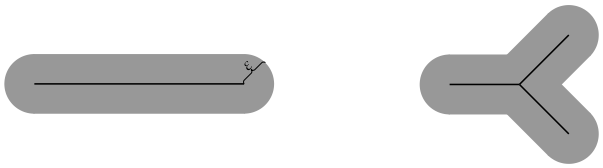

(a) (b)

Figure 3.7: The neighborhoods $N_\epsilon(T)$ for two trees of the same length, a line segment (3.7a) and a generic tree (3.7b).

3.2.1 Lower bounds on a given convex polygon

In this section we introduce some lower bounds for the function $F(X, C)$ defined on a given convex polygon C.

Theorem 14. *Suppose that $X = \{x_1, \ldots, x_k\}$ is a set of points in a convex polygon C such that $\mathrm{MST}(X) = \ell$ and $\mathrm{Area}(C) = A$. Then $\mathrm{FW}(X, C) \geq \frac{2A^2}{8\ell + 3\sqrt{\pi A}}$.*

Proof. This follows via two simple lemmas, which we will now prove. When we refer to a "tree" we implicitly concern ourselves only with those trees in the plane that consist of a finite number of line segments. We first make the observation that if T is a spanning tree of the points X, then obviously $\mathrm{FW}(X, C) \geq \mathrm{FW}(T, C)$ (since $X \subset T$), and therefore we can consider bounding the quantity $\mathrm{FW}(T, C)$ over all trees with a given length.

Lemma 15. *For any tree T of length ℓ and any ϵ, we have $\mathrm{Area}(N_\epsilon(T)) \leq \pi\epsilon^2 + 2\epsilon\ell$, which is tight when T is a line segment.*

Proof. We prove this by induction on the number of line segments k that comprise T. The base case $k = 1$ is simply a line segment for which $N_\epsilon(T)$ is shown in Figure 3.7. To complete the induction, consider a tree consisting of k line segments, which we can think of as the union of a tree T' with length ℓ' with $k - 1$ line segments, and a line segment s of length ℓ'' such that $\ell = \ell' + \ell''$. Let $T' \cup s = T$ denote their union. Since T' and s are joined at a point, the neighborhoods $N_\epsilon(T')$ and $N_\epsilon(S)$ must intersect in

a ball of radius ϵ and consequently we have

$$\begin{aligned}\text{Area}\left(N_\epsilon\left(T\right)\right) &= \text{Area}\left(N_\epsilon\left(T^{'}\cup s\right)\right) = \text{Area}\left(N_\epsilon\left(T^{'}\right)\cup N_\epsilon\left(s\right)\right)\\ &= \underbrace{\text{Area}\left(N_\epsilon\left(T^{'}\right)\right)}_{\leq\pi\epsilon^2+2\epsilon\ell^{'}} + \underbrace{\text{Area}\left(N_\epsilon\left(s\right)\right)}_{\leq\pi\epsilon^2+2\epsilon\ell^{''}} - \underbrace{\text{Area}\left(N_\epsilon\left(T^{'}\right)\cap N_\epsilon\left(s\right)\right)}_{\geq\pi\epsilon^2}\end{aligned}$$

and the desired result follows. □

Lemma 16. *Let T denote a tree with length ℓ and let C denote a planar region with area A containing T. Further let L denote a line segment with length ℓ and let $\epsilon_L^{\max}$ be chosen so that* $\text{Area}(N_{\epsilon_L^{\max}}(L)) = A$. *Then* $\text{FW}(L, N_{\epsilon_L^{\max}}(L)) \leq \text{FW}(T, C)$*; in other words, for a given area A, among all trees with fixed length ℓ, a line segment and its appropriately-chosen neighborhood have the minimal Fermat-Weber value.*

Proof. Assume without loss of generality that $A = 1$ and let $\epsilon_T^{\max}$ be chosen so that $\text{Area}(N_{\epsilon_T^{\max}}(T)) = A = 1$. It is obvious that $\text{FW}(T, N_{\epsilon_T^{\max}}(T)) \leq \text{FW}(T, C)$ for all regions C with area 1. Thus it will suffice to show that $\text{FW}(T, N_{\epsilon_T^{\max}}(T)) \geq \text{FW}(L, N_{\epsilon_L^{\max}}(L))$. Consider a random variable ϵ_T defined by setting $\epsilon_T := D\left(z, T\right)$, where z is a random variable sampled uniformly from $N_{\epsilon_T^{\max}}(T)$, and define ϵ_L similarly. Note that the cumulative distribution functions for ϵ_T and ϵ_L are given by

$$\begin{aligned}F_T(\epsilon_T) &= \min\left\{1, \text{Area}\left(N_{\epsilon_T}(T)\right)\right\}\\ F_L(\epsilon_L) &= \min\left\{1, \text{Area}\left(N_{\epsilon_L}(L)\right)\right\}.\end{aligned}$$

By Lemma 15, for any $\epsilon > 0$, we have $F_L(\epsilon) \geq F_T(\epsilon)$. Next note that

$$\mathbf{E}(\epsilon_L) = \int_0^\infty 1 - F_L(\epsilon)\, d\epsilon \leq \int_0^\infty 1 - F_T(\epsilon)\, d\epsilon = \mathbf{E}(\epsilon_T)\,,$$

a well-known result of first-order stochastic dominance (see page 249 of [33], for instance). The proof is complete by observing that by definition, $\mathbf{E}(\epsilon_L) = \mathrm{FW}(L, N_{\epsilon_L}(L))$ and $\mathbf{E}(\epsilon_T) = \mathrm{FW}(T, N_{\epsilon_T}(T))$. □

Having established the two preceding lemmas, we next note that for any line segment L with length ℓ and any ϵ, we can compute

$$\begin{aligned} \mathrm{Area}(N_\epsilon(L)) &= \pi\epsilon^2 + 2\epsilon\ell \\ \mathrm{FW}\left(L, N_\epsilon\left(L\right)\right) &= \frac{2\pi\epsilon^3}{3} + \epsilon^2\ell\,. \end{aligned} \tag{3.8}$$

Solving equation (3.8) in terms of $\epsilon > 0$ and substituting, we find that

$$\mathrm{FW}\left(L, N_\epsilon\left(L\right)\right) = \frac{-2\ell^3 - 3\pi\ell A + \left(2\ell^2 + 2\pi A\right)\sqrt{\ell^2 + \pi A}}{3\pi^2}\,.$$

where $A = \mathrm{Area}(N_\epsilon\left(L\right))$. We can easily show that the above quantity is bounded below by $\frac{2A^2}{8\ell + 3\sqrt{\pi A}}$. This is equivalent to showing that

$$\frac{\left[2\left(\ell^2 + \pi A\right)^{3/2} - 3\pi A\ell - 2\ell^3\right]\left(8\ell + 3\sqrt{\pi A}\right)}{6\pi^2 A^2} \geq 1\,.$$

Defining $t := A/\ell^2$ so that $A = \ell^2 t$, the above expression is equivalent to

$$\frac{\left[(2 + 2\pi t)\sqrt{1 + \pi t} - 3\pi t - 2\right]\left(8 + 3\sqrt{\pi t}\right)}{6\pi^2 t^2} \geq 1$$

which is easily verified using single-variable calculus.

Our proof of Theorem 14 is complete; if we let T be the minimum spanning tree of any point set X, contained in a region C with area A, then

$$\mathrm{FW}\left(X, C\right) \geq \mathrm{FW}\left(T, C\right) \geq \mathrm{FW}\left(T, N_{\epsilon_T^{\max}}(T)\right) \geq \mathrm{FW}\left(L, N_{\epsilon_L^{\max}}(L)\right) \geq \frac{2A^2}{8\ell + 3\sqrt{\pi A}}$$

where length(T) = length(L) and $\epsilon_T^{\max}$ and $\epsilon_L^{\max}$ are chosen so as to induce the appropriate areas. □

Before describing our approximation algorithm, we must introduce an additional lower bound which applies when C is a particularly long, skinny region. To quantify this, we orient C so that diam (C) is aligned with the coordinate x-axis, and we assume without loss of generality that C is contained in a box of dimensions (diam$(C) = 1/h = w) \times h$, where $w \geq h$. It immediately follows that

$$1/2 = wh/2 \leq \text{Area}\,(C) \leq wh = 1\,.$$

For purposes of clarity, we will use the terms w and $1/h$ interchangeably.

Theorem 17. *Suppose that $X = \{x_1, \ldots, x_k\}$ is a set of points in a convex polygon C such that* MST $(X) = \ell < A/h$. *Then* FW $(X, C) \geq \frac{(A-h\ell)^2}{4h}$.

Proof. Consider the rectangle of dimensions $w \times h$ containing C so that $1/2 \leq$ Area $(C) \leq 1$ as mentioned previously. Assume without loss of generality that $x_1 = \left(x_1^1, x_2^1\right)$ is the leftmost point in X and $x_k = \left(x_1^k, x_2^k\right)$ is the rightmost point in X. Clearly $x_1^k - x_1^1 \leq \ell$. The maximum amount of area of C that can be contained in the slab S between the lines $\ell_1 = \left\{(x_1, x_2) : x_1 = x_1^1\right\}$ and $\ell_2 = \left\{(x_1, x_2) : x_1 = x_1^k\right\}$ is $h\ell$. Thus, we have at least $A - h\ell$ units of area of C remaining to distribute outside S. Let $x^{'} = \left(x_1^{'}, x_2^{'}\right)$ be a dummy variable and consider the function $f\left(x^{'}\right)$ defined by

$$f\left(x^{'}\right) = \begin{cases} x_1^1 - x_1^{'} & \text{if } x_1^{'} \leq x_1^1 \\ 0 & \text{if } x_1^1 < x_1^{'} < x_1^k \\ x_1^{'} - x_1^k & \text{otherwise} \end{cases}$$

and note that clearly $f(x^{'}) \leq \min_{x_i \in X} \|x^{'} - x_i\|$. We now consider the problem of

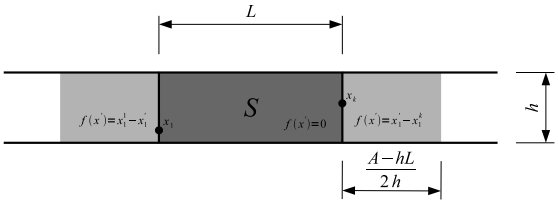

Figure 3.8: The distribution of area that minimizes $f\left(x^{'}\right)$.

distributing the remaining $A - h\ell$ units of area in the rectangle so as to minimize the integral of $f(x^{'})$. The obvious solution is to distribute $\frac{A-h\ell}{2}$ units of area to the right and to the left of S in rectangles of dimensions $\frac{A-h\ell}{2h} \times h$ as shown in Figure 3.8. The integral of $f(x^{'})$ over this shape is precisely $\frac{(A-h\ell)^2}{4h}$ as desired. □

Having established the two preceding results, we may find a lower bound to our original problem by minimizing

$$G\left(\ell\right) := \phi\ell + \max\left\{\frac{2A^2}{8\ell + 3\sqrt{\pi A}}, \frac{\left(A - h\ell\right)^2}{4h}\mathbb{1}(\ell < A/h)\right\}$$

where $\mathbb{1}(\cdot)$ denotes the indicator function, $\phi = c_2/c_1$. Since

$$\arg\min_{\ell \geq 0} \phi\ell + \frac{2A^2}{8\ell + 3\sqrt{\pi A}} = \begin{cases} \frac{4A\sqrt{\phi} - 3\phi\sqrt{\pi A}}{8\phi} & \text{if } \phi \leq \frac{16A}{9\pi} \\ 0 & \text{otherwise} \end{cases}$$

$$\arg\min_{\ell \geq 0} \phi\ell + \frac{\left(A - h\ell\right)^2}{4h} = \begin{cases} \frac{A-2\phi}{h} & \text{if } \phi \leq A/2 \\ 0 & \text{otherwise} \end{cases}$$

we find that

$$\min_{\ell \geq 0} \phi\ell + \frac{2A^2}{8\ell + 3\sqrt{\pi A}} = \begin{cases} A\sqrt{\phi} - \frac{3\phi\sqrt{\pi A}}{8} & \text{if } \phi \leq \frac{16A}{9\pi} \\ \frac{2A^{3/2}}{3\sqrt{\pi}} & \text{otherwise} \end{cases}$$

$$\min_{\ell \geq 0} \phi\ell + \frac{(A - h\ell)^2}{4h} = \begin{cases} \frac{\phi(A-\phi)}{h} & \text{if } \phi \leq A/2 \\ \frac{A^2}{4h} & \text{otherwise} \end{cases}$$

and therefore a lower bound for our objective function 2.1 is

$$\Phi_{\text{LB}}(A, \phi, h) = \begin{cases} \max\left\{A\sqrt{\phi} - \frac{3\phi\sqrt{\pi A}}{8}, \frac{\phi(A-\phi)}{h}\right\} & \text{if } \phi \leq A/2 \\ \max\left\{A\sqrt{\phi} - \frac{3\phi\sqrt{\pi A}}{8}, \frac{A^2}{4h}\right\} & \text{if } A/2 < \phi \leq \frac{16A}{9\pi} \\ \max\left\{\frac{2A^{3/2}}{3\sqrt{\pi}}, \frac{A^2}{4h}\right\} & \text{otherwise.} \end{cases} \tag{3.9}$$

Note that this proves that the Archimedes heuristic is asymptotically optimal as $\phi \to 0$ since we have $F(X, C) \sim A\sqrt{\phi}$.

3.2.2 Upper bounds for Algorithm 4

We next define

$$\begin{aligned} \alpha(A) &= H_1\left(A, \sqrt{3}, 1/\sqrt{3}\right) \in (0.3090, 0.5022) \\ \beta &= \sqrt{3} \approx 1.7321 \end{aligned}$$

where $H_1(A, w, h)$ is defined in Lemma 12. Simply put, $\alpha(A)$ is an upper bound on the Fermat-Weber value of a convex object with area $A \in [0.5, 1]$ contained in a rectangle of area 1 and aspect ratio 3. The value β is simply the length of the long side of this rectangle. We hereafter abbreviate $\alpha(A)$ by α (suppressing the dependency on A in the

interests of notation).

Lemma 18. *Suppose that Algorithm 2 is applied to a convex region C contained in a rectangle of dimensions $(w = 1/h) \times h$, with $k \geq w/3h$. Then*

$$\begin{aligned} \mathrm{FW}\,(X, C) &\leq \alpha/\sqrt{k} \\ \mathrm{MST}\,(X) &\leq \beta\left(\sqrt{k} - 1/\sqrt{k}\right) \end{aligned}$$

so that $F\,(X, C) \leq \alpha/\sqrt{k} + \phi\beta(\sqrt{k} - 1/\sqrt{k}) < \alpha/\sqrt{k} + \phi\beta\sqrt{k}$.

Proof. If $k \geq \frac{w}{3h}$, then all sub-rectangles that are output by Algorithm 1 have area $1/k$ and an aspect ratio not exceeding 3 by Lemma 5. Since α is concave in A, the total Fermat-Weber objective value in all of the k sub-rectangles is maximized when each rectangle contains area A/k of the original polygon C, which gives a Fermat-Weber value of $\alpha k^{-3/2}$ in each rectangle. The total Fermat-Weber contribution to the objective function (over all k facilities) is at most $k \cdot (\alpha k^{-3/2}) = \alpha/\sqrt{k}$.

We now turn our attention to bounding $\mathrm{MST}\,(X)$; we shall prove the desired result using induction, with the base case $k = 1$ being immediately evident. Specifically we will prove that there exists a spanning tree of X in which each edge has length not exceeding $\beta/\sqrt{k}$; the desired result follows. First, note that the sides of each of the k rectangles output by Algorithm 1 are at most $\beta/\sqrt{k}$. Suppose that $k > 1$ and let $\tilde{R} \subseteq \square C$ be an intermediate rectangle obtained throughout Algorithm 1, which is further subdivided into intermediate rectangles $\tilde{R}'$ and $\tilde{R}''$ by a (without loss of generality, vertical) line segment s. By the induction hypothesis, the spanning trees of the points in $\tilde{R}'$ and $\tilde{R}''$, i.e. $\mathrm{MST}(X \cap \tilde{R}')$ and $\mathrm{MST}(X \cap \tilde{R}'')$, each consist of edges with length at most $\beta/\sqrt{k}$, and therefore we merely must show that there exists an edge of length at most $\beta/\sqrt{k}$ that connects $X \cap \tilde{R}'$ and $X \cap \tilde{R}''$. To see this, let R_1 and R_2 be the uppermost *final* rectangles that touch the cutting segment s, with center points X_1 and X_2. Since the

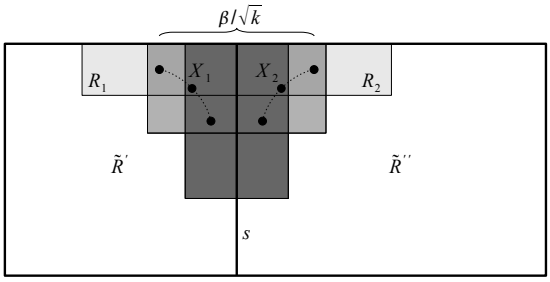

Figure 3.9: The hyperbolic arcs representing the locus of possible locations of X_1 and X_2.

aspect ratios of R_1 and R_2 are at most 3 and both have area $1/k$, the locus of possible locations of X_1 and X_2 are simply hyperbolic arcs, and the maximum possible distance between X_1 and X_2 is $\beta/\sqrt{k}$; see Figure 3.9. This completes the proof. □

We now consider the objective function value $F(X, C)$ when we let X be the output of Algorithm 2, for three particular values of k:

- If $k = 1$, then $\mathrm{MST}(X) = 0$ and therefore

$$F(X, C) \leq \min\{H_1(A, w, h), H_2(A, w/2)\} .$$

- If $k = \lceil w/h \rceil$, then C is divided into $\lceil w/h \rceil$ rectangles with almost-equal dimensions, so $\mathrm{FW}(X, C) \leq \lceil w/h \rceil \cdot H_2\left(\frac{A}{\lceil w/h \rceil}, h/2\right)$ and $\mathrm{MST}(X) = \frac{\lceil w/h \rceil - 1}{\lceil w/h \rceil} w$, and therefore

$$F(X, C) \leq \lceil w/h \rceil \cdot H_2\left(\frac{A}{\lceil w/h \rceil}, h/2\right) + \phi\left(\frac{\lceil w/h \rceil - 1}{\lceil w/h \rceil}\right) w .$$

- If $k = \left\lceil \frac{\alpha}{\phi\beta} \right\rceil$ and $\left\lceil \frac{\alpha}{\phi\beta} \right\rceil \geq \frac{w}{3h}$, then C is divided into $\left\lceil \frac{\alpha}{\phi\beta} \right\rceil$ rectangles with aspect

ratio at most 3, so

$$F(X,C) \leq \alpha/\sqrt{\left\lceil \frac{\alpha}{\phi\beta} \right\rceil} + \phi\beta\sqrt{\left\lceil \frac{\alpha}{\phi\beta} \right\rceil}$$

from Lemma 18.

By analogy with equation (3.9), we define the function $\Phi_{\mathrm{UB}}(A,\phi,h)$ that gives an upper bound of the objective function of Algorithm 4 by

$$\Phi_{\mathrm{UB}}(A,\phi,h) = \begin{cases} \min\left\{ \begin{array}{l} H_1(A,1/h,h), H_2\left(A,\frac{1}{2h}\right), \\ \lceil 1/h^2 \rceil \cdot H_2\left(\frac{A}{\lceil 1/h^2 \rceil}, h/2\right) + \phi\left(\frac{\lceil 1/h^2 \rceil - 1}{h\lceil 1/h^2 \rceil}\right), \\ \frac{\alpha}{\sqrt{\left\lceil \frac{\alpha}{\phi\beta} \right\rceil}} + \phi\beta\sqrt{\left\lceil \frac{\alpha}{\phi\beta} \right\rceil} \end{array} \right\} & \text{if } \left\lceil \frac{\alpha}{\phi\beta} \right\rceil \geq 1/3h^2 \\ \min\left\{ \begin{array}{l} H_1(A,1/h,h), H_2\left(A,\frac{1}{2h}\right), \\ \lceil 1/h^2 \rceil \cdot H_2\left(\frac{A}{\lceil 1/h^2 \rceil}, h/2\right) + \phi\left(\frac{\lceil 1/h^2 \rceil - 1}{h\lceil 1/h^2 \rceil}\right) \end{array} \right\} & \text{otherwise.} \end{cases}$$

3.2.3 Approximation algorithm

In this section we describe our simple algorithm for placing facilities in C so as to (approximately) minimize the objective function (2.1). The input to our algorithm is a convex polygon C and a constant ϕ. The algorithm first evaluates the three possible placement strategies (a single facility, evenly distributed facilities along the longer dimension of the polygon, general positions of facilities, see Figure 3.10) based on the problem input, and then output the one with the best performance. Algorithm 2 is called for the general position case. This is formally described in Algorithm 4.

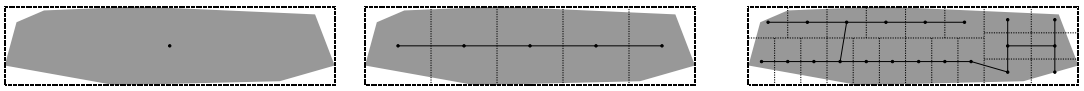

(a) $k = 1$ (b) $k = \lceil w/h \rceil = 5$ (c) $k = \left\lceil \frac{\alpha}{\phi\beta} \right\rceil = 21$

Figure 3.10: The three candidate outputs of Algorithm 4, with spanning trees shown. For visual clarity, the Voronoi diagrams of the point sets have been omitted and instead we show the rectangular partition from Algorithm 1 that led to their placement.

Input: A convex polygon C with area $A \in [1/2, 1]$ contained in a minimum bounding box of dimensions $(\text{diam}(C) = 1/h = w) \times h$ and a positive scalar ϕ.

Output: The locations of a finite set of points X in C that approximately minimize $\text{FW}(X, C) + \phi\,\text{MST}(X)$ within a factor of 3.21.

Let $\alpha := H_1\left(A, \sqrt{3}, 1/\sqrt{3}\right)$ and $\beta := \sqrt{3}$;

if $\left\lceil \frac{\alpha}{\phi\beta} \right\rceil < \frac{w}{3h}$ **then**

`/* This only occurs when the input shape is very long and thin, and` ϕ `is large. */`

Let $v_1 := \min\{H_1(A, w, h), H_2(A, w/2)\}$ and $v_2 := \lceil w/h \rceil \cdot H_2\left(\frac{A}{\lceil w/h \rceil}, h/2\right) + \phi\left(\frac{\lceil w/h \rceil - 1}{\lceil w/h \rceil}\right)$;

if $v_1 < v_2$ **then**

Set $k := 1$;

else

Set $k := \lceil w/h \rceil$;

end

else

Let $v_1 := \min\{H_1(A, w, h), H_2(A, w/2)\}$, $v_2 := \lceil w/h \rceil \cdot H_2\left(\frac{A}{\lceil w/h \rceil}, h/2\right) + \phi\left(\frac{\lceil w/h \rceil - 1}{\lceil w/h \rceil}\right)$, and $v_3 := \alpha/\sqrt{\left\lceil \frac{\alpha}{\phi\beta} \right\rceil} + \beta\sqrt{\left\lceil \frac{\alpha}{\phi\beta} \right\rceil}$;

switch $\min\{v_1, v_2, v_3\}$ **do**

case v_1 Set $k := 1$;

case v_2 Set $k := \lceil w/h \rceil$;

case v_3 Set $k = \left\lceil \frac{\alpha}{\phi\beta} \right\rceil$;

endsw

end

return *ApproxFW*(C, k);

Algorithm 3: Algorithm FacilityPlacement (C, ϕ) takes as input a convex polygon C and a positive scalar ϕ.

3.2.4 Approximation bounds for Algorithm 4

In this section we will prove that $\Phi_{\mathrm{UB}}(A,\phi,h)/\Phi_{\mathrm{LB}}(A,\phi,h)$ is bounded above by 3.21 on the problem domain $\mathcal{D}$, defined by $\mathcal{D} := (A,h,\phi) \in [1/2,1]\times(0,1]\times(0,\infty)$. In order to make this domain bounded, we first observe that if $\phi > \frac{16}{9\pi}$, then our lower bounding function is

$$\Phi_{\mathrm{LB}}(A,\phi,h) = \max\left\{\frac{2A^{3/2}}{3\sqrt{\pi}}, \frac{A^2}{4h}\right\} = \begin{cases} \frac{A^2}{4h} & \text{if } h < \frac{3}{8}\sqrt{\pi A} \\ \frac{2A^{3/2}}{3\sqrt{\pi}} & \text{otherwise.} \end{cases}$$

which does not depend on ϕ. It is easy to verify that the approximately optimal solution is to use a single facility, in which case our approximation ratio is simply

$$\frac{\min\left\{H_1(A,1/h,h), H_2(A,1/2h)\right\}}{\max\left\{\frac{2A^{3/2}}{3\sqrt{\pi}}, \frac{A^2}{4h}\right\}}.$$

As it turns out, the second upper bound is not even necessary and merely using $H_1(A,1/h,h)$ suffices. It is straightforward to verify that the above ratio is always at most 3 using a simple case-by-case analysis.

We can thus restrict our attention to the bounded domain $\mathcal{D} := (A,h,\phi) \in [1/2,1]\times(0,1]\times(0,16/9\pi]$, on which we want to show that $\Phi_{\mathrm{UB}}(\cdot)/\Phi_{\mathrm{LB}}(\cdot) < 3.21$ everywhere. Our strategy will be to divide $\mathcal{D}$ into 6 subdomains as illustrated in Figure 3.11. We will explicitly deal with the limiting cases where $h \to 0$ and $\phi \to 0$ in subdomains I through V, and then handle subdomain VI using a branch-and-bound algorithm.

Subdomain I We will use a lower bound of $A^2/4h$ and an upper bound of $H_1(A,1/h,h)$.

We have already addressed this case.

Subdomain II We will use a lower bound of $\phi(A-\phi)/h$ and an upper bound of

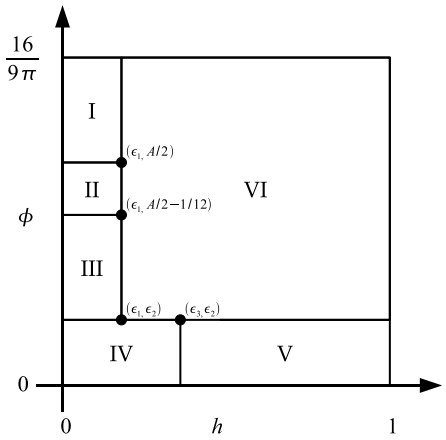

Figure 3.11: The domain $\mathcal{D}$, for $A \in [0.5, 1]$ and the subdomains I through VI (not to scale), with $\epsilon_1, \epsilon_2, \epsilon_3 = 0.001, 0.0002, 0.1$.

$H_1(A, 1/h, h)$. The quantity

$$\frac{H_1(A, 1/h, h)}{\phi(A - \phi)/h}$$

is maximized on this subdomain at $\phi = A/2 - 1/12$, and thus our approximation ratio is

$$F(X, C) \leq \frac{144}{36A^2 - 1} \cdot \begin{cases} a_0 + (a_1 A - a_2) h^2 & \\ -a_3 (1 - A) \sqrt{1 - h^4} & \\ -a_4 h^4 & \text{if } A \leq 1 - \frac{h}{2}\sqrt{1/h^2 - h^2} \\ -b_0 A^2 + b_1 A - b_2 & \\ +(b_3 A - b_4) h^2 & \text{if } 1 - \frac{h}{2}\sqrt{1/h^2 - h^2} < A \leq 1 - \frac{h^2}{2} \\ -c_0 A^2 + c_1 A + c_2 & \\ +(c_3 A - c_4) h^2 + c_5 h^4 & \text{otherwise .} \end{cases}$$

which is bounded above by 3.01 for $A \in [0.5, 1]$ and $h \in [0, \epsilon_1]$.

Subdomain III We will use a lower bound of $\phi\left(A-\phi\right)/h$ and an upper bound of

$$\begin{aligned}\left\lceil\frac{w}{h}\right\rceil\cdot H_2\left(\frac{A}{\lceil w/h\rceil},\frac{h}{2}\right)+\phi\left(\frac{\lceil w/h\rceil-1}{\lceil w/h\rceil}\right)w &= \left\lceil\frac{1}{h^2}\right\rceil\cdot H_2\left(\frac{A}{\lceil 1/h^2\rceil},\frac{h}{2}\right)\\ &\quad+\phi\left(\frac{\lceil 1/h^2\rceil-1}{\lceil 1/h^2\rceil}\right)/h\\ &\leq \left(\frac{1+h^2}{h^2}\right)\cdot H_2\left(Ah^2,\frac{h}{2}\right)+\frac{\phi}{h}\end{aligned}$$

and thus our approximation ratio is

$$\begin{aligned}\frac{\left(\frac{1+h^2}{h^2}\right)\cdot H_2\left(Ah^2,h/2\right)+\phi/h}{\phi\left(A-\phi\right)/h} &= \frac{\left(\frac{1}{h}+h\right)\cdot H_2\left(Ah^2,h/2\right)+\phi}{\phi\left(A-\phi\right)}\\ &= \frac{\left(\frac{1}{h}+h\right)\cdot H_2\left(Ah^2,h/2\right)}{\phi\left(A-\phi\right)}+\frac{1}{\left(A-\phi\right)}\\ &\leq \frac{\left(\frac{1}{h}+h\right)\cdot H_2\left(Ah^2,h/2\right)}{\epsilon_2\left(A-\epsilon_2\right)}+\frac{1}{A/2+1/12}\\ &\leq \frac{\frac{\sqrt{2}}{3}A-\frac{\sqrt{2}-1}{6}A^2}{0.0000996}\left(h^4+h^2\right)+3\\ &\leq 3.005\,.\end{aligned}$$

Subdomain IV It is easy to see that, since $\phi\leq\epsilon_2$ on this domain, we know that

$$\alpha/\sqrt{\left\lceil\frac{\alpha}{\phi\beta}\right\rceil}+\beta\sqrt{\left\lceil\frac{\alpha}{\phi\beta}\right\rceil}\leq 2c\sqrt{\alpha/\phi\beta}$$

where $c=\frac{101}{100}$ and

$$\lceil 1/h^2\rceil\cdot H_2\left(\frac{A}{\lceil 1/h^2\rceil},h/2\right)+\phi\left(\frac{\lceil 1/h^2\rceil-1}{\lceil 1/h^2\rceil}\right)\leq c\left[\left(\frac{\sqrt{2}}{3}A-\frac{\sqrt{2}-1}{6}A^2\right)h+\phi/h\right]$$

since $h \leq \epsilon_3$. We will therefore use an upper bound of

$$\begin{cases} 2c\sqrt{\alpha\phi\beta} & \text{if } \phi \leq \frac{3\alpha}{\beta}h^2 \\ c\left[\left(\frac{\sqrt{2}}{3}A - \frac{\sqrt{2}-1}{6}A^2h^2\right) + \phi\right] & \text{otherwise} \end{cases}$$

and a lower bound of

$$\begin{cases} A - \frac{3}{8}\sqrt{\pi\phi A} & \text{if } \phi \leq \frac{3\alpha}{\beta}h^2 \\ \phi\left(A-\phi\right)/h & \text{otherwise.} \end{cases}$$

If $\phi \geq \frac{3\alpha}{\beta}h^2$ then the ratio is

$$\frac{2c\sqrt{\alpha\phi\beta}}{A - \frac{3}{8}\sqrt{\pi\phi A}}$$

which is increasing in ϕ and is therefore maximized at $\phi = \frac{3\alpha}{\beta}h^2$. The resulting function is bounded above by 3.18 for $A \in [0.5, 1]$. If $\phi > \frac{3\alpha}{\beta}h^2$ then the ratio is

$$\frac{c\left[\left(\frac{\sqrt{2}}{3}A - \frac{\sqrt{2}-1}{6}A^2\right)h^2 + \phi\right]}{\phi\left(A-\phi\right)}$$

which is increasing in h and is thus maximized by increasing h until $\phi = \frac{3\alpha}{\beta}h^2$. The ratio is equal to

$$\frac{c\left[\left(\frac{\sqrt{2}}{3}A - \frac{\sqrt{2}-1}{6}A^2\right)\frac{\beta\phi}{3\alpha} + \phi\right]}{\phi\left(A-\phi\right)} = \frac{c\left[\left(\frac{\sqrt{2}}{3}A - \frac{\sqrt{2}-1}{6}A^2\right)\frac{\beta}{3\alpha} + 1\right]}{\left(A-\phi\right)}$$

which is increasing in ϕ; setting $\phi = \epsilon_2$ the resulting expression is bounded above by 3 for $A \in [0.5, 1]$.

Subdomain V It is easy to see that $\frac{\alpha}{\phi\beta} \geq \frac{1}{3h^2}$ everywhere on this subdomain, and therefore a valid upper bound is $2c\sqrt{\alpha\phi\beta}$, where $c = \frac{101}{100}$ as before. We will use a

lower bound of $A\sqrt{\phi} - \frac{3\phi\sqrt{\pi A}}{8}$ and conclude that the ratio is

$$\frac{2c\sqrt{a\phi\beta}}{A\sqrt{\phi} - \frac{3\phi\sqrt{\pi A}}{8}}$$

which is increasing in ϕ and is therefore maximized at $\phi = \epsilon_2$. The resulting function in A is bounded above by 3 for $A \in [0.5, 1]$.

Subdomain VI Since $h > 0$ and $\phi > 0$ on this subdomain, we do not have to concern ourselves with any limiting cases and can prove that our approximation ratio is bounded above by 3.21 by performing a branch-and-bound search on this entire region.

We have therefore shown that our algorithm produces a placement of facilities that is always within a constant factor 3.21 of optimality.

Chapter 4

Continuous connected facility location problem: various backbone networks

4.1 Introduction

In this chapter, we generalize our model in (2.1) in two aspects. First, we introduce a *fixed cost* that is incurred by each facility itself and is independent of the location of the facilities. This generally includes any cost from installing, operating and maintaining the facilities. Second, we generalize the backbone network to various different network topologies. The generalized problem is stated as the follows. We consider the problem of selecting the optimal locations of a set of facilitis $X = \{x_1, \ldots, x_k\}$ in a planar Euclidean region R where the demands are continuously and uniformly distributed in the region; specifically, our optimization problem is given by

$$\underset{X}{\text{minimize}}\, \text{Fix}(|X|) + \phi\, \text{BBN}(X) + \psi\, \text{FW}(X, R) \tag{4.1}$$

where ϕ and ψ are given scalar parameters. Here the term $\text{Fix}(|X|) = \text{Fix}(k)$ represents the fixed costs and depends only on the number of elements of X, i.e. k (which is a decision variable), and not their geographic locations. The term $\phi\,\text{BBN}(X)$ represents the cost of the backbone network of the points X, which may be a Euclidean Steiner or minimum spanning tree(MST), a traveling salesman (TSP) tour, a star network(SN), a collection of capacitated vehicle routing(VRP) tours, a complete bipartite graph(CBG), or a complete graph(CG) on the points X. These three costs are illustrated in Figure 4.1, which shows the seven backbone network structures of interest and the Voronoi partition of the service region.

4.1.1 Backbone network topologies

Before proceeding further, it may be useful to briefly give some context to the seven backbone network topologies that we study in this chapter.

Steiner trees, MSTs, and TSPs The Steiner tree, minimum spanning tree, and traveling salesman tour are all *sub additive Euclidean functionals* ([35], [40]) whose lengths in a bounded region increase at a rate proportional to $\sqrt{k}$ in the worst case (here $k = |X|$ represents the number of facilities we place). It is well-known [44] that the lengths of these configurations are always within a constant factor of each other; specifically, in Euclidean space, we have

$$Steiner(X) \leq MST(X) \leq TSP(X) \leq 2Steiner(X).$$

Star networks The discrete case of problem (4.1) with a star network SN(X) as a backbone structure is known as a "star-star" hub location problem [23] (because we have a star network that connects hubs together as well as small-scale star networks that connect the hubs to end demands), which is commonly encountered in communication

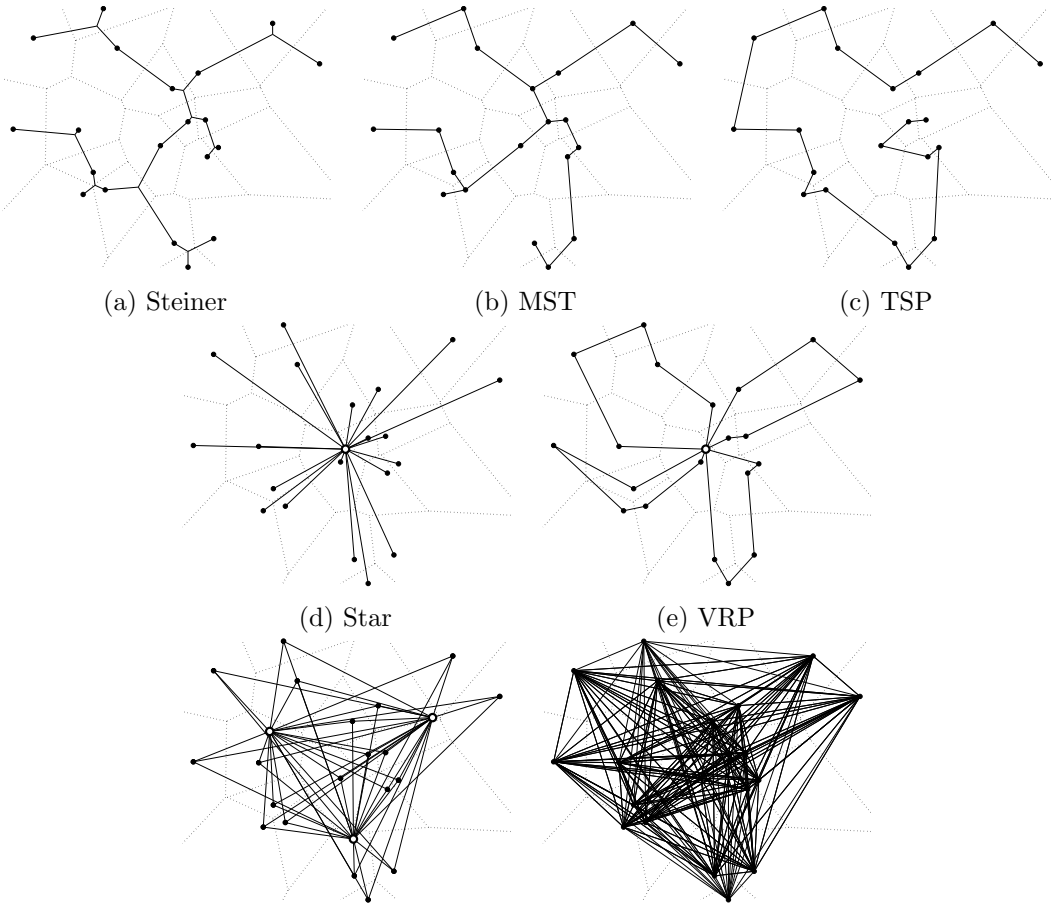

(a) Steiner (b) MST (c) TSP

(d) Star (e) VRP

(f) Complete bipartite graph (g) Complete graph

Figure 4.1: The seven backbone network structures considered in this chapter for a fixed point set X, together with the induced Voronoi partition.

network design ([32], [45])and satellite allocation [19]. Section 5.3.5 of the monograph [11] explains that such a network also occurs in air transportation of valuable goods because "the cost (and delay) of a stop is large compared with that of the moving portion of the trip." In the worst case, the length of the star network in a bounded region R increases at a rate proportional to k. In this chapter, unless otherwise stated, we will assume that the root node of SN(X) is the geometric median of X, which we write as $\bar{x}$ (this allows us to treat the points of X homogeneously, i.e. to not identify a distinct "root node" and treat it separately from the others).

VRP tours A VRP tour of the points X is a generalization of the TSP tour in which vehicles departs from a central depot and visit the points X. The vehicle, however, is now *capacitated*: it can only visit a given number of stops κ before it is required to return to the depot. We therefore see that the TSP tour and the star network are special cases of the VRP tour in which $\kappa = \infty$ and $\kappa = 1$ respectively. Such a distribution model is canonical in a wide variety of contexts for modeling "one-to-many" relationships; see for example Chapter 4 of [11].

Complete bipartite graphs The complete bipartite graph is a "many-to-many" backbone structure that arises when our facilities X are interconnected with a second set of facilities Y. This might arise in a supply chain in which each facility $y_j \in Y$ produces a specific component that is used to construct a product at each facility x_i. Since components from *each* facility y_j are needed to construct the product, we must therefore connect each facility $y_j \in Y$ to each facility $x_i \in X$. Distribution networks of this type are sometimes referred to as *point-to-point* networks [36]. In the worst case, the length of a complete bipartite graph in a bounded region R increases at a rate proportional to $k_1 k_2$, where $k_1 = |X|$ and $k_2 = |Y|$.

Complete graphs The *complete graph* CG(X) is the most frequently used backbone structure in hub location problems [6] and is commonly encountered in airline network

design [21], freight delivery [30], and urban transportation [29]. In the worst case, the length of the complete graph in a bounded region R increases at a rate proportional to k^2.

4.2 Asymptotic analysis

4.2.1 Special cases of (4.1)

In this section, we will examine the optimal solutions to certain special cases of problem (4.1). Before doing anything else, we find it useful to state a classical result of continuous location theory proven in [17], as well as an immediate corollary thereof:

Theorem 19. *If R is a bounded region in the plane with area (i.e. Lebesgue measure) A, then*

$$\inf_{X:|X|=k} FW(X,R) \sim \frac{\alpha_1 A^{3/2}}{\sqrt{k}}$$

as $k \to \infty$, where $X = \{x_1, \ldots, x_k$ denotes a finite subset of $\Re^2$ and α_1 is the Fermat-Weber value of a regular hexagon with unit area:

$$\alpha_1 = FW(Hexagon) = \frac{3^{3/4}(4 + 3\log 3)\sqrt{6}}{108} \approx 0.37721.$$

Theorem 19 says that, for sufficiently large point sets X, the optimal configuration that minimizes FW(X,R) is always a regular hexagonal lattice, i.e. the *honeycomb heuristic*. The paper [17] actually generalizes Theorem 19 to a more versatile setting in which, rather than minimizing the quantity

$$\mathrm{FW}(X,R) = \iint_R \min_i \{||x - x_i||\}\, dA\,,$$

we are interested in the general form

$$\mathrm{FW}_f(X,R) := \iint_R \min_i \{f(||x - x_i||)\}\, dA\,,$$

where $f(\cdot) : [0,\infty) \to [0,\infty)$ is a monotonically increasing function:

Theorem 20. *If R is a bounded region in the plane with area (i.e. Lebesgue measure) A, and $f(\cdot) : [0,\infty) \to [0,\infty)$ is a monotonically increasing function, then*

$$\inf_{X:|X|=k} \mathrm{FW}_f(X,R) \sim k \cdot \mathrm{FW}_f(\mathrm{Hex}(A/k))$$

as $k \to \infty$, where $X = \{x_1, \ldots, x_k\}$ denotes a finite subset of $\mathbb{R}^2$, $\mathrm{Hex}(A/k)$ denotes a regular hexagon of area A/k, and

$$\mathrm{FW}_f(\mathrm{Hex}(A/k)) := \iint_{\mathrm{Hex}(A/k)} f(\|x - x_0\|)\, dA$$

where x_0 is the centroid of the hexagon in question.

Simply put, Theorem 20 says that the honeycomb heuristic is an asymptotically optimal configuration whenever our objective is to minimize any monotonically increasing *function* of the distances from the landmark points x_i to the region R.

The case $\phi = 0$: the honeycomb heuristic

Before studying our problem (4.1) for various forms of $\mathrm{BBN}(\cdot)$, we remark that it is obvious that the solution to (4.1) when backbone network costs are ignored, i.e.

$$\underset{X}{\text{minimize}}\ \mathrm{Fix}(|X|) + \psi\, \mathrm{FW}(X,R)\,, \tag{4.2}$$

is the honeycomb heuristic (Figure 4.2a). In particular, provided the optimal number of points X to place is sufficiently large, we can apply Theorem 19 to obtain a nearly optimal solution by minimizing the expression

$$\mathrm{Fix}(k) + \frac{\psi\alpha_1}{\sqrt{k}} \tag{4.3}$$

over k.

The case $\mathrm{Fix}(\cdot) = 0$ **and** $\mathrm{BBN}(\cdot) \in \{\mathrm{Steiner}(\cdot), \mathrm{MST}(\cdot), \mathrm{TSP}(\cdot)\}$**: the Archimedes heuristic**

If $\mathrm{Fix}(k) = 0$ for all k, then we do not incur any penalty for placing hubs in the region if they do not lengthen the backbone network.

Thus, when $\mathrm{BBN}(\cdot) \in \{\mathrm{Steiner}(\cdot), \mathrm{MST}(\cdot), \mathrm{TSP}(\cdot)\}$, our optimal configuration will be to place infinitely many hubs along the backbone network. Using Theorem 14, we can determine a lower bound for the problem

$$\underset{X}{\text{minimize}}\, \phi\,\mathrm{BBN}(X) + \psi\,\mathrm{FW}(X, R) \tag{4.4}$$

via

$$\min_{\ell} \phi\ell + \psi\frac{2A^2}{8\ell + 3\sqrt{\pi A}} \sim A\sqrt{\phi\psi}$$

provided that the ratio ψ/ϕ is sufficiently large (this ensures that the optimal ℓ^* is long enough that the boundary of R does not contribute significantly to the objective function and that $8\ell^* \gg 3\sqrt{\pi A}$). We conclude by observing that if we configure an infinite number of hubs X on an Archimedean spiral of the form $r = a\theta$ in polar coordinates, where $a = \sqrt{\phi/\psi}/\pi$, then for a sufficiently large ratio ψ/ϕ we have $\phi\,\mathrm{BBN}(X) + \psi\,\mathrm{FW}(X, R) \sim A\sqrt{\phi\psi}$, thus proving that the Archimedes heuristic is an

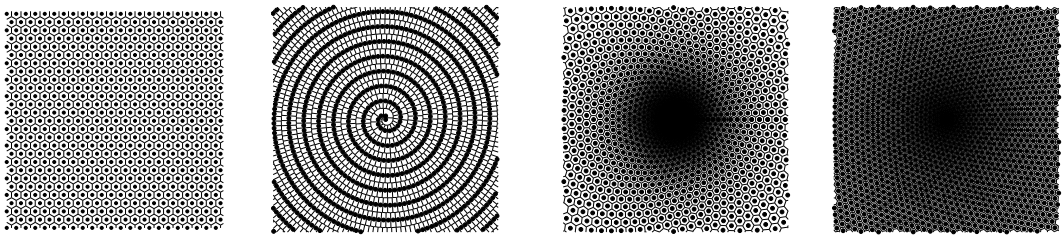

(a) Honeycomb (b) Archimedes (c) "Contracted honeycomb" (d) "Less contracted honeycomb"

Figure 4.2: Optimal configurations for the four special instances of (4.1) described throughout Section 4.2.1 and their Voronoi diagrams.

optimal configuration for minimizing (4.4) when we use a Steiner tree, MST, or TSP tour of X as a backbone network. This configuration is shown in Figure 4.2b.

The case $\mathrm{Fix}(\cdot) = 0$ **and** $\mathrm{BBN}(\cdot) = \mathrm{SN}(\cdot)$**: the "contracted honeycomb"**

We next consider the case where (4.1) takes the form

$$\underset{X}{\text{minimize}}\, \phi\, \mathrm{SN}(X) + \psi\, \mathrm{FW}(X, R)\,. \tag{4.5}$$

Suppose without loss of generality that the center of the star network $\bar{x}$ is the origin, and that we divide R into N cells $\square_i$ of size $\epsilon = A/N$. Let $d_i = \min_{x \in \square_i} \|x\|$ and let the variable $k_i = |X \cap \square_i|$ denote the number of points in $\square_i$ (so that $k = \sum_{i=1}^{N} k_i$). Consider a particular cell $\square_i$: provided that k_i is large, Theorem 19 says that

$$\min_{X_i : |X_i| = k_i} \mathrm{FW}(X_i, \square_i) \sim \frac{\alpha_1 \epsilon^{3/2}}{\sqrt{k_i}}\,.$$

We therefore find that, as k becomes large, a lower bound of (4.5) is given by

$$\underset{(k_1,\ldots,k_N)}{\text{minimize}}\, \phi \underbrace{\sum_{i=1}^{N} d_i k_i}_{\leq \mathrm{SN}(X)} + \psi \underbrace{\alpha_1 \epsilon^{3/2} \sum_{i=1}^{N} \frac{1}{\sqrt{k_i}}}_{\leq \mathrm{FW}(X,R)}\,.$$

The above problem is convex in $(k_1, \ldots, k_N)$. Setting first derivatives to zero, we find that for each i we must have

$$\phi d_i = \frac{1}{2} \cdot \frac{\psi \alpha_1 \epsilon^{3/2}}{k_i^{3/2}} \,.$$

Introducing a variable $f_i := {}^{k_i}/_{\epsilon k}$, the above can equivalently be written as

$$f_i = (\alpha_1/2)^{2/3} \cdot \frac{(\psi/\phi)^{2/3}}{d_i^{2/3} k}$$

which is simply a finite discretization of the expression

$$f(x) = (\alpha_1/2)^{2/3} \cdot \frac{(\psi/\phi)^{2/3}}{\|x\|^{2/3} k}$$

where $f(x)$ describes the "density" of the points X. Introducing $c = (\alpha_1/2)^{2/3}(\psi/\phi)^{2/3}/k$, the above can equivalently be written as

$$f(x) = c\|x\|^{-2/3} \,.$$

This tells us that as k becomes large, the optimal X that minimizes (4.5) is a "contracted honeycomb" configuration: we define $c = \left(\iint_R \|x\|^{-2/3}\, dA\right)^{-1}$, and then place a total of $k = (\alpha_1/2)^{2/3}(\psi/\phi)^{2/3}/c$ points in R in a honeycomb configuration that follows the distribution $f(x) = c\|x\|^{-2/3}$ on R. This configuration is shown in Figure 4.2c. Note that the optimal number of points k is proportional to $(\psi/\phi)^{2/3}$, the backbone network cost is

$$\phi \sum_{i=1}^{N} d_i k_i \sim \left(\frac{\alpha_1}{2}\right)^{2/3} \left(\iint_R \|x\|^{1/3}\, dA\right) \phi^{1/3} \psi^{2/3} \,, \tag{4.6}$$

and the coverage cost is

$$\psi \alpha_1 \epsilon^{3/2} \sum_{i=1}^{N} \frac{1}{\sqrt{k_i}} \sim \left(2^{1/3} \alpha_1^{2/3}\right) \left(\iint_R ||x||^{1/3}\, dA\right) \phi^{1/3} \psi^{2/3} \,.$$

If we assume that the shape of R is fixed, we see that $\iint_R \|x\|^{1/3}\, dA \propto A^{7/6}$, so that the optimal objective function value is proportional to $A^{7/6}\phi^{1/3}\psi^{2/3}$. It is also worth noting that the density of points X decays proportionally to $||x||^{-2/3}$, or equivalently, that the area of the sub-region assigned to hub point x_i (i.e. the Voronoi cell) is proportional to $||x||^{2/3}$.

The case $\mathrm{Fix}(\cdot) = 0$ **and** $\mathrm{BBN}(\cdot) = \mathrm{VRP}(\cdot)$

A *VRP tour* of the points X is a generalization of the TSP tour in which vehicles depart from a central depot $\bar{x}$ (which we will again assume to be the origin) and visit the points X. The vehicle, however, is now *capacitated*: it can only visit a given number of stops κ before it is required to return to the depot. We therefore see that the TSP tour and the Star network are special cases of the VRP tour in which $\kappa = \infty$ and $\kappa = 1$ respectively. We will consider here the case where (4.1) takes the form

$$\underset{X}{\text{minimize}}\, \phi\, \mathrm{VRP}(X) + \psi\, \mathrm{FW}(X, R)\,. \tag{4.7}$$

The following bounds are due to [18]: for any point set X, we have

$$\mathrm{VRP}(X) \geq \max\left\{ \mathrm{TSP}(X), \frac{2}{\kappa}\, \mathrm{SN}(X) \right\}.$$

The fact that $\mathrm{VRP}(X) \geq \mathrm{TSP}(X)$ allows us to immediately conclude (owing to the result of Section 4.2.1) that a valid lower bound of (4.7) is $A\sqrt{\phi\psi}$. Similarly, the fact that $\mathrm{VRP}(X) \geq {}^{2}/_{\kappa}\, \mathrm{SN}(X)$ allows us to conclude (owing to the result of Section 4.2.1) that another valid lower bound of (4.7) is

$$\underbrace{\left(2^{2/3} + 2^{-1/3}\right) \alpha_1 \left(\iint_R \|x\|^{1/3}\, dA \right)}_{=:cA^{7/6}} \left(\frac{\phi}{\kappa}\right)^{1/3} \psi^{2/3}\,.$$

Some simple algebra shows that the two lower bounds are equal when $\kappa = c^3\sqrt{A\psi/\phi}$. Moreover, as κ becomes small relative to $c^3\sqrt{A\psi/\phi}$, we find that $\mathrm{VRP}(X) \sim {}^2\!/\!_\kappa\,\mathrm{SN}(X)$, and as κ becomes large relative to $c^3\sqrt{A\psi/\phi}$, we find that $\mathrm{VRP}(X) \sim \mathrm{TSP}(X)$. Thus, when $\kappa \ll c^3\sqrt{A\psi/\phi}$, we find that a "contracted honeycomb" configuration becomes optimal (i.e. treating our problem as that of Section 4.2.1, making the substitution $\phi \mapsto {}^2\!/\!_\kappa \cdot \phi$), and when $\kappa \gg c^3\sqrt{A\psi/\phi}$, the Archimedes heuristic becomes optimal (with the same coefficients ϕ and ψ).

The case $\mathrm{Fix}(\cdot) = 0$ **and** $\mathrm{BBN}(\cdot) = \mathrm{CBG}(\cdot)$

When the backbone network is a complete bipartite graph, we have an additional set of hub nodes Y and our problem takes the form

$$\underset{X}{\text{minimize}}\; \phi\,\mathrm{CBG}(X, Y) + \psi\,\mathrm{FW}(X, R) \tag{4.8}$$

where we have

$$\mathrm{CBG}(X, Y) = \sum_{i=1}^{|X|}\sum_{j=1}^{|Y|} \|x_i - y_j\|\,.$$

Note that in (4.8) we are only treating X as an optimization variable and assuming that Y is exogenous. This is because, if Y were an optimization variable as well, the optimal solution to (4.8) would be to set $Y = \emptyset$, thus incurring no backbone network costs whatseover. When Y is given and fixed, we simply have a generalization of problem (4.5) in which we define

$$c = \left[\iint_R \left(\sum_{j=1}^{|Y|} \|x - y_j\|\right)^{-2/3} dA\right]^{-1}$$

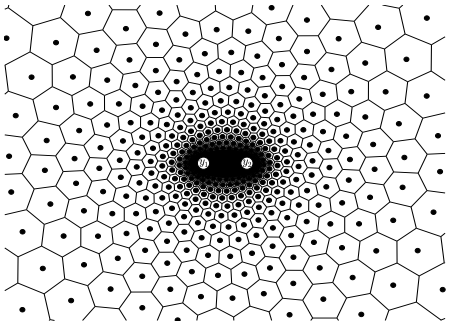

Figure 4.3: A contracted honeycomb configuration derived for a complete bipartite graph with $|Y| = 2$.

and then place a total of $k = (\alpha_1/2)^{2/3}(\psi/\phi)^{2/3}/c$ points in R in a honeycomb configuration that follows the distribution

$$f(x) = c\left(\sum_{j=1}^{|Y|} \|x - y_j\|\right)^{-2/3}$$

on R. The optimal objective function value is again proportional to $A^{7/6}\phi^{1/3}\psi^{2/3}$. Figure 4.3 shows a picture of this configuration for the case where $|Y| = 2$.

The case $\mathrm{Fix}(\cdot) = 0$ and $\mathrm{BBN}(\cdot) = \mathrm{CG}(\cdot)$: the "less contracted honeycomb"

When (4.1) takes the form

$$\underset{X}{\text{minimize}}\, \phi\,\mathrm{CG}(X) + \psi\,\mathrm{FW}(X, R)\,, \tag{4.9}$$

it is difficult to determine a closed-form solution for the optimal configuration of the hubs X as in the previous examples, although it is straightforward to find a solution whose objective value is guaranteed to fall within $2^{1/5} - 1 \approx 15\%$ of the optimum. Our argument proceeds as follows: let $\bar{x}$ denote the geometric median of X. By definition,

we have

$$\sum_{j=1}^{k} \|\bar{x} - x_j\| \leq \sum_{j=1}^{k} \|x - x_j\| \quad \forall x \in R$$

and so in particular, for any point $x_i \in X$, we have $\sum_{j=1}^{k} \|\bar{x} - x_j\| \leq \sum_{j=1}^{k} \|x_i - x_j\|$. It follows that

$$\mathrm{CG}(X) = \frac{1}{2} \sum_{i=1}^{k} \sum_{j=1}^{k} \|x_i - x_j\| \geq \frac{1}{2} \sum_{i=1}^{k} \sum_{j=1}^{k} \|\bar{x} - x_j\| = \frac{k}{2} \sum_{j=1}^{k} \|\bar{x} - x_j\| = \frac{k}{2} \mathrm{SN}(X)\,.$$

However, by the triangle inequality, it also holds that

$$\mathrm{CG}(X) \leq \frac{1}{2} \sum_{i=1}^{k} \sum_{j=1}^{k} \|x_i - \bar{x}\| + \|\bar{x} - x_j\| = k\,\mathrm{SN}(X)$$

so that $k/2 \cdot \mathrm{SN}(X) \leq \mathrm{CG}(X) \leq k \cdot \mathrm{SN}(X)$. Thus, it will suffice to consider the problem

$$\underset{X}{\text{minimize}}\; \phi k\,\mathrm{SN}(X) + \psi\,\mathrm{FW}(X, R)\,. \tag{4.10}$$

Treating this problem in precisely the same manner as Section 4.2.1, and assuming that $\bar{x}$ is the origin, we find that the optimal "density" of the points that minimizes (4.10) is given by

$$\phi k^{5/2} \left(\|x\| + \iint_R \|x\| f(x)\, dA \right) = \frac{1}{2} \cdot \frac{\psi \alpha_1}{f(x)^{3/2}}$$

i.e.

$$f(x) \;=\; (\alpha_1/2)^{-2/3} \left(\psi k^{-5/2} / \phi \right)^{2/3} \left(\|x\| + \iint_R \|x\| f(x)\, dA \right)^{-2/3}.$$

$$f(x) = k^{-5/3} (\alpha_1/2)^{-2/3} \left(\psi/\phi \right)^{2/3} \left(\|x\| + \iint_R \|x\| f(x)\, dA \right)^{-2/3}.$$

Finally, introducing c such that $k = \frac{\psi^{2/5}}{c^{3/5}\phi^{2/5}}$, we can write

$$\begin{aligned} f(x) &= c(\alpha_1/2)^{-2/3}\left(\|x\| + \iint_R \|x\| f(x)\, dA\right)^{-2/3} \\ &= (\alpha_1/2)^{-2/3}\left(\underbrace{c^{-3/2}}_{c'}\|x\| + \underbrace{c^{-3/2}\iint_R \|x\| f(x)\, dA}_{c''}\right)^{-2/3} \\ &= (\alpha_1/2)^{-2/3}\left(c'\|x\| + c''\right)^{-2/3} \end{aligned} \tag{4.11}$$

so that we merely need to find constants c' and c'' such that

$$(\alpha_1/2)^{-2/3}\iint_R \left(c'\|x\| + c''\right)^{-2/3} dA = 1 \tag{4.12}$$

$$(\alpha_1/2)^{-2/3}\iint_R \|x\|\left(c'\|x\| + c''\right)^{-2/3} dA = c''. \tag{4.13}$$

It is easy to verify that such constants c' and c'' always exist using a simple monotonicity argument (although they depend on the region R). We thus find that the approximately optimal solution to (4.9) is to distribute a total of $k = \frac{\psi^{2/5}}{c^{3/5}\phi^{2/5}}$ hub points in a honeycomb lattice that follows the distribution $f(x) = (\alpha_1/2)^{-2/3}(c'\|x\| + c'')^{-2/3}$ for appropriate constants c, c' and c''. This configuration is shown in Figure 4.2d.

To conclude this section, we note that the optimal number of points k is proportional to $(\psi/\phi)^{2/5}$, the backbone network cost approaches

$$\phi k \sum_{i=1}^{N} d_i k_i \to \frac{(\alpha_1/2)^{-2/3}}{c^{6/5}}\left[\iint_R ||x||\left(c'\|x\| + c''\right)^{-2/3} dA\right]\phi^{1/5}\psi^{4/5}, \tag{4.14}$$

and the coverage cost approaches

$$\psi\alpha_1\epsilon^{3/2}\sum_{i=1}^{N}\frac{1}{\sqrt{k_i}} \to \left[2^{-1/3}\alpha_1 c^{3/10}\iint_R \left(c'\|x\| + c''\right)^{1/3} dA\right]\phi^{1/5}\psi^{4/5}.$$

Objective function	Optimal configuration	Optimal objective value
$\mathrm{Fix}(\lvert X\rvert) + \psi\,\mathrm{FW}(X, R)$	Honeycomb	Depends on $\mathrm{Fix}(\cdot)$
$\phi\,\mathrm{Steiner}(X) + \psi\,\mathrm{FW}(X, R)$	Archimedes	$\mathcal{O}(A\sqrt{\phi\psi})$
$\phi\,\mathrm{MST}(X) + \psi\,\mathrm{FW}(X, R)$	Archimedes	$\mathcal{O}(A\sqrt{\phi\psi})$
$\phi\,\mathrm{TSP}(X) + \psi\,\mathrm{FW}(X, R)$	Archimedes	$\mathcal{O}(A\sqrt{\phi\psi})$
$\phi\,\mathrm{SN}(X) + \psi\,\mathrm{FW}(X, R)$	Contracted honeycomb	$\mathcal{O}\left(A^{7/6}\phi^{1/3}\psi^{2/3}\right)$
$\phi\,\mathrm{VRP}(X) + \psi\,\mathrm{FW}(X, R)$	$\kappa \ll c^3\sqrt{A\psi/\phi}$: Contracted honeycomb $\kappa \gg c^3\sqrt{A\psi/\phi}$: Archimedes	$\mathcal{O}(A^{7/6}\phi^{1/3}\psi^{2/3}/\kappa^{1/3})$ $\mathcal{O}(A\sqrt{\phi\psi})$
$\phi\,\mathrm{CG}(X) + \psi\,\mathrm{FW}(X, R)$	Less contracted honeycomb	$\mathcal{O}\left(A^{13/10}\phi^{1/5}\psi^{4/5}\right)$
$\phi\,\mathrm{CBG}(X) + \psi\,\mathrm{FW}(X, R)$	Contracted honeycomb	$\mathcal{O}(A^{7/6}\phi^{1/3}\psi^{2/3})$

Table 4.1: Summary of the major results from Section 4.2.1.

If we assume that the shape of R is fixed, we see that the optimal objective function value is proportional to $A^{13/10}\phi^{1/5}\psi^{4/5}$. Note that the lower bound of our problem is given by solving

$$\underset{X}{\text{minimize}}\, \phi\left(\frac{k}{2}\right)\mathrm{SN}(X) + \psi\,\mathrm{FW}(X, R)$$

which has an objective function value within a factor of $2^{1/5} \approx 1.15$ of the upper bound that we just computed.

Summary table

We summarize the major results of this section in Table 4.1.

4.2.2 Asymptotic solutions to (4.1)

In this section, we analyze the solutions to problem (4.1) as the various coefficients become large or small. Since we are only concerned with the limiting behavior of the model, we find it useful to express the utility functions in their highest-order terms. To this end, we assume that the service region R has a population t and we impose the following functional forms on $\mathrm{Fix}(\cdot)$, ϕ, and ψ:

- We assume that the fixed cost for $|X| = k$ hubs to serve the population t takes the form $\mathrm{Fix}(k; t) = k \cdot f(t/k)$, where $f(\tau)$ denotes the fixed cost associated with

a single hub that provides service to a population of size τ. If we assume that the fixed costs follow an economy of scale, it is natural to assume that $f(\tau)$ is concave and increasing, and (since we are only concerned with the limiting behavior, i.e. the highest-order terms) we make the further assumption that $f(\tau) = a\tau^p$, where $0 \leq p \leq 1$ (this is equivalent to assuming that the fixed costs follow the simplest possible Cobb-Douglas production function with increasing returns to scale [26]).

- We assume that the backbone network cost for the hubs X to serve the population t takes the form $\phi_t \,\mathrm{BBN}(X)$, where $\mathrm{BBN}(\cdot)$ is of the form $\mathrm{Steiner}(\cdot)$, $\mathrm{MST}(\cdot)$, $\mathrm{TSP}(\cdot)$, $\mathrm{SN}(\cdot)$, or $\mathrm{CG}(\cdot)$, and ϕ_t is a concave increasing function of the population t. This models the case where a higher population results in higher backbone network costs (since there are more "things" to transport), but the network benefits from an economy of scale (see for example Section 3.1 of [10]). As in the fixed costs, we therefore assume that ϕ_t takes the form $\phi_t = bt^q$, where $0 \leq q \leq 1$.

- We assume that the coverage costs take the form $t\,\mathrm{FW}(X, R)$. This simply says that the coverage cost increases proportionally to the population in the region, which is justified by assuming that local coverage does not benefit from an economy of scale.

Our model in this section then takes the form

$$\underset{X}{\text{minimize}}\ ka\,(t/k)^p + bt^q\,\mathrm{BBN}(X) + t\,\mathrm{FW}(X, R)\,. \tag{4.15}$$

We shall assume throughout this section that $\mathrm{Area}(R) = 1$ since we are considering the limiting behavior as $t \to \infty$. We now proceed to describe the optimal solution to (4.15) as $t \to \infty$ for the various forms of $\mathrm{BBN}(\cdot)$.

The case $b = 0$

Note first that if we do not impose backbone network costs, then by Section 4.2.1 it will suffice to consider the problem

$$\underset{k}{\text{minimize}}\ ka\,(t/k)^p + t\alpha_1/\sqrt{k}$$

where $\alpha_1 \approx 0.37721$ as before, which is minimized at $k = ct^{\frac{2-2p}{3-2p}}$, where

$$c = \left[\frac{\alpha_1}{2a(1-p)}\right]^{\frac{2}{3-2p}}.$$

The optimal objective function value is then proportional to $t^{\frac{2-p}{3-2p}}$ (the proportionality constant can be computed, but we omit it here for brevity).

The case $\text{BBN}(\cdot) \in \{\text{Steiner}(\cdot), \text{MST}(\cdot), \text{TSP}(\cdot)\}$

Suppose that we adopt a Steiner tree, minimum spanning tree, or travelling salesman tour as our backbone network. We will show that the optimal solution to (4.15) depends on the relationship between p and $3/2 - 1/2q$:

- If $p > 3/2 - 1/2q$, then we claim that the uniform honeycomb heuristic, with $c = \left[\frac{\alpha_1}{2a(1-p)}\right]^{\frac{2}{3-2p}}$ and $k = ct^{\frac{2-2p}{3-2p}}$ as in Section 4.2.2, is asymptotically optimal as $t \to \infty$. Under a honeycomb configuration, we see that

  $$\text{MST}(X), \text{TSP}(X) \sim \beta_0\sqrt{k} := \frac{\sqrt{6}}{3^{3/4}}\sqrt{k} \approx 1.0746\sqrt{k}$$

  as explained in [5], and therefore that $\text{Steiner}(X) \in \mathcal{O}(\sqrt{k})$ as well (this is because $1/2\,\text{MST}(X) \leq \text{Steiner}(X) \leq \text{MST}(X)$ [44]). Thus, objective function (4.15) is at most

  $$ka\,(t/k)^p + bt^q \cdot \beta_0\sqrt{k} + t\alpha_1/\sqrt{k}\,. \tag{4.16}$$

We take the ratio of the fixed costs to the backbone network costs

$$\left.\frac{ka\,(t/k)^p}{bt^q \cdot \beta_0\sqrt{k}}\right|_{k=ct^{\frac{2-2p}{3-2p}}} \in \mathcal{O}\left(t^{\frac{1}{3-2p}-q}\right)$$

which is increasing in t provided that $p > 3/2 - 1/2q$. This shows that as $t \to \infty$, the backbone network cost becomes arbitrarily small relative to the fixed costs, and therefore

$$\left.\frac{ka\,(t/k)^p + bt^q \cdot \beta_0\sqrt{k} + t\alpha_1/\sqrt{k}}{ka\,(t/k)^p + t\alpha_1/\sqrt{k}}\right|_{k=ct^{\frac{2-2p}{3-2p}}} \to 1$$

which proves asymptotic optimality, since the denominator in the above expression is clearly a lower bound on problem (4.17).

- If $p < 3/2 - 1/2q$, then we claim that the Archimedes heuristic, with $k = t^{\frac{3-q-2p}{4-2p}}$ points placed equidistantly along an Archimedean spiral with length $\ell^* = \frac{t^{(1-q)/2}}{2\sqrt{b}}$ (i.e. with polar equation $r = \theta/2\pi\ell^*$), is optimal as $t \to \infty$. First, we note that from Section 4.2.1, it is clear that a lower bound for our problem is $\sqrt{b}t^{(q+1)/2}$; this is simply the optimal objective value $\sqrt{\phi\psi}$ with $\phi = bt^q$ and $\psi = t$. when fixed costs are ignored. When X consists of k points distributed along a spiral of length ℓ, then provided k is sufficiently large, we have

$$\mathrm{FW}(X, R) \leq \frac{\ell}{4k} + \frac{1}{4\ell}$$

(this is true because the Voronoi diagram of X approximately consists of k rectangles having dimensions $\ell/k \times 1/\ell$, which is apparent from Figure 4.2b; the right-hand side of the above expression is the Fermat-Weber value of these under

the ℓ_1 norm). Objective function (4.15) is then at most

$$\begin{aligned} & ka\,(t/k)^p + bt^q \cdot \ell^* + t\left(\frac{\ell}{4k} + \frac{1}{4\ell}\right)\Big|_{k=t^{\frac{3-q-2p}{4-2p}},\ell^*=t^{(1-q)/2}/(2\sqrt{b})} \\ & = \sqrt{b}t^{(q+1)/2} + \mathcal{O}\left(t^{\frac{3+qp-q-p}{4-2p}}\right) \sim \sqrt{b}t^{(q+1)/2} \end{aligned}$$

because $\frac{3+qp-q-p}{4-2p} < (q+1)/2$.

The case $\mathrm{BBN}(\cdot) = \mathrm{SN}(\cdot)$

Suppose that we adopt a star network topology as our backbone network. We will show that the optimal solution to (4.15) depends on the relationship between p and $\frac{3q}{2q+1}$:

- If $p > \frac{3q}{2q+1}$, then we claim that the uniform honeycomb heuristic, with $c = \left[\frac{\alpha_1}{2a(1-p)}\right]^{\frac{2}{3-2p}}$ and $k = ct^{\frac{2-2p}{3-2p}}$ as in Section 4.2.2, is asymptotically optimal as $t \to \infty$. Under this configuration, we can write (4.15) as

$$ka\,(t/k)^p + bt^q \cdot \beta k + t\alpha_1/\sqrt{k} \tag{4.17}$$

where $\beta = \mathrm{FW}(R)$ represents the average distance between a uniformly sampled point in R (or, for large k, a point in X) and $\bar{x}$, which we again assume to be the origin. We take the ratio of the fixed costs to the backbone network costs

$$\frac{ka\,(t/k)^p}{bt^q \cdot \beta k}\Big|_{k=ct^{\frac{2-2p}{3-2p}}} \in \mathcal{O}\left(t^{\frac{p}{3-2p}-q}\right)$$

which is increasing in t provided $p > \frac{3q}{2q+1}$. This shows that as $t \to \infty$, the backbone network cost becomes arbitrarily small relative to the fixed costs, and therefore

$$\frac{ka\,(t/k)^p + bt^q \cdot \beta k + t\alpha_1/\sqrt{k}}{ka\,(t/k)^p + t\alpha_1/\sqrt{k}}\Big|_{k=ct^{\frac{2-2p}{3-2p}}} \to 1$$

which proves asymptotic optimality, since the denominator in the above expression is clearly a lower bound on problem (4.17).

- Conversely, if $p < \frac{3q}{2q+1}$, then we claim that the "contracted honeycomb" configuration, with $c = \left(\iint_R \|x\|^{-2/3}\, dA\right)^{-1}$ and $k = (\alpha_1/2)^{2/3}(t/bt^q)^{2/3}/c$, is asymptotically optimal as $t \to \infty$. This is because, by (4.6), the backbone network costs approach

$$\left(\iint_R \|x\|^{1/3}\, dA\right)(bt^q)^{1/3}t^{2/3} \in \mathcal{O}\left(t^{(2+q)/3}\right),$$

whereas the fixed costs approach

$$ka\,(t/k)^p|_{k=(\alpha_1/2)^{2/3}(t/bt^q)^{2/3}/c} \in \mathcal{O}\left(t^{(2-2q+p+2qp)/3}\right),$$

and thus we find that the backbone network costs dwarf the fixed costs as $t \to \infty$ since $(2+q)/3 > (2-2q+p+2qp)/3$.

The case $\mathrm{BBN}(\cdot) = \mathrm{VRP}(\cdot)$

Suppose that we adopt a capacitated VRP tour as our backbone network. As we have seen in Section 4.2.1, the backbone network costs incurred under such a topology are essentially inherited from either a star network or a TSP tour depending on the vehicle capacity κ. We will assume that $\kappa = \kappa_0 t^r$, i.e. that the vehicle capacities vary with respect to the population t; this simply models the case where different modes of transportation are available to provide service to the region as demand increases. Applying the result of Section 4.2.1 to our model (4.15), we find that the capacity constraints become increasingly restrictive when $r < (1-q)/2$, so that the star network approximation of $\mathrm{VRP}(\cdot)$ becomes tight as $t \to \infty$, and similarly the TSP tour approximation becomes tight when $r > (1-q)/2$. The optimal solution to (4.15) can then be classified as follows:

- If $r < (1-q)/2$, then our problem can be approximated as

$$\underset{X}{\text{minimize}}\ ka\,(t/k)^p + \frac{2b}{\kappa_0} t^{q-r}\,\mathrm{BBN}(X) + t\,\mathrm{FW}(X,R)$$

  as $t \to \infty$, and consequently the optimal solution depends on the relationship between p and $\frac{3(q-r)}{2(q-r)+1}$ (this is nothing more than a restatement of the result of Section 4.2.1, making the substitution $q \mapsto q-r$):

  - If $p > \frac{3(q-r)}{2(q-r)+1}$, then the uniform honeycomb heuristic is asymptotically optimal as $t \to \infty$ because the fixed costs dominate the backbone network costs.
  - If $p < \frac{3(q-r)}{2(q-r)+1}$, then the "contracted honeycomb" configuration is asymptotically optimal as $t \to \infty$ because the backbone network costs dominate the fixed costs.

- If $r > (1-q)/2$, then our problem can be approximated as

$$\underset{X}{\text{minimize}}\ ka\,(t/k)^p + bt^q\,\mathrm{TSP}(X) + t\,\mathrm{FW}(X,R)$$

  as $t \to \infty$, and consequently the optimal solution depends on the relationship between p and $3/2 - 1/2q$ in the same fashion as in Section 4.2.2.

The case $\mathrm{BBN}(\cdot) = \mathrm{CBG}(\cdot)$

As we have seen previously in Section 4.2.1, the case where $\mathrm{BBN}(\cdot) = \mathrm{CBG}(\cdot)$ is a straightforward generalization of the case where $\mathrm{BBN}(\cdot) = \mathrm{SN}(\cdot)$. Thus, there is nothing more to do in this section because the result of Section 4.2.1 carries over without incident.

Backbone network	Conditions		Optimal configuration	k^*	Optimal objective value
Steiner/MST/TSP	$p > \frac{3}{2} - \frac{1}{2q}$		Honeycomb	$\mathcal{O}\left(t^{\frac{2-2p}{3-2p}}\right)$	$\mathcal{O}\left(t^{\frac{2-p}{3-2p}}\right)$
	$p < \frac{3}{2} - \frac{1}{2q}$		Archimedes	$\mathcal{O}\left(t^{\frac{3-2p-q}{4-2p}}\right)$	$\mathcal{O}\left(t^{(q+1)/2}\right)$
Star network/CBG	$p > \frac{3q}{2q+1}$		Honeycomb	$\mathcal{O}\left(t^{\frac{2-2p}{3-2p}}\right)$	$\mathcal{O}\left(t^{\frac{2-p}{3-2p}}\right)$
	$p < \frac{3q}{2q+1}$		Contracted honeycomb	$\mathcal{O}\left(t^{2(1-q)/3}\right)$	$\mathcal{O}\left(t^{(q+2)/3}\right)$
VRP	$r < (1-q)/2$	$p > \frac{3(q-r)}{2(q-r)+1}$	Honeycomb	$\mathcal{O}\left(t^{\frac{2-2p}{3-2p}}\right)$	$\mathcal{O}\left(t^{\frac{2-p}{3-2p}}\right)$
		$p < \frac{3(q-r)}{2(q-r)+1}$	Contracted honeycomb	$\mathcal{O}\left(t^{2[1-(q-r)]/3}\right)$	$\mathcal{O}\left(t^{(q-r+2)/3}\right)$
	$r > (1-q)/2$	$p > \frac{3}{2} - \frac{1}{2q}$	Honeycomb	$\mathcal{O}\left(t^{\frac{2-2p}{3-2p}}\right)$	$\mathcal{O}\left(t^{\frac{2-p}{3-2p}}\right)$
		$p < \frac{3}{2} - \frac{1}{2q}$	Archimedes	$\mathcal{O}\left(t^{\frac{3-2p-q}{4-2p}}\right)$	$\mathcal{O}\left(t^{(q+1)/2}\right)$
Complete graph	$p > \frac{3q+2}{2q+3}$		Honeycomb	$\mathcal{O}\left(t^{\frac{2-2p}{3-2p}}\right)$	$\mathcal{O}\left(t^{\frac{2-p}{3-2p}}\right)$
	$p < \frac{3q+2}{2q+3}$		Less contracted honeycomb	$\mathcal{O}\left(t^{2(1-q)/5}\right)$	$\mathcal{O}\left(t^{(q+4)/5}\right)$

Table 4.2: The optimal configurations, numbers of hubs, and objective values for various values of p and q and backbone network structures in (4.15).

The case $\mathrm{BBN}(\cdot) = \mathrm{CG}(\cdot)$

When we adopt a complete graph as the backbone network, we can follow precisely the same line of reasoning as in Section 4.2.2 to show that the optimal solution to (4.15) depends on the relationship between p and $\frac{3q+2}{2q+3}$:

- If $p > \frac{3q+2}{2q+3}$, the uniform honeycomb heuristic with with $c = \left[\frac{\alpha_1}{2a(1-p)}\right]^{\frac{2}{3-2p}}$ and $k = ct^{\frac{2-2p}{3-2p}}$ as in Section 4.2.2 gives an asymptotically optimal solution with objective value $\mathcal{O}(t^{\frac{2-p}{3-2p}})$.

- If $p < \frac{3q+2}{2q+3}$, the "less contracted honeycomb" configuration, with $k = \frac{t^{2/5}}{c^{3/5}(bt^q)^{2/5}}$ and c, $c^{'}$, and $c^{''}$ defined in (4.11), (4.12), and (4.13), is asymptotically optimal (within a factor of 15%) with objective value $\mathcal{O}(t^{(q+4)/5})$.

Summary table and discussion

Table 4.2 and Figure 4.4 summarize the results of this section. Another interpretation of these results allows us to understand the benefits of improving infrastructures in either the fixed costs or the backbone network: for all five backbone network topologies, the optimal configuration is either the honeycomb heuristic or a heuristic that is associated

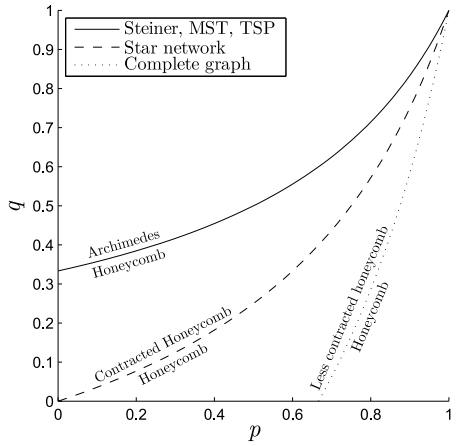

Figure 4.4: The boundary curves that distinguish different optimal solution configurations for various values of p and q in five of the backbone network structures (we have omitted the cases where $\mathrm{BBN}(\cdot) \in \{\mathrm{VRP}(\cdot), \mathrm{CBG}(\cdot)\}$ because they can be described in terms of the others). If the pair (p, q) lies above the curve associated with a particular backbone network configuration, then the backbone network costs dominate the fixed costs as $t \to \infty$. Conversely, if (p, q) lies below the curve of interest, then the fixed costs dominate the backbone network costs.

with that backbone network topology. One can also observe that, under the various conditions on p and q, it is always the case that either the fixed costs dominate the backbone network costs or that the backbone network costs dominate the fixed costs. Thus, for example, if we use a star network to connect our hubs and $p < \frac{3q}{2q+1}$, then there is little to be gained by reducing our fixed costs because they are already dwarfed by the backbone network costs as it is. Similarly, if we use a TSP tour as our backbone network and $p > 3/2 - 1/2q$, we gain little by cheapening our backbone network because the fixed costs are the dominant term. This allows us to quantify (in a very highly stylized sense, of course) the intrinsic trade-offs between such fixed costs and transportation costs as a function of the input parameters [39].

4.3 Algorithmic analysis

4.3.1 An algorithmic formulation of (4.1)

In this section we describe an algorithm for approximately minimizing objective function (4.1). We will assume without loss of generality that $\psi = 1$, and for purposes of clarity we will treat the fixed costs as a hard constraint that $|X| \leq k_0$ for some fixed input k_0. We will also assume that the service region R is a convex polygon C and that C is oriented in such a way that $\text{diam}(C)$ is aligned with the x-axis, so that C is contained in a box of dimensions $(w = \text{diam}(C)) \times h$. We will further assume without loss of generality that $w = 1/h$, which implies by convexity of C that $1/2 \leq A = \text{Area}(C) \leq 1$. For purposes of clarity, we will use the terms w and $1/h$ interchangeably depending on the context. In summary, we will show how to obtain an approximately optimal solution for the problem

$$\begin{aligned} \underset{X}{\text{minimize}}\, F(X) = \phi\, \text{BBN}(X) + \text{FW}(X, C) \qquad & s.t. \\ |X| \quad &\leq \quad k_0 \end{aligned} \tag{4.18}$$

for a given convex polygon C, a backbone network topology $\text{BBN}(\cdot)$, a positive scalar ϕ, and a positive integer k_0. Our general procedure will be to run a simple subroutine, ApproxFW as described in Algorithm 2 in Chapter 3 on C, applying several "strategic" choices of $k = |X|$.

In order to simplify our exposition as much as possible, we will apply a rigorous analysis only to the case where $\text{BBN}(\cdot) = \text{SN}(\cdot)$. This is because the case where $\text{BBN}(\cdot) = \text{MST}(\cdot)$ was already discussed in Chapter **??**, and the analysis can be extended to the cases $\text{BBN}(\cdot) = \text{Steiner}(\cdot)$ and $\text{BBN}(\cdot) = \text{TSP}(\cdot)$ in a straightforward way. Our analysis here also suggests a natural approach for the case where $\text{BBN}(\cdot) = \text{CG}(\cdot)$

because for any point set X we have already seen that $k/2\,\mathrm{SN}(X) \leq \mathrm{CG}(X) \leq k\,\mathrm{SN}(X)$. We will list all of the approximation constants associated with these five backbone network topologies in Table 4.3.

Lower bounds

In this section we introduce some lower bounding functions that we will use in proving that Algorithm 4 to be presented later in this section minimizes (4.18) within a constant factor.

Lower bounds for $\mathrm{BBN}(\cdot) = \mathrm{SN}(\cdot)$ When we adopt a star network as our backbone network topology, we find three useful lower bounds which follow below.

Theorem 21. *Suppose that* $X = \{x_1, \ldots, x_k\}$ *is a set of points in a convex polygon* C *with area* A*. Then*

$$\begin{aligned}&\phi\,\mathrm{SN}(X) + \mathrm{FW}(X, C)\\ &\geq \phi k^{'}\sqrt{\frac{Ap}{\pi}} + \frac{A^{3/2}}{3\sqrt{\pi}} \cdot \frac{\left(\sqrt{p(k'+1) - k'p^2} - p\right)^2 \left(p + 2\sqrt{p(k'+1) - k'p^2}\right)}{(k'+1)^2\, p^{3/2}}\,, \end{aligned} \tag{4.19}$$

with $p = 1/7$ *and*

$$k^{'} = \max\left\{0\,,\ \frac{2 \cdot 21^{1/3}}{21}\left(\frac{3A^{2/3}}{\phi^{2/3}} - \frac{A^{1/3}}{\phi^{1/3}}\right) - 1\right\}.$$

Proof. Suppose without loss of generality that $\bar{x}$ is the origin. Consider a ball B_r about the origin with radius r. Consider the lower bound for $\mathrm{SN}(X)$ defined by

$$\mathrm{SNLB}_r(X) = \begin{cases} 0 & \text{if } ||x_i|| \leq r \\ r & \text{otherwise.} \end{cases}$$

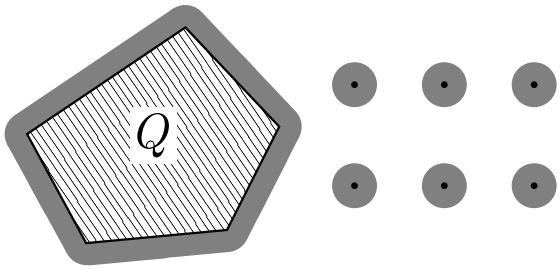

Figure 4.5: The optimal region R that minimizes $\mathrm{FW}(X^{'} \cup Q, R)$ in gray, where $k^{'} = |X^{'}| = 6$.

We can consider the related problem of minimizing $\phi\,\mathrm{SNLB}_r(X) + \mathrm{FW}(X, C)$, or equivalently

$$\phi r|X \setminus B_r| + \mathrm{FW}(X, C \setminus B_r)\,,$$

since we can place infinitely many elements of X inside B_r without incurring any additional penalty on the backbone network. We now attempt to find a lower bound for $\mathrm{FW}(X, C \setminus B_r)$, and to this end we require the following lemma:

Lemma 22. *Suppose that Q is a convex region in the plane with boundary length $\ell^{'}$ and that $X^{'} = \{x_1, \ldots, x_{k'}\}$ is a finite set of points in the plane. Then for any region R outside of Q with area $A^{'}$, we have*

$$\mathrm{FW}(X^{'} \cup Q, R) \geq \frac{\left(\sqrt{\ell'^2 + 4A'\pi(k'+1)} - \ell'\right)^2 \left(2\sqrt{\ell'^2 + 4A'\pi(k'+1)} + \ell'\right)}{24\pi^2(k'+1)^2} \tag{4.20}$$

where we define

$$\mathrm{FW}(X^{'} \cup Q, R) = \iint_R \min\left\{\min_{i \in 1,\ldots,k'} ||x - x_i||, d(x, Q)\right\} dA\,.$$

Proof. It is clear that if Q is convex then $\mathrm{Area}(N_\epsilon(Q)) = \epsilon\ell^{'} + \pi\epsilon^2$ for all ϵ. It is also clear that the region R that minimizes $\mathrm{FW}(X^{'} \cup Q, R)$ is precisely given by $N_\epsilon(Q \cup X^{'})$ for an appropriate choice of ϵ such that $\mathrm{Area}(N_\epsilon(X^{'} \cup Q)) = A^{'}$; see Figure 4.5. It

follows that we should solve

$$(\epsilon\ell^{'} + \pi\epsilon^2) + k^{'}\pi\epsilon^2 = A^{'}$$

for ϵ, which gives

$$\epsilon = \frac{\sqrt{\ell'^2 + 4A'\pi(k'+1)} - \ell'}{2\pi(k'+1)}\,.$$

The minimal Fermat-Weber value is attained when R is the disjoint union of $k^{'}$ balls of radius ϵ about the points x_i plus the neighborhood $N_\epsilon(Q)$, as shown in Figure 4.5. Their Fermat-Weber value is precisely the right-hand side of (4.20). □

It is straightforward to verify (either algebraically or via geometric intuition) that the right-hand side of (4.20) is decreasing in $\ell^{'}$. Having established the preceding result, we let p denote the fraction of area of C that is contained in B_r, so that $\text{Area}(C \setminus B_r) = A(1-p)$. It is easy to see that $\text{length}(\partial B_r \cap C) \leq 2\sqrt{\pi A p}$ and therefore, applying Lemma 22 with $Q = B_r$, $A^{'} = A(1-p)$ and $\ell^{'} = 2\sqrt{\pi A p}$, we find that

$$\text{FW}(X \cup B_r, R) \geq \frac{A^{3/2}}{3\sqrt{\pi}} \cdot \frac{\left(\sqrt{p(k'+1) - k'p^2} - p\right)^2 \left(p + 2\sqrt{p(k'+1) - k'p^2}\right)}{(k'+1)^2 p^{3/2}}$$

where $k^{'} = |X \setminus B_r|$ as before, and, using the fact that $r \geq \sqrt{Ap/\pi}$, we find that for any point set X,

$$\begin{aligned}
&\phi\,\text{SN}(X) + \text{FW}(X, C) \\
&\geq \min_{k'} \left\{ \phi k^{'}\sqrt{\frac{Ap}{\pi}} + \frac{A^{3/2}}{3\sqrt{\pi}} \cdot \frac{\left(\sqrt{p(k'+1) - k'p^2} - p\right)^2 \left(p + 2\sqrt{p(k'+1) - kp^2}\right)}{(k'+1)^2 p^{3/2}} \right\}.
\end{aligned}$$

It is not hard to show that, for large $k^{'}$, the optimal value of p (i.e. that maximizes the right-hand side of the above) is $p = 1/7$; plugging this value in and differentiating, we

find that the optimal value of $k^{'}$ is

$$k^{'} = \max\left\{0\,,\ \frac{2\cdot 21^{1/3}}{21}\left(\frac{3A^{2/3}}{\phi^{2/3}} - \frac{A^{1/3}}{\phi^{1/3}}\right) - 1\right\}$$

which completes the proof. □

Remark 23. It is not hard to see that, as $\phi \to 0$, the lower bound satisfies

$$\phi k^{'}\sqrt{\frac{Ap}{\pi}} + \frac{A^{3/2}}{3\sqrt{\pi}}\cdot\frac{\left(\sqrt{p(k^{'}+1)-k^{'}p^2}-p\right)^2\left(p+2\sqrt{p(k^{'}+1)-k^{'}p^2}\right)}{\left(k^{'}+1\right)^2 p^{3/2}} \sim \frac{6\cdot\sqrt{7}\cdot 21^{1/3}A^{7/6}}{49\sqrt{\pi}}\cdot\phi^{1/3}\,.$$

Theorem 24. *Suppose that $X = \{x_1, \ldots, x_k\}$ is a set of points in a convex polygon C with area A, which is itself contained in a minimum bounding box $\square C$ of dimensions $w \times h$. Then*

$$\begin{aligned}\phi\,\mathrm{SN}(X) + \psi\,\mathrm{FW}(X,C) \geq\ & \phi k^{'}\cdot\frac{Ap}{2h} + \left(\sqrt{16h^2+4A(1-p)\pi(k^{'}+1)}-4h\right)^2 \\ & \cdot\left(2\sqrt{16h^2+4A(1-p)\pi(k^{'}+1)}+4h\right) \\ & \cdot\left(24\pi^2(k^{'}+1)^2\right)^{-1}, \quad (4.21)\end{aligned}$$

where $p = 1/4$ and

$$k^{'} = \max\left\{0\,,\ \frac{3^{1/3}A^{1/3}}{\pi^{1/3}}\cdot\frac{h^{2/3}}{\phi^{2/3}} - \frac{8\cdot 3^{2/3}}{3\pi^{2/3}A^{1/3}}\cdot\frac{h^{4/3}}{\phi^{1/3}} - 1\right\}.$$

Proof. See Section B in Appendix □

Remark 25. It is not hard to show that, as $\max\{\phi, h\} \to 0$, the lower bound satisfies

$$\phi k^{'} \cdot \frac{Ap}{2h} + \frac{\left(\sqrt{16h^2 + 4A(1-p)\pi(k^{'}+1)} - 4h\right)^2 \left(2\sqrt{16h^2 + 4A(1-p)\pi(k^{'}+1)} + 4h\right)}{24\pi^2(k^{'}+1)^2} \sim \frac{3^{4/3}A^{4/3}}{8\pi^{1/3}} \cdot \frac{\phi^{1/3}}{h^{1/3}} - \frac{A}{8} \cdot \frac{\phi}{h}.$$

Theorem 26. *Suppose that $X = \{x_1, \ldots, x_k\}$ is a set of points in a convex polygon C with area A, which is itself contained in a minimum bounding box $\square C$ of dimensions $w \times h$. Then for any $p \in (0, 1)$, we have*

$$\phi\,\mathrm{SN}(X) + \mathrm{FW}(X, C) \geq \phi k^{'} \cdot \frac{Ap}{2h} + \frac{A^2(1-p)^2}{4h(k^{'}+1)}$$

where

$$k^{'} = \max\left\{\frac{\sqrt{A}(1-p)}{\sqrt{2p\phi}} - 1\,,\, 0\right\}. \tag{4.22}$$

Proof. See Section C in Appendix. □

Remark 27. Substituting $k^{'}$, the lower bound can be expressed equivalently as

$$\phi k^{'} \cdot \frac{Ap}{2h} + \frac{A^2(1-p)^2}{4h(k^{'}+1)} = \frac{(2A)^{3/2}(1-p)\sqrt{p\phi} - 2Ap\phi}{4h}.$$

Upper bounds

We begin this section by defining a function $H(A, w, h)$, which we will use in all of the forthcoming backbone network topologies, which is an upper bound on the Fermat-Weber value of a convex region with area A contained in a box of dimensions $w \times h$:

Theorem 28. *Suppose that C is a convex region with area A in a rectangle R having*

dimensions $w \times h$, with $w \geq h$. We have

$$\mathrm{FW}(C) \leq H(A,w,h) := \begin{cases} \left[\log\left(\frac{h+\sqrt{w^2+h^2}}{wa+w\sqrt{1+a^2}}\right) - a\sqrt{1+a^2}\right]\frac{w^3}{12} \\ + \left[\log\left(\frac{bw+b\sqrt{w^2+h^2}}{h+h\sqrt{b^2+1}}\right) - \frac{\sqrt{b^2+1}}{b^2}\right]\frac{h^3}{12} \\ + \frac{wh\sqrt{w^2+h^2}}{6} \qquad \textit{if } A < wh - \frac{h}{2}\sqrt{w^2-h^2} \\ \log\left(\frac{h+\sqrt{w^2+h^2}}{w}\right)\cdot\frac{w^3}{12} \\ + \left[\log\left(\frac{cw+c\sqrt{w^2+h^2}}{h+h\sqrt{c^2+1}}\right) - \frac{\sqrt{1+c^2}}{c^2}\right]\frac{h^3}{12} \\ + \frac{1}{6}wh\sqrt{w^2+h^2} \qquad \textit{otherwise}, \end{cases}$$

where

$$\begin{aligned} a &= \frac{w^3h - wh^3 - 2(wh-A)\sqrt{(w^2+h^2)^2 - 8hwA + 4A^2}}{2Awh - 2w^2h^2 - w^2\sqrt{(w^2+h^2)^2 - 8hwA + 4A^2}} \\ b &= \frac{2(wh^3 - Ah^2) + wh\sqrt{h^4 + 2w^2h^2 + w^4 - 8Awh + 4A^2}}{w^4 + 3w^2h^2 - 8Awh + 4A^2} \\ c &= \frac{h^2}{2(wh-A)}\,. \end{aligned}$$

Proof. See Section D in Appendix. □

Remark 29. It is not hard to show that, if we fix the product wh, then as $h/w \to 0$, we have

$$H(A,w,h) \sim \frac{2}{3}Aw - \frac{1}{12}w^2h - \frac{1}{3}\cdot\frac{A^2}{h} \tag{4.23}$$

for all A (see the end of Section D of the Online Supplement). It can also be shown that, for fixed w and h, the function $H(A,w,h)$ is concave in A, and that the function $H(A,1/h,h)$ is decreasing in h whenever $h \leq 1$.

Before defining the appropriate values of k that should be passed to Algorithm 2 to solve problem (4.18), we find it useful to state four claims regarding Algorithms 1 and

2 which are easy to verify:

Claim 30. Suppose that R is a box of dimensions $w \times h$, where $w \geq h$, and that $\{R_1, \ldots, R_k\} = \mathsf{RectanglePartition}(R, k)$ is the output of Algorithm 1. If $k \geq {}^{w}/_{3h}$, then we have $\mathrm{AR}(R_i) \leq 3$ for all sub-rectangles R_i. If $k < {}^{w}/_{3h}$, then $\mathrm{AR}(R_i) = {}^{w}/_{hk}$ for all R_i.

Proof. Observing that if $k = \frac{w}{3h}$, then the algorithm will produce k sub-rectangles with the same aspect ratio of 3 along dimension w, this claim is simply an application of Lemma 5. □

Claim 31. Suppose that R is a box of dimensions $w \times h$, where $w \geq h$, and that $\{R_1, \ldots, R_k\} = \mathsf{RectanglePartition}(R, k)$ is the output of Algorithm 1. If $k \leq 2w/h$, then all sub-rectangles R_i are identical, with width w/k and height h .

Proof. Trivial. □

Claim 32. Suppose that C is a convex polygon, $\{R_1, \ldots, R_k\} = \mathsf{RectanglePartition}(\square C, k)$ is the output of Algorithm 1 applied to $\square C$. Further suppose that $\{c_1, \ldots, c_k\}$ is the set of centers of the rectangles $\{R_1, \ldots, R_k\}$ and that $\{x_1, \ldots, x_k\} = \mathsf{ApproxFW}(C, k)$ is the output of Algorithm 2. Then $\mathrm{FW}(\{c_1, \ldots, c_k\}, C) \geq \mathrm{FW}(\{x_1, \ldots, x_k\}, C)$ and $\mathrm{BBN}(\{c_1, \ldots, c_k\}) \geq \mathrm{BBN}(\{x_1, \ldots, x_k\})$ for any of the five backbone network configurations under consideration.

Proof. It is clear from Algorithm 2 that we only have $c_i \neq x_i$ if $c_i \notin C$, so that x_i is the *projection* of c_i on C. It is a well-known fact [46] of convex analysis that projection operators onto closed convex sets are *nonexpansive*, i.e. that if $P_C(x)$ denotes the projection of x onto a convex set C, then $||x - y|| \geq ||P_C(x) - P_C(y)||$. The above claim immediately follows from this fact. □

Claim 32 is helpful to us because it allows us to assume, in our upper bounding analysis below, that $p_i = c_i$ for all $i \in \{1, \ldots, k\}$, because the case where $c_i \neq p_i$ can only *decrease* our objective function (4.18).

Claim 33. Suppose that C is a convex polygon whose bounding box has dimensions $(w = 1/h) \times h$, where $w \geq h$, and that $\{x_1, \ldots, x_k\} = \mathsf{ApproxFW}(C, k)$ is the output of Algorithm 2. Then if $k \geq w/3h$, we have $\mathrm{FW}(X, C) \leq \alpha/\sqrt{k}$, where $\alpha = H(A, \sqrt{3}, 1/\sqrt{3})$.

Proof. As in Claim 30, we know that the sub-rectangles R_i that led to the points x_i all have an aspect ratio of at most 3, and therefore the maximum value of $\mathrm{FW}(X, C)$ is attained when each of the rectangles has an aspect ratio of exactly 3 and contains area A/k (here we are using concavity of $H(\cdot)$ in its first argument which we observed in Remark 29). Thus, $\mathrm{FW}(X, C)$ is bounded above by $k \cdot H(A/k, \sqrt{3/k}, 1/\sqrt{3k}) = k \cdot (H(A, \sqrt{3}, 1/\sqrt{3})/k^{3/2}) = \alpha/\sqrt{k}$. □

Using the preceding results we can now present our approximation algorithm HubPlacement for placing hubs so as to minimize (4.18), which is given in Algorithm 4. In the following section we will prove that this is a constant-factor approximation algorithm by introducing the various values of k that are input to Algorithm 2 as a subroutine in Algorithm 4. Observe that in Algorithm 4 we consider only those elements of the set

$$K = \left\{1, \left\lfloor \sqrt{\frac{24A - 12A^2 - 3}{9\phi}} \right\rceil, \left\lfloor \frac{2^{1/3}\alpha^{2/3}}{2\,\mathrm{FW}(\square C)^{2/3}\phi^{2/3}} \right\rceil, k_0 \right\}$$

that are bounded above by k_0. For purposes of brevity, we will consider the case where all elements of K are at most k_0, so that our upper and lower bounds are not affected by k_0; the general case merely requires a case-by-case analysis on the relationships between k_0 and the other elements of K and can be solved using precisely the same kind of approach we take here.

Input: A convex polygon C with area $A \in [1/2, 1]$ contained in a minimum bounding box of dimensions $(\text{diam}(C) = 1/h = w) \times h$, a backbone network topology $\text{BBN}(\cdot)$, a positive scalar ϕ, and a positive integer k_0.

Output: The locations of a set of points X^* in C that approximately minimize, within a constant factor, the objective function

$$F(X) = \phi\,\text{BBN}(X) + \text{FW}(X, C)\,,$$

subject to the constraint that $|X| \leq k_0$.

Let $\alpha = H(A, \sqrt{3}, 1/\sqrt{3})$;

if $\text{BBN}(\cdot) \in \{\text{Steiner}(\cdot), \text{MST}(\cdot), \text{TSP}(\cdot)\}$ **then**

  Set $K = \{1, \lfloor w/h \rceil\,, \lfloor \alpha/2\phi \rceil, \lfloor \alpha/\sqrt{3}\phi \rceil, k_0\}$;

else if $\text{BBN}(\cdot) \in \text{SN}(\cdot)$ **then**

  Set $K = \left\{1, \left\lfloor \sqrt{\frac{8A-4A^2-1}{3\phi}} \right\rceil\,, \left\lfloor \left(\frac{\alpha}{2\,\text{FW}(\square C)\phi}\right)^{2/3} \right\rceil\,, k_0 \right\}$;

else if $\text{BBN}(\cdot) \in \text{CG}(\cdot)$ **then**

  Set $K = \left\{1, \left\lfloor \left(\frac{8A-4A^2-1}{6\phi}\right)^{1/3} \right\rceil\,, \left\lfloor \left(\frac{\alpha}{4\,\text{FW}(\square C)\phi}\right)^{2/5} \right\rceil\,, k_0 \right\}$;

end

Remove from K all those elements k that are greater than k_0;

for $k \in K$ **do**

  Set $X^k = \mathsf{ApproxFW}(C, k)$;

end

Let X^* denote the set X^k for which $F(X^k)$ is minimal;

return X^*;

Algorithm 4: Algorithm $\mathsf{HubPlacement}(C, \phi, k_0)$ takes as input a convex polygon C, a backbone network topology $\text{BBN}(\cdot)$, a positive scalar ϕ, and a positive integer k_0.

Upper bound I When $k = 1$, it is clear that $F(X)$ is bounded above by $\mathrm{FW}(C) \leq H(A, 1/h, h)$.

Upper bound II When $k = \left\lfloor \sqrt{\frac{8A-4A^2-1}{3\phi}} \right\rceil$, then provided that $w/k \geq h/2$, we know from Claim 31 that Algorithm 1 divides $\square C$ into k identical rectangles with dimensions $w/k \times h$ and places the points X at their centers. The backbone network cost of such a configuration is clearly

$$\sum_{i=1}^{k} |i - (k+1)/2| \cdot w/k = \begin{cases} \frac{wk}{4} & \text{if } k \text{ is even} \\ \frac{w(k^2-1)}{4k} & \text{if } k \text{ is odd} \end{cases}$$

and the Fermat-Weber cost is at most $k \cdot H(A/k, w/k, h)$ (here we have used the monotonicity and concavity properties in Remark 29). Thus, objective function (4.18) is at most

$$\phi \left(\sum_{i=1}^{k} |i - (k+1)/2| \cdot w/k \right) + k \cdot H(A/k, w/k, h)\,. \tag{4.24}$$

It turns out that when $w/k < h/2$ the case $k = \left\lfloor \sqrt{\frac{8A-4A^2-1}{3\phi}} \right\rceil$ is never optimal (we prefer upper bound III, described below).

Upper bound III When $k = \left\lfloor \left(\frac{\alpha}{2\,\mathrm{FW}(\square C)\phi} \right)^{2/3} \right\rceil$, then provided that $k \geq w/3h$, we are guaranteed (by Claim 30) that all rectangles output by Algorithm 1 have an aspect ratio not exceeding 3, and therefore $\mathrm{FW}(X, C) \leq \alpha/\sqrt{k}$ as in Claim 33. We can also show that $\mathrm{SN}(X) \leq k \cdot \mathrm{FW}(\square C)$: if we assume that $\square C$ is oriented so that its center is the origin, then letting Z denote a point selected uniformly at random in $\square C$, it is obvious that $\mathbf{E}(||Z||) = \mathrm{FW}(\square C)$ (since $\mathrm{Area}(\square C) = 1$). We can also think of Z as being generated by selecting one of the rectangles R_i output by Algorithm 1, then sampling a point Z_i uniformly within R_i. It follows

that

$$\begin{aligned} k \cdot \mathrm{FW}(C) &= k \cdot \mathbf{E}(||Z||) \\ &= k \cdot \mathbf{E}\left(\mathbf{E}\left(\,||Z_i|||\, Z_i \in R_i\right)\right) \\ &\leq k \cdot \mathbf{E}\left(c_i\right) = k \cdot \left(\frac{1}{k}\sum_{i=1}^{k} ||c_i||\right) = \mathrm{SN}(X) \end{aligned}$$

where we have applied the law of iterated expectation and Jensen's inequality. Thus, we we find that objective function (4.18) is at most

$$\phi k \cdot \mathrm{FW}(\square C) + \alpha/\sqrt{k}\,.$$

It is not hard to verify that as $\phi \to 0$, the above expression is approximately

$$\frac{3\alpha^{2/3}}{2^{2/3}}\,\mathrm{FW}(\square C)^{1/3}\phi^{1/3}\,.$$

We do not use this upper bound when $k < w/3h$ because Claim 30, and therefore Claim 33, does not apply (we must use either upper bound I or II).

4.3.2 Proof of approximation bounds

We note here that the preceding upper and lower bounds for the objective function $\phi\,\mathrm{SN}(X) + \mathrm{FW}(X, C)$ depend only on the input parameters A, h, and ϕ. Thus, in order to prove that Algorithm 4 minimizes (4.18) within a constant factor, it will suffice to show that for any triplet $(A, h, \phi) \in [1/2, 1] \times (0, 1] \times (0, \infty)$, there exists an upper bound UB and a lower bound LB such that UB/LB is less than some constant factor. In our particular case we will show that UB/LB ≤ 3.7. In what follows we will decompose the domain $[1/2, 1] \times (0, 1] \times (0, \infty)$ into a collection of sub-domains that we will address individually. Alternatively, for fixed A, one can visualize the approximation ratio over

varying h and ϕ by plotting the ratio of the minimum of upper bounds I, II, and III to the maximum of the lower bounds; see Figure 4.6, for example.

Case-by-case analysis of the input domain

Throughout this section we set $\epsilon_1 = 1/10$ and $\epsilon_2 = 1/4$.

- Suppose that $\phi > 1$. Then it is easy to see that upper bound I of $\mathrm{FW}(C) \leq H(A, 1/h, h)$ is always within a factor of 5.5 of the lower bound of Theorem 26 with $p = 1/5$; the approximation ratio is

$$\frac{\mathrm{UB}}{\mathrm{LB}} = \frac{H(A, 1/h, h)}{\frac{4\sqrt{10}A^{3/2}\sqrt{\phi} - 5A\phi}{50h}} < 5.5$$

  for $A \in [1/2, 1]$, $h \in (0, 1)$, and $\phi > 1$.

- Suppose that $(h, \phi) \in (0, \epsilon_1] \times (0, \epsilon_2]$. Consider the curves in this box of the form $\{(h, \phi) : \phi = ch^4\}$ for $c \geq 0.05$. If we use upper bound II, then it is not hard to see that, as k is large (since ϕ is small), the aspect ratios of the rectangles R_i are all approximately constant along the curve. The upper bound for our objective function is then approximately

$$\phi \left(\sum_{i=1}^{k} |i - (k+1)/2| \cdot w/k \right) + k \cdot H(A/k, w/k, h) \approx \left[\frac{\sqrt{24A - 12A^2 - 3}}{12} \sqrt{c} + \left(\frac{3}{8A - 4A^2 - 1} \right)^{1/4} \alpha' c^{1/4} \right] h$$

  where we define

$$\alpha' = H\left(A, \left(\frac{3c}{8A - 4A^2 - 1} \right)^{1/4}, \left(\frac{8A - 4A^2 - 1}{3c} \right)^{1/4} \right).$$

  Using the lower bound of Theorem 26 with $p = 1/3$, the approximation ratio is

therefore

$$\begin{aligned}\frac{\text{UB}}{\text{LB}} &= \frac{\left[\frac{\sqrt{24A-12A^2-3}}{12}\sqrt{c}+\left(\frac{3}{8A-4A^2-1}\right)^{1/4}\alpha' c^{1/4}\right]h}{\frac{\sqrt{6}A^{3/2}\sqrt{\phi}}{9h}-\frac{\phi A}{6h}} \\ &= \frac{\left[\frac{\sqrt{24A-12A^2-3}}{12}\sqrt{c}+\left(\frac{3}{8A-4A^2-1}\right)^{1/4}\alpha' c^{1/4}\right]h}{\frac{\sqrt{6}A^{3/2}\sqrt{ch}}{9}-\frac{Ach^3}{6}} \\ &\approx \frac{\frac{3\sqrt{24A-12A^2-3}}{4}\sqrt{c}+9\left(\frac{3}{8A-4A^2-1}\right)^{1/4}\alpha' c^{1/4}}{\sqrt{6}A^{3/2}\sqrt{c}}\end{aligned}$$

which is bounded above by 5.5 for $c \geq 0.05$ and $A \in [1/2, 1]$. Conversely, if $c < 0.05$, then it is easy to verify that $k = \left\lfloor \frac{2^{1/3}\alpha^{2/3}}{2\,\mathrm{FW}(\Box C)^{2/3}\phi^{2/3}} \right\rfloor \geq w/3h$, so we can apply upper bound III. Since k is large and h and ϕ are both small, the upper bound is approximately

$$\frac{3\alpha^{2/3}}{2^{2/3}}\,\mathrm{FW}(\Box C)^{1/3}\phi^{1/3} \approx \frac{3\cdot 2^{\dot{2}/3}\alpha^{2/3}}{4}c^{1/3}h\,.$$

Using the lower bound of Theorem 24, the approximation ratio is therefore

$$\begin{aligned}\frac{\text{UB}}{\text{LB}} &= \frac{\frac{3\cdot 2^{\dot{2}/3}\alpha^{2/3}}{4}c^{1/3}h}{\frac{3^{4/3}A^{4/3}}{8\pi^{1/3}}\cdot\frac{\phi^{1/3}}{h^{1/3}}-\frac{A}{8}\cdot\frac{\phi}{h}} = \frac{\frac{3\cdot 2^{\dot{2}/3}\alpha^{2/3}}{4}c^{1/3}h}{\frac{3^{4/3}A^{4/3}}{8\pi^{1/3}}\cdot\frac{(ch^4)^{1/3}}{h^{1/3}}-\frac{A}{8}\cdot\frac{ch^4}{h}} \\ &\approx \frac{2^{5/3}3^{2/3}\pi^{1/3}\alpha^{2/3}}{3A^{4/3}} < 4\end{aligned}$$

for $A \in [1/2, 1]$.

- Suppose that $(h, \phi) \in [\epsilon_1, 1] \times (0, \epsilon_2]$. As before, the upper bound is approximately

$$\frac{3\alpha^{2/3}}{2^{2/3}}\,\mathrm{FW}(\Box C)^{1/3}\phi^{1/3} \approx \frac{3\cdot 2^{\dot{2}/3}\alpha^{2/3}}{4}c^{1/3}h$$

and the lower bound of Theorem 21 is approximately

$$\frac{6 \cdot \sqrt{7} \cdot 21^{1/3} A^{7/6}}{49\sqrt{\pi}} \cdot \phi^{1/3}$$

so that

$$\frac{\text{UB}}{\text{LB}} = \frac{\frac{3\alpha^{2/3}}{2^{2/3}} \text{FW}(\square C)^{1/3} \phi^{1/3}}{\frac{6 \cdot \sqrt{7} \cdot 21^{1/3} A^{7/6}}{49\sqrt{\pi}} \cdot \phi^{1/3}} = \frac{\frac{3\alpha^{2/3}}{2^{2/3}} 49\sqrt{\pi}\, \text{FW}(\square C)^{1/3}}{6 \cdot \sqrt{7} \cdot 21^{1/3} A^{7/6}} < 5$$

since $h \geq \epsilon_1$ (this allows us to bound the term $\text{FW}(\square C)^{1/3}$).

- Suppose that $(h, \phi) \in (0, \epsilon_1] \times [\epsilon_2, 1])$. We can use upper bound I of $\text{FW}(C) \leq H(A, 1/h, h)$ and the lower bound of Theorem 26 with $p = 1/5$ so that the approximation ratio is

$$\frac{\text{UB}}{\text{LB}} = \frac{H(A, 1/h, h)}{\frac{4\sqrt{10}A^{3/2}\sqrt{\phi} - 5A\phi}{50h}} \sim \frac{\frac{2}{3}A/h - \frac{1}{12h} - \frac{1}{3} \cdot \frac{A^2}{h}}{\frac{4\sqrt{10}A^{3/2}\sqrt{\phi} - 5A\phi}{50h}} = \frac{100A/3 - 50A^2/3 - 25/6}{4\sqrt{10}A^{3/2}\sqrt{\phi} - 5A\phi} \leq 5.2$$

for $\phi \geq \epsilon_2$ and $A \in [1/2, 1]$.

- The final sub-domain is $(h, \phi) \in [\epsilon_1, 1] \times [\epsilon_2, 1]$. This domain is compact and closed and therefore we can verify that the approximation ratio is bounded above by 3.7 using a computational branch-and-bound procedure (one can easily verify this for the case $A = 1/2$, for example, by inspecting Figure 4.6).

Summary table

Table 4.3 lists the values of k that we use in Algorithm 4 for the various backbone network topologies and the resulting approximation ratios.

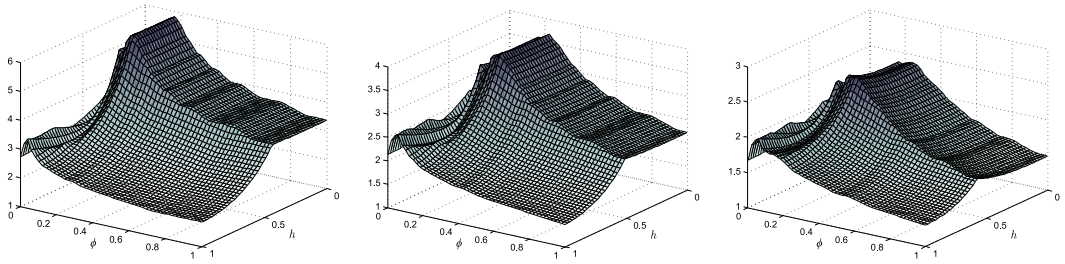

(a) $A = 1/2$ (b) $A = 3/4$ (c) $A = 1$

Figure 4.6: Surface plots of the approximation ratio for $h \in (0, 1]$, $\phi \in (0, 1]$, and $A \in \{1/2, 3/4, 1\}$.

Backbone network	Values of k	Approximation ratio
Steiner, MST	$1, \lfloor 1/h^2 \rceil, \lfloor \alpha/\sqrt{3}\phi \rceil$	3.12
TSP	$1, \lfloor 1/h^2 \rceil, \lfloor \alpha/2\phi \rceil$	3.70
Star network	$1, \left\lfloor \sqrt{\frac{8A-4A^2-1}{3\phi}} \right\rceil, \left\lfloor \left(\frac{\alpha}{2\,\mathrm{FW}(\Box C)\phi} \right)^{2/3} \right\rceil$	3.7
Complete graph	$1, \left\lfloor \left(\frac{8A-4A^2-1}{6\phi} \right)^{1/3} \right\rceil, \left\lfloor \left(\frac{\alpha}{4\,\mathrm{FW}(\Box C)\phi} \right)^{2/5} \right\rceil$	7.69

Table 4.3: Values of k that Algorithm 4 inputs to Algorithm 2 in order to achieve the approximation guarantees for (4.18) shown.

Chapter 5

Extensions to CCFL

In this chapter, we consider two types of extensions to the continuous connected facility location model (4.1) discussed in previous chapters. First, we consider two alternative cost models other than the direct trip cost in our original problem and provide some insights for these settings. Second, we extend our two layer network model, namely facilities and demands, to a multilevel network configuration and derive asymptotic results in this scenario.

5.1 Alternative cost models

A gravity model of demand The *gravity hypothesis* [37] is a well-known geographic theory that states that the "interaction" between two points x and y decays at a rate proportional to the inverse square of the distance between them, i.e. $1/\|x-y\|^2$. Here "interaction" might be measured by economic activity [43] or transport [36], for example. We can design a spatial utility model based around the gravity hypothesis by postulating that, if a customer at point x is within the service region of point x_i (i.e. nearer to x_i

than any other facility point x_j), then

$$\Pr(\text{customer at } x \text{ uses } x_i) = \frac{1}{(1+\alpha\|x-x_i\|)^2}$$

where α is a decay parameter (the "1+" term in the denominator ensures that we have quadratic decay but that the customer uses the facility with probability 1 if $x = x_i$). The total amount of demand served by the facilities X is then proportional to

$$D(X,C) := \iint_C \frac{dA}{(1+\alpha \min_i\{\|x-x_i\|\})^2} = \sum_{i=1}^{k} \iint_{V_i} \frac{dA}{(1+\alpha\|x-x_i\|)^2}$$

where $\mathcal{V} = \{V_1, \ldots, V_k\}$ denotes a Voronoi partition of C with respect to the points X. Since a firm wants $D(X,C)$ to be as large as possible while keeping fixed costs and backbone network costs small, we thus consider the alternative model of (4.1) given by minimizing

$$\bar{F}(X) = \gamma \cdot |X| + \phi\, \mathrm{MST}(X) - \psi D(X,C)\,.$$

As in the preceding section, we can analyze the asymptotic behavior of this model when $\psi \to \infty$ by considering the optimal facility placement under the special cases where $\phi = 0$ and $\gamma = 0$. Applying a monotonicity argument to that of [20], it is intuitive that when $\phi = 0$, the optimal solution is again the honeycomb heuristic. When $\gamma = 0$, the optimal solution is an Archimedean spiral with length $\sqrt{\alpha\psi/2} - \alpha/2 \sim \sqrt{\alpha\psi/2}$.

Multi-trip costs As described in the introduction, the transportation costs $\psi\,\mathrm{FW}(X,C)$ model the case where we have a continuum of customers distributed uniformly in C and the cost due to each customer is proportional to the distance between that customer and its nearest facility x_i (a single round trip between the facility and the customer). Suppose that a total of N customers are distributed uniformly in C, and let $\psi' = \psi/N$ so that the transportation costs can equivalently be written as $\psi' N \cdot \mathrm{FW}(X,C)$; this

allows us to describe the transportation costs in terms of the number of customers. We may consider an alternative model in which m customers can be serviced before a return trip to the facility: specifically, let V_i denote the service sub-region (the Voronoi cell) associated with x_i, and suppose that a "service vehicle" based at x_i visits the customers in V_i, of which there are N_i in total. The vehicle can visit up to m customers before it is required to return to x_i for re-stocking cargo. We write the cost of servicing the set of customers $Y = \{y_1, \ldots, y_{N_i}\}$ in V_i as $\mathrm{tsp}_m(Y; x_i)$, where we use the lowercase notation to reflect the notion that this travel is happening locally *within* V_i, as opposed to the backbone network costs $\mathrm{TSP}(X)$ which occur between facilities. The original case where transportation costs are $\psi\,\mathrm{FW}(X, C)$ is simply the special case of this new formulation in which $m = 1$. Finally, since we assume that the customers are distributed uniformly at random in V_i, we define

$$\mathrm{Etsp}_m(V_i, x_i) = \mathbf{E}\,\mathrm{tsp}_m(Y; x_i)$$

as the expected transportation workload in V_i. Provided m is fixed, it is not difficult to show that (see Theorem 4 of [18])

$$\mathrm{Etsp}_m(V_i, x_i) \sim \frac{N_i}{m} \cdot \frac{\iint_{V_i} \|x - x_i\|\, dA}{\mathrm{Area}(V_i)}$$

as $N_i \to \infty$. Since $N_i \sim N \cdot \mathrm{Area}(V_i)$ as $N \to \infty$ (with probability 1), we find that the total transportation cost in the region is then

$$\begin{aligned}
\sum_{i=1}^{k} \psi'\,\mathrm{Etsp}_m(V_i, x_i) &= \sum_{i=1}^{k} \psi' \left(\frac{N_i}{m} \cdot \frac{\iint_{V_i} \|x - x_i\|\, dA}{\mathrm{Area}(V_i)} \right) \\
&= \sum_{i=1}^{k} \frac{\psi' \cdot N}{m} \iint_{V_i} \|x - x_i\|\, dA = \frac{\psi}{m}\,\mathrm{FW}(X, C)
\end{aligned}$$

which differs from the transportation cost in our initial formulation merely by a factor of $1/m$. Thus, we find that the introduction of a multi-stop model for transportation cost within sub-regions does not alter our model in a fundamental way.

5.2 Multilevel networks

The problems we have considered thus far can be thought of as belonging to the class of two-level location and design problems: goods are first transported along the backbone network to facilities, then to the customers in the service region via direct trips. It is natural to generalize problem (4.1) to the case where we have multiple levels of distribution that occur between the facilities and the customers,

$$\underset{X^1,\ldots,X^n}{\text{minimize}} \sum_{i=1}^{n} \text{Fix}_i(|X^i|) + \sum_{i=1}^{n} \phi_i \, \text{BBN}_i(X^i) + \psi \, \text{FW}(X^1, R), \tag{5.1}$$

where X^i denotes the set of facilities at the ith level; note that it is only the lowest-level facilities X^1 that provide service to the customers in the region (which they do via direct trips). This setup is shown in Figure 5.1. In this section, we will consider the structure of the optimal solution to (5.1) when all backbone networks are star networks (which is also suggested in Figure 5.1). Thus, a facility $x_j^{i-1} \in X^{i-1}$ will be connected to the facility in X^i that is closest to it; let $\text{NN}(X^i, X^{i-1})$ denote the "nearest neighbor" graph that is induced by this assumption. Since there are no facilities above the nth level, we simply assume that those facilities at the nth level are connected with a star network rooted at the geometric median of X^n, i.e., that $\text{BBN}_n(X^n) = \text{SN}(X^n)$. For simplicity, we will consider the case where no fixed costs are imposed on any of the facilities, i.e., $\text{Fix}_i(\cdot) = 0$ for all levels. We devote the remainder of this section to a proof of the following theorem:

Theorem 34. *The optimal objective function value to the problem*

$$\underset{X^1,\ldots,X^n}{\text{minimize}}\, \phi_n \,\mathrm{SN}(X^n) + \sum_{i=1}^{n-1} \phi_i \,\mathrm{NN}(X^{i+1}, X^i) + \phi_0 \,\mathrm{FW}(X^1, R) \tag{5.2}$$

takes the form

$$\left(\frac{2^{n+1}-1}{2^{(2+2^{n+1}(n-1))/(2^{n+1}-1)}}\right)\left(\prod_{i=0}^{n-1} a_i^{2^{n+1}-2^{n-i}}\right)^{1/\left(2^{n+1}-1\right)} \cdot \left(\prod_{i=0}^{n} \phi_i^{2^{n-i}}\right)^{1/\left(2^{n+1}-1\right)} \iint_R \|x\|^{1/\left(2^{n+1}-1\right)} dA \tag{5.3}$$

as $\phi_0/\phi_i \to \infty$ *for all* $i \geq 1$*, where we define*

$$a_i = \iint_{\mathrm{Hex}(1)} \|x\|^{1/\left(2^{i+1}-1\right)} dA$$

with $\mathrm{Hex}(1)$ *denoting a regular hexagon with unit area, which simplifies to*

$$\left(\frac{2^{n+1}-1}{2^{(2+2^{n+1}(n-1))/(2^{n+1}-1)}}\right)\left(\prod_{i=0}^{n} a_i^{2^{n+1}-2^{n-i}}\right)^{1/\left(2^{n+1}-1\right)} \cdot \left(\prod_{i=0}^{n} \phi_i^{2^{n-i}}\right)^{1/\left(2^{n+1}-1\right)} A^{\left(2^{n+2}-1\right)/\left(2^{n+2}-2\right)} \tag{5.4}$$

when R *is a regular hexagon of area* A*. The optimal configuration of points at the* n*th level is a contracted honeycomb configuration that follows the distribution* $f(x) = c\|x\|^{-2/(q+2)}$ *for a suitable constant* c*, where* $q = 1/\left(2^n - 1\right)$*.*

The above expression is quite unwieldy but becomes clearer when we write out its first few values, which are show in Table 5.1. Note that higher-level facilities are more concentrated about their centers than lower-level facilities because the exponent $-2/(q+2)$ approaches -1 from the right as n increases. We require a fairly simple

Table 5.1: Values of (5.4) for $n \in \{1, 2, 3, 4\}$

n	Optimal value to (5.2)
1	$\frac{3}{2^{2/3}}\left(a_0^2 a_1^3\right)^{1/3}\left(\phi_0^2\phi_1\right)^{1/3} A^{7/6}$
2	$\frac{7}{2^{10/7}}\left(a_0^4 a_1^6 a_2^7\right)^{1/7}\left(\phi_0^4\phi_1^2\phi_2\right)^{1/7} A^{15/14}$
3	$\frac{15}{2^{34/15}}\left(a_0^8 a_1^{12} a_2^{14} a_3^{15}\right)^{1/15}\left(\phi_0^8\phi_1^4\phi_2^2\phi_3\right)^{1/15} A^{31/30}$
4	$\frac{31}{2^{98/31}}\left(a_0^1 6 a_1^{24} a_2^{28} a_3^{30} a_4^{31}\right)^{1/31}\left(\phi_0^{16}\phi_1^8\phi_2^4\phi_3^2\phi_4\right)^{1/31} A^{63/62}$

lemma in order to prove this result:

Lemma 35. *Let R be a compact planar region with area A. As $\phi/\psi \to 0$, the optimal objective value to the problem*

$$\underset{X}{\text{minimize}}\, \phi\, \mathrm{SN}(X) + \psi\, \mathrm{FW}_f(X, R), \tag{5.5}$$

where $f(\tau) = \tau^q$ and $\mathrm{FW}_f(\cdot,\cdot)$ is as defined in Theorem 20, is given by

$$c\left(\phi^q\psi^2\right)^{1/(q+2)} \iint_R \|x\|^{q/(q+2)} dA,$$

where we define

$$c = \left(\frac{\alpha_q^2}{4q^q}\right)^{1/(q+2)} (q+2)$$

and

$$\alpha_q = \iint_{\mathrm{Hex}(1)} \|x\|^q dA.$$

Proof. Note that this is a generalization of section 4.2.1 (which deals with the special case $q = 1$) and that our values α_q generalize our previous definition of α_1. This result is proven in an entirely analogous manner to section 4.2.1. □

Remark 36. If we vary the area A but retain the same shape, the integral $\iint_R \|x\|^{q/(q+2)} dA$

in the above scales proportionally to $A^{(3q+4)/(2q+4)}$.

We ca now proceed to prove Theorem 34 by induction:

Proof of Theorem 34. It is clearly true that Theorem 34 holds for the base case where $n = 1$, which was demonstrated in section 4.2.1. Assume that Theorem 34 holds for networks of up to $n-1$ levels and consider the problem with n levels; for any placement of the points $X^n = \{x_1^n, \ldots, x_k^n\}$ (with k obviously a variable) let V_j denote the Voronoi cell of point x_j^n. By the induction hypothesis, we see that the optimal cost to cover cell V_j with those facilities at levels 1 through $n-1$ is given by

$$\left(\frac{2^n-1}{2^{(2+2^n(n-2))/(2^n-1)}}\right)\left(\prod_{i=0}^{n-2} a_i^{2^n-2^{n-1-i}}\right)^{1/(2^n-1)} \cdot \left(\prod_{i=0}^{n-1}\phi_i^{2^n-1-i}\right)^{1/(2^n-1)} \iint_{V_i} \|x - x_j^n\|^{1/(2^n-1)} dA,$$

and therefore the total cost of coverage of these regions is simply the sum of this over all cells:

$$\begin{aligned}
&\sum_{i=1}^{n-1}\phi_i \,\mathrm{NN}(X^{i+1}, X^i) + \phi_0\,\mathrm{FW}(X^1, R) \\
&\sim \left(\frac{2^n-1}{2^{(2+2^n(n-2))/(2^n-1)}}\right)\left(\prod_{i=0}^{n-2} a_i^{2^n-2^{n-1-i}}\right)^{1/(2^n-1)} \\
&\quad \cdot \left(\prod_{i=0}^{n-1}\phi_i^{2^n-1-i}\right)^{1/(2^n-1)} \sum_{j=1}^{k}\iint_{V_i}\|x - x_j^n\|^{1/(2^n-1)} dA \\
&= \underbrace{\left(\frac{2^n-1}{2^{(2+2^n(n-2))/(2^n-1)}}\right)\left(\prod_{i=0}^{n-2} a_i^{2^n-2^{n-1-i}}\right)^{1/(2^n-1)} \left(\prod_{i=0}^{n-1}\phi_i^{2^n-1-i}\right)^{1/(2^n-1)}}_{\psi} \\
&\quad \cdot \mathrm{FW}_f(X^n, R),
\end{aligned}$$

where $f(\tau) = \tau^{1/(2^n-1)}$. We therefore find that problem (5.1) can be written as

$$\underset{X^n}{\text{minimize}}\, \phi_n \,\mathrm{SN}(X^n) + \psi \,\mathrm{FW}_f(X^n, R),$$

whose optimal objective value is given by Lemma 35; the reminder of the proof then becomes a tedious calculation by substituting for ψ, which we omit for brevity. □

To conclude this section, Figure 5.2 shows an optimal configuration of a three-level network.

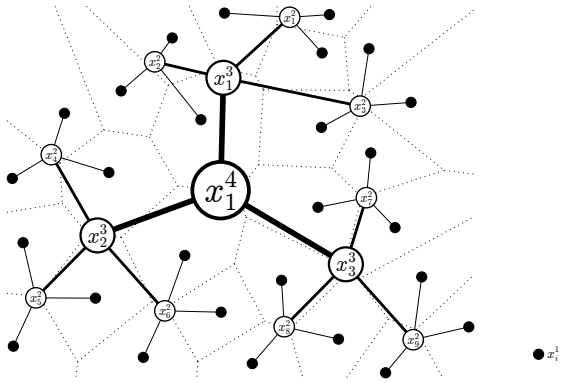

Figure 5.1: A four-stage hub-and-spoke network with star backbone networks at each level.

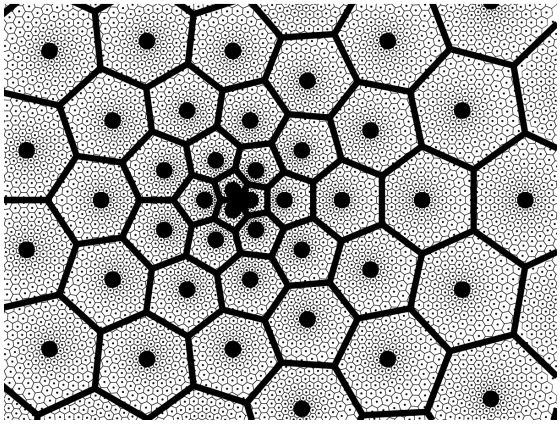

Figure 5.2: An optimal configuration of a three-level network

Chapter 6

Conclusions and future directions

We have considered a class of location problems called the *Continuous Connected Facility Location Problems* which arise in distribution network design and also seen their applications in fields including telecommunication network design and public transportation service and emergency service deployment. Inherent computational complexity and intractability makes solving this problem with exact solution very hard. We tackle the problem from two aspects. First, we conduct asymptotic analysis on the model and derive insights on the optimal solution from the limiting behavior of various model parameters. In this effort, a spiral shaped network configuration is discovered that yields the asymptotically optimal solution to the problem. Second, we take an algorithmic approach with the goal of developing approximation solutions with guaranteed bounds. To this end, we have developed a fast and simple algorithm that solves the problem with a constant approximation factor. We then generalize our model in two folds. First, we allow the connection between facilities to take a number of different network topologies besides the minimum spanning tree configuration in the original model. A total of seven topologies are studied and, as we discover, the asymptotically optimal configurations

for these variations essentially have two forms that are represented by either a minimum spanning tree or star shaped back bone network. The analysis unifies our model with the different network constructs under a single analysis framework and gives more insights about the connections between each network structure. The second generalization of our original model aim at the underlying cost models specifying the interaction between facilities and demand points. We consider two alternative cost models in this case. The gravity model applies an inverse square function to model the attractiveness of the facility to the customers with the distance between the two. The multi-trip model represents a setting where delivery service is explicitly included and achieved by routing capacitated vehicles. We show that in both cases, our asymptotic analysis can be applied to find asymptotic optimal solutions that do not differ fundamentally from our original model.

6.1 Future directions

Questions remain that could enhance our understanding of the problem but we are not able to achieve at this time. In the following, we point out a few of them that worth exploring.

As we discussed in section 3.1.7, our partition algorithm works well for k-median problems in the simulation experiment. This suggests that the lower bound used in our analysis is fairly tight. However, it is less clear how good our upper bound is. We conjecture that a refined upper bound would bring our approximation factor for the k-median problem down to under 2. In fact, a new result in [12] shows that this is indeed very promising.

Throughout our analysis, we made the assumption that the demand distribution is uniform. It is natural to consider problems with a nonuniform demand distribution. Unfortunately, our algorithm does not generalize in this case. For the continuous 1-median

problem, [15] provides an $O(n)$ algorithm that extends to the nonuniform demand density for L_1 norm distance. However, as proved in that work, the problem becomes NP-hard when there are multiple median points to be placed. One possible way to tackle the continuous k-median problem with nonuniform demand distribution may be to combine a Voronoi partition algorithm with a median finding algorithm. Intuitively, this is done by iteratively assigning demand to its nearest facility and relocating the facilities to the median of each subregion until convergence. Convergence is guaranteed because each of the two steps decreases the objective function value. However, there is no guarantee for global optimum and obtaining performance bound for this algorithm appears to be quite challenging.

Bibliography

[1] B. Aronov, P. Carmi, and M.J. Katz. Minimum-cost load-balancing partitions. *Algorithmica*, 54(3):318–336, July 2009.

[2] Sanjeev Arora, Prabhakar Raghavan, and Satish Rao. Approximation schemes for euclidean k-medians and related problems. In *Proceedings of the thirtieth annual ACM symposium on Theory of computing*, pages 106–113. ACM, 1998.

[3] Jillian Beardwood, John H Halton, and John Michael Hammersley. The shortest path through many points. In *Mathematical Proceedings of the Cambridge Philosophical Society*, volume 55, pages 299–327. Cambridge Univ Press, 1959.

[4] Dimitris J Bertsimas and David Simchi-Levi. A new generation of vehicle routing research: robust algorithms, addressing uncertainty. *Operations Research*, 44(2):286–304, 1996.

[5] Gérard P Cachon. Retail store density and the cost of greenhouse gas emissions. *Management Science*, 60(8):1907–1925, 2014.

[6] J. F. Campbell. Hub location and the p-hub median problem. *Operations Research*, 44(6):pp. 923–935, 1996.

[7] John Gunnar Carlsson and Fan Jia. Euclidean hub-and-spoke networks. *Operations Research*, 61(6):1360–1382, 2013.

[8] John Gunnar Carlsson and Fan Jia. Continuous facility location with backbone network costs. *Transportation Science*, 2014.

[9] John Gunnar Carlsson, Fan Jia, and Ying Li. An approximation algorithm for the continuous k-medians problem in a convex polygon. *INFORMS Journal on Computing*, 26(2):280–289, 2013.

[10] C. F. Daganzo and G. F. Newell. Configuration of physical distribution networks. *Networks*, 16(2):113–132, 1986.

[11] Carlos F Daganzo. *Logistics systems analysis*. Springer Science & Business Media, 2005.

[12] Raghuveer Devulapalli. *Geometric partitioning algorithms for fair division of geographic resources*. PhD thesis, University of Minnesota, 2014.

[13] Horst A Eiselt and Vladimir Marianov. *Foundations of location analysis*, volume 155. Springer Science & Business Media, 2011.

[14] Friedrich Eisenbrand, Fabrizio Grandoni, Thomas Rothvoß, and Guido Schäfer. Approximating connected facility location problems via random facility sampling and core detouring. In *Proceedings of the nineteenth annual ACM-SIAM symposium on Discrete algorithms*, pages 1174–1183. Society for Industrial and Applied Mathematics, 2008.

[15] Sándor P Fekete, Joseph SB Mitchell, and Karin Beurer. On the continuous fermat-weber problem. *Operations Research*, 53(1):61–76, 2005.

[16] Anupam Gupta, Jon Kleinberg, Amit Kumar, Rajeev Rastogi, and Bulent Yener. Provisioning a virtual private network: a network design problem for multicommodity flow. In *Proceedings of the thirty-third annual ACM symposium on Theory of computing*, pages 389–398. ACM, 2001.

[17] M. Haimovich and Thomas L. Magnanti. Extremum properties of hexagonal partitioning and the uniform distribution in Euclidean location. *SIAM J. Discrete Math.*, 1:50–64, 1988.

[18] M. Haimovich and A. H. G. Rinnooy Kan. Bounds and heuristics for capacitated routing problems. *Mathematics of Operations Research*, 10(4):527–542, 1985.

[19] M. P. Helme and T. L. Magnanti. Designing satellite communication networks by zero-one quadratic programming. *Networks*, 19(4):427–450, 1989.

[20] Dorit S Hochbaum. When are np-hard location problems easy? *Annals of Operations Research*, 1(3):201–214, 1984.

[21] P. Jaillet, G. Song, and G. Yu. Airline network design and hub location problems. *Location Science*, 4(3):195–212, October 1996.

[22] Hyunwoo Jung, Mohammad Khairul Hasan, and Kyung-Yong Chwa. Improved primal-dual approximation algorithm for the connected facility location problem. In *Combinatorial Optimization and Applications*, pages 265–277. Springer, 2008.

[23] M. Labb and H. Yaman. Solving the hub location problem in a star-star network. *Networks*, 51(1):19–33, 2008.

[24] André Langevin, Pontien Mbaraga, and James F Campbell. Continuous approximation models in freight distribution: an overview. *Transportation Research Part B: Methodological*, 30(3):163–188, 1996.

[25] James N Lyness and Ronald Cools. A survey of numerical cubature over triangles. In *Proceedings of Symposia in Applied Mathematics*, volume 48, pages 127–150, 1994.

[26] A. Mas-Colell, M.D. Whinston, and J.R. Green. *Microeconomic Theory*. Oxford University Press, USA, 1995.

[27] Joseph SB Mitchell. Guillotine subdivisions approximate polygonal subdivisions: A simple polynomial-time approximation scheme for geometric tsp, k-mst, and related problems. *SIAM Journal on Computing*, 28(4):1298–1309, 1999.

[28] Gordon Frank Newell. Scheduling, location, transportation, and continuum mechanics: some simple approximations to optimization problems. *SIAM Journal on Applied Mathematics*, 25(3):346–360, 1973.

[29] S. Nickel, A. Schobel, and T. Sonnebon. Hub location problems in urban traffic networks. In M. Pursula and J. Niittymhaki, editors, *Mathematical Methods on Optimization in Transportation Systems*, pages 95–107. Kluwer Academic Publishers, 2000.

[30] M. O'Kelly. A geographer's analysis of hub-and-spoke networks. *Journal of Transport Geography*, 6(3):171 – 186, 1998.

[31] C. H. Papadimitriou. Worst-case and probabilistic analysis of a geometric location problem. *SIAM Journal on Computing*, 10:542, 1981.

[32] J. Petrek and V. Sledt. A large hierarchical network star-star topology design algorithm. *European Transactions on Telecommunications*, 12(6):511–522, 2001.

[33] M. Pinedo. *Scheduling: theory, algorithms, and systems*. Springer, 2008.

[34] Franco P. Preparata and Michael I. Shamos. *Computational geometry: an introduction*. Springer-Verlag New York, Inc., New York, NY, USA, 1985.

[35] C Redmond and JE Yukich. Limit theorems and rates of convergence for euclidean functionals. *The Annals of Applied Probability*, pages 1057–1073, 1994.

[36] J.P. Rodrigue, C. Comtois, and B. Slack. *The Geography of Transport Systems*. Routledge, 2009.

[37] E. Sheppard. Theoretical underpinnings of the gravity hypothesis. *Geographical Analysis*, 10(4):386–402, 1978.

[38] David B Shmoys, Éva Tardos, and Karen Aardal. Approximation algorithms for facility location problems. In *Proceedings of the twenty-ninth annual ACM symposium on Theory of computing*, pages 265–274. ACM, 1997.

[39] D. Simchi-Levi, J. P. Peruvankal, N. Mulani, B. Read, and J. Ferreira. Is it time to rethink your manufacturing strategy? *MIT Sloan Management Review*, 53(2):19–22, 2012.

[40] J Michael Steele. Subadditive euclidean functionals and nonlinear growth in geometric probability. *The Annals of Probability*, pages 365–376, 1981.

[41] Chaitanya Swamy and Amit Kumar. Primal–dual algorithms for connected facility location problems. *Algorithmica*, 40(4):245–269, 2004.

[42] Godfried T Toussaint. Solving geometric problems with the rotating calipers. In *Proc. IEEE Melecon*, volume 83, page A10, 1983.

[43] Peter AG van Bergeijk and Steven Brakman. *The gravity model in international trade: Advances and applications*. Cambridge University Press, 2010.

[44] V. V. Vazirani. *Approximation Algorithms*. Springer, 2004.

[45] H. Yaman and S. Elloumi. Star p-hub center problem and star p-hub median problem with bounded path lengths. *Computers & Operations Research*, 39(11):2725 – 2732, 2012.

[46] D. C. Youla and H. Webb. Image restoration by the method of convex projections: Part 1: Theory. *Medical Imaging, IEEE Transactions on*, 1(2):81–94, October 1982.

[47] Eitan Zemel. Probabilistic analysis of geometric location problems. *Annals of Operations Research*, 1(3):215–238, 1984.

Appendix A

Proof of approximation factor for Algorithm 2

A.1 The case $k \leq w/\rho h$

If $k \leq w/\rho h$, then our algorithm will divide $\square C$ into k identical rectangles of dimensions $(w/k) \times h$. Thus we set $w_{\text{rect}} = w/k \geq \rho$ and assume without loss of generality that $h = 1$. We will use lower bound (3.4). Note that we may either have $\frac{(2\sqrt{2}-2)\gamma+1}{\sqrt{2}-1}h^2 < wh - \frac{h}{2}\sqrt{w^2-h^2}$ or $\frac{(2\sqrt{2}-2)\gamma+1}{\sqrt{2}-1}h^2 \geq wh - \frac{h}{2}\sqrt{w^2-h^2}$, depending on the dimensions of $\square C$, and therefore we have to consider these cases separately. In total, there are five cases that we have to consider:

1. $A \leq wh - \frac{h}{2}\sqrt{w^2-h^2}$ and $A \leq \frac{(2\sqrt{2}-2)\gamma+1}{\sqrt{2}-1}h^2$.
2. $\frac{(2\sqrt{2}-2)\gamma+1}{\sqrt{2}-1}h^2 < A \leq wh - \frac{h}{2}\sqrt{w^2-h^2}$.
3. $wh - \frac{h}{2}\sqrt{w^2-h^2} < A \leq \frac{(2\sqrt{2}-2)\gamma+1}{\sqrt{2}-1}h^2$.
4. $A > wh - \frac{h}{2}\sqrt{w^2-h^2}$, $A > \frac{(2\sqrt{2}-2)\gamma+1}{\sqrt{2}-1}h^2$, and $A \leq wh - h^2/2$.

5. $A > wh - h^2/2$.

We consider each case separately below.

A.1.1 Case 1

By assumption we have $\alpha \leq w_{\text{rect}} - \frac{1}{2}\sqrt{w_{\text{rect}}^2 - 1}$ and $\alpha \leq \frac{(2\sqrt{2}-2)\gamma+1}{\sqrt{2}-1}$ and the approximation ratio is given by

$$\frac{\frac{\sqrt{2}-1}{3}\alpha - \frac{\sqrt{2}-1}{12}w_{\text{rect}} - \frac{\sqrt{w_{\text{rect}}^2-1}}{3}(w_{\text{rect}} - \alpha) + \frac{1}{3}w_{\text{rect}}^2 - \frac{1}{12}}{\frac{(16+12\sqrt{2})\gamma(\gamma-1)+\sqrt{2}}{24(\sqrt{2}+1)^2} + \frac{8+6\sqrt{2}-(28+20\sqrt{2})\gamma}{24(\sqrt{2}+1)^2}\alpha + \frac{16+11\sqrt{2}}{24(\sqrt{2}+1)^2}\alpha^2}.$$

We notice that the denominator is quadratic in α and the numerator is linear in α, and it is therefore not hard to show that the ratio is maximized when α is as small as possible, i.e. that $\alpha = w_{\text{rect}}/2$. Since we have $\alpha \leq \frac{(2\sqrt{2}-2)\gamma+1}{\sqrt{2}-1}$, it must be the case that $w_{\text{rect}} \leq \frac{(4\sqrt{2}-4)\gamma+2}{\sqrt{2}-1} < 5.30$. The approximation ratio is therefore

$$\frac{\frac{\sqrt{2}-1}{6}w_{\text{rect}} - \frac{\sqrt{2}-1}{12}w_{\text{rect}} - \frac{\sqrt{w_{\text{rect}}^2-1}}{6}w_{\text{rect}} + \frac{1}{3}w_{\text{rect}}^2 - \frac{1}{12}}{\frac{(16+12\sqrt{2})\gamma(\gamma-1)+\sqrt{2}}{24(\sqrt{2}+1)^2} + \frac{8+6\sqrt{2}-(28+20\sqrt{2})\gamma}{48(\sqrt{2}+1)^2}w_{\text{rect}} + \frac{16+11\sqrt{2}}{96(\sqrt{2}+1)^2}w_{\text{rect}}^2}$$

which is bounded above by 2.74 for $w_{\text{rect}} \in [\rho, 5.30]$.

A.1.2 Case 2

By assumption we have $\frac{(2\sqrt{2}-2)\gamma+1}{\sqrt{2}-1} < \alpha \leq w_{\text{rect}} - \frac{1}{2}\sqrt{w_{\text{rect}}^2 - 1}$ and the approximation ratio is given by

$$\frac{\frac{\sqrt{2}-1}{3}\alpha - \frac{\sqrt{2}-1}{12}w_{\text{rect}} - \frac{\sqrt{w_{\text{rect}}^2-1}}{3}(w_{\text{rect}} - \alpha) + \frac{1}{3}w_{\text{rect}}^2 - \frac{1}{12}}{\left(\gamma^3/3 + \sqrt{2}/6 - 1/12\right) - (\gamma/2)\,\alpha + (1/4)\,\alpha^2}.$$

We again observe that the denominator is quadratic in α and the numerator is linear in α, and it is therefore not hard to show that the ratio is maximized when α is as small as possible, i.e. the maximizer $\alpha^* = \max\left\{\frac{(2\sqrt{2}-2)\gamma+1}{\sqrt{2}-1}, w_{\text{rect}}/2\right\}$. The approximation ratio is given by

$$\frac{\frac{\sqrt{2}-1}{3}\alpha^* - \frac{\sqrt{2}-1}{12}w_{\text{rect}} - \frac{\sqrt{w_{\text{rect}}^2-1}}{3}(w_{\text{rect}} - \alpha^*) + \frac{1}{3}w_{\text{rect}}^2 - \frac{1}{12}}{\left(\gamma^3/3 + \sqrt{2}/6 - 1/12\right) - (\gamma/2)\,\alpha^* + (1/4)\,\alpha^{*2}}$$

which is bounded above by 2.74 for $w_{\text{rect}} \geq \rho$.

A.1.3 Case 3

By assumption we have $w_{\text{rect}} - \frac{1}{2}\sqrt{w_{\text{rect}}^2 - 1} < \alpha \leq \frac{(2\sqrt{2}-2)\gamma+1}{\sqrt{2}-1}$ and the approximation ratio is given by

$$\frac{\frac{2}{3}\alpha w_{\text{rect}} + \frac{\sqrt{2}-1}{3}\alpha - \frac{1}{3}\alpha^2 - \frac{1}{12}w_{\text{rect}}^2 - \frac{\sqrt{2}-1}{12}w_{\text{rect}}}{\frac{(16+12\sqrt{2})\gamma(\gamma-1)+\sqrt{2}}{24\left(\sqrt{2}+1\right)^2} + \frac{8+6\sqrt{2}-(28+20\sqrt{2})\gamma}{24\left(\sqrt{2}+1\right)^2}\alpha + \frac{16+11\sqrt{2}}{24\left(\sqrt{2}+1\right)^2}\alpha^2}.$$

We notice that the numerator is increasing in w_{rect}, and therefore we assume that w_{rect} is as large as possible so that $\alpha^* = w_{\text{rect}} - \frac{1}{2}\sqrt{w_{\text{rect}}^2 - 1}$. Furthermore, since $w_{\text{rect}} - \frac{1}{2}\sqrt{w_{\text{rect}}^2 - 1} < \frac{(2\sqrt{2}-2)\gamma+1}{\sqrt{2}-1}$, it must be the case that $w_{\text{rect}} < 5.2002$. The approximation ratio is given by

$$\frac{\frac{2}{3}\alpha^* w_{\text{rect}} + \frac{\sqrt{2}-1}{3}\alpha^* - \frac{1}{3}\alpha^{*2} - \frac{1}{12}w_{\text{rect}}^2 - \frac{\sqrt{2}-1}{12}w_{\text{rect}}}{\frac{(16+12\sqrt{2})\gamma(\gamma-1)+\sqrt{2}}{24\left(\sqrt{2}+1\right)^2} + \frac{8+6\sqrt{2}-(28+20\sqrt{2})\gamma}{24\left(\sqrt{2}+1\right)^2}\alpha^* + \frac{16+11\sqrt{2}}{24\left(\sqrt{2}+1\right)^2}\alpha^{*2}}$$

which is bounded above by 2.74 for $w_{\text{rect}} \in [\rho, 5.2002]$.

A.1.4 Case 4

By assumption we have $\alpha > w_{\text{rect}} - \frac{1}{2}\sqrt{w_{\text{rect}}^2 - 1}$, $\alpha > \frac{\left(2\sqrt{2}-2\right)\gamma+1}{\sqrt{2}-1}$, and $\alpha \leq w_{\text{rect}} - 1/2$ and the approximation ratio is given by

$$\frac{\frac{2}{3}\alpha w_{\text{rect}} + \frac{\sqrt{2}-1}{3}\alpha - \frac{1}{3}\alpha^2 - \frac{1}{12}w_{\text{rect}}^2 - \frac{\sqrt{2}-1}{12}w_{\text{rect}}}{\left(\gamma^3/3 + \sqrt{2}/6 - 1/12\right) - (\gamma/2)\,\alpha + (1/4)\,\alpha^2}\,.$$

We notice that the numerator is increasing in w_{rect} in this domain, and therefore we assume that w_{rect} is as large as possible so that $\alpha^* = w_{\text{rect}} - \frac{1}{2}\sqrt{w_{\text{rect}}^2 - 1}$. The approximation ratio is therefore

$$\frac{\frac{2}{3}\alpha^* w_{\text{rect}} + \frac{\sqrt{2}-1}{3}\alpha^* - \frac{1}{3}\alpha^{*2} - \frac{1}{12}w_{\text{rect}}^2 - \frac{\sqrt{2}-1}{12}w_{\text{rect}}}{\left(\gamma^3/3 + \sqrt{2}/6 - 1/12\right) - (\gamma/2)\,\alpha^* + (1/4)\,\alpha^{*2}}$$

which is bounded above by 2.74 for $w_{\text{rect}} \geq \rho$.

A.1.5 Case 5

By assumption we have $\alpha > w_{\text{rect}} - 1/2$ and the approximation ratio is given by

$$\frac{\frac{2\sqrt{2}-2}{3}\alpha w_{\text{rect}} + \frac{1}{3}\alpha + \frac{7-4\sqrt{2}}{12}w_{\text{rect}}^2 + \frac{2-\sqrt{2}}{12} - \frac{\sqrt{2}-1}{3}\alpha^2 - \frac{7-3\sqrt{2}}{12}w_{\text{rect}}}{\left(\gamma^3/3 + \sqrt{2}/6 - 1/12\right) - (\gamma/2)\,\alpha + (1/4)\,\alpha^2}\,.$$

We notice that the numerator is increasing in w_{rect}, and therefore we assume that w_{rect} is as large as possible so that $\alpha^* = w_{\text{rect}} - 1/2$. The approximation ratio is therefore

$$\frac{\frac{2\sqrt{2}-2}{3}\alpha^* w_{\text{rect}} + \frac{1}{3}\alpha^* + \frac{7-4\sqrt{2}}{12}w_{\text{rect}}^2 + \frac{2-\sqrt{2}}{12} - \frac{\sqrt{2}-1}{3}\alpha^{*2} - \frac{7-3\sqrt{2}}{12}w_{\text{rect}}}{\left(\gamma^3/3 + \sqrt{2}/6 - 1/12\right) - (\gamma/2)\,\alpha^* + (1/4)\,\alpha^{*2}}$$

which is bounded above by 1.4 for $w_{\text{rect}} \geq \rho$.

A.2 The case $k > w/\rho h$

If $k > w/\rho h$, then our algorithm will divide $\square C$ into k rectangles with aspect ratio at most ρ. Thus we assume that we have k rectangles with height 1 and width $w_{\text{rect}} \in [1, \rho]$. We will use lower bound (3.3). In total, there are three cases that we have to consider:

6. $A \leq wh - \frac{h}{2}\sqrt{w^2 - h^2}$.
7. $wh - \frac{h}{2}\sqrt{w^2 - h^2} < A \leq wh - h^2/2$.
8. $A > wh - h^2/2$.

A.2.1 Case 6

By assumption we have $\alpha \leq w_{\text{rect}} - \frac{1}{2}\sqrt{w_{\text{rect}}^2 - 1}$ and the approximation ratio is given by

$$\frac{\frac{\sqrt{2}-1}{3}\alpha - \frac{\sqrt{2}-1}{12}w_{\text{rect}} - \frac{\sqrt{w_{\text{rect}}^2-1}}{3}(w_{\text{rect}} - \alpha) + \frac{1}{3}w_{\text{rect}}^2 - \frac{1}{12}}{\frac{2}{3\sqrt{\pi}}\alpha^{3/2}}.$$

It is not hard to verify that the above ratio is decreasing in α, and therefore we assume that α is as small as possible, i.e. that $\alpha = w_{\text{rect}}/2$. The approximation ratio is therefore

$$\frac{\frac{\sqrt{2}-1}{6}w_{\text{rect}} - \frac{\sqrt{2}-1}{12}w_{\text{rect}} - \frac{\sqrt{w_{\text{rect}}^2-1}}{6}w_{\text{rect}} + \frac{1}{3}w_{\text{rect}}^2 - \frac{1}{12}}{\frac{2}{3\sqrt{\pi}}\left(w_{\text{rect}}/2\right)^{3/2}}$$

which is bounded above by 2.74 for $w_{\text{rect}} \in [1, \rho]$.

A.2.2 Case 7

By assumption we have $w_{\text{rect}} - \frac{1}{2}\sqrt{w_{\text{rect}}^2 - 1} < \alpha \leq w_{\text{rect}} - 1/2$ and the approximation ratio is given by

$$\frac{\frac{2}{3}\alpha w_{\text{rect}} + \frac{\sqrt{2}-1}{3}\alpha - \frac{1}{3}\alpha^2 - \frac{1}{12}w_{\text{rect}}^2 - \frac{\sqrt{2}-1}{12}w_{\text{rect}}}{\frac{2}{3\sqrt{\pi}}\alpha^{3/2}}.$$

We notice that the numerator is increasing in w_{rect} in this domain and therefore we assume that $\alpha^* = w_{\text{rect}} - \frac{1}{2}\sqrt{w_{\text{rect}}^2 - 1}$. The approximation ratio is therefore

$$\frac{\frac{2}{3}\alpha^* w_{\text{rect}} + \frac{\sqrt{2}-1}{3}\alpha^* - \frac{1}{3}\alpha^{*2} - \frac{1}{12}w_{\text{rect}}^2 - \frac{\sqrt{2}-1}{12}w_{\text{rect}}}{\frac{2}{3\sqrt{\pi}}\alpha^{*3/2}}$$

which is bounded above by 2.71 for $w_{\text{rect}} \in [1, \rho]$.

A.2.3 Case 8

By assumption we have $\alpha > w_{\text{rect}} - 1/2$ and the approximation ratio is given by

$$\frac{\frac{2\sqrt{2}-2}{3}\alpha w_{\text{rect}} + \frac{1}{3}\alpha + \frac{7-4\sqrt{2}}{12}w_{\text{rect}}^2 + \frac{2-\sqrt{2}}{12} - \frac{\sqrt{2}-1}{3}\alpha^2 - \frac{7-3\sqrt{2}}{12}w_{\text{rect}}}{\frac{2}{3\sqrt{\pi}}\alpha^{3/2}}.$$

We notice that the numerator is increasing in w_{rect}, and therefore we assume that w_{rect} is as large as possible so that $\alpha^* = w_{\text{rect}} - 1/2$. The approximation ratio is therefore

$$\frac{\frac{2\sqrt{2}-2}{3}\alpha^* w_{\text{rect}} + \frac{1}{3}\alpha^* + \frac{7-4\sqrt{2}}{12}w_{\text{rect}}^2 + \frac{2-\sqrt{2}}{12} - \frac{\sqrt{2}-1}{3}\alpha^{*2} - \frac{7-3\sqrt{2}}{12}w_{\text{rect}}}{\frac{2}{3\sqrt{\pi}}\alpha^{*3/2}}$$

which is bounded above by 1.8 for $w_{\text{rect}} \in [1, \rho]$.

Appendix B

Proof of Theorem 24

Proof. As in our proof of Theorem 4.20, we suppose without loss of generality that $\bar{x}$ is the origin, and define B_r about the origin as before. However, we now note that, since C is contained between a "slab" of height h, it must be the case that $\text{Area}(B_r \cap C) \leq \text{Area}(B_r \cap \square C) \leq 2hr$ (see Figure B.1). We again consider the lower bound for $\text{SN}(X)$ defined by

$$\text{SNLB}_r(X) = \begin{cases} 0 & \text{if } ||x_i|| \leq r \\ r & \text{otherwise} \end{cases}$$

and look at the related problem of minimizing $\phi\,\text{SNLB}_r(X) + \text{FW}(X, C)$, or equivalently

$$\phi r|X \setminus B_r| + \text{FW}(X, C \setminus B_r)\,.$$

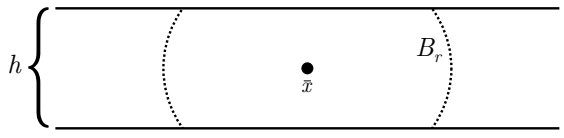

Figure B.1: The setup for our proof of Theorem 24.

We also note now that length$(\partial B_r \cap C) \leq 4h$ (again, see Figure B.1), and therefore, substituting applying Lemma 22 with $A^{'} = A(1-p)$ and $\ell^{'} = 4h$, we find that

$$\mathrm{FW}(X,C) \geq \frac{\left(\sqrt{16h^2 + 4A(1-p)\pi(k^{'}+1)} - 4h\right)^2 \left(2\sqrt{16h^2 + 4A(1-p)\pi(k^{'}+1)} + 4h\right)}{24\pi^2(k^{'}+1)^2}$$

and, using the fact that $r \geq {Ap}/{2h}$, we find that for any point set X,

$$\phi\,\mathrm{SN}(X) + \mathrm{FW}(X,C) \geq \min_{k^{'}} \left\{ \phi k^{'} \cdot \frac{Ap}{2h} + \frac{\left(\sqrt{16h^2 + 4A(1-p)\pi(k^{'}+1)} - 4h\right)^2}{24\pi^2(k^{'}+1)^2} \right.$$
$$\left. \cdot \left(2\sqrt{16h^2 + 4A(1-p)\pi(k^{'}+1)} + 4h\right) \right\}.$$

For large $k^{'}$, the optimal value of p is $p = 1/4$; plugging this value in and differentiating, we find that the optimal value of $k^{'}$ is

$$k^{'} = \max\left\{0\,,\ \frac{3^{1/3}A^{1/3}}{\pi^{1/3}} \cdot \frac{h^{2/3}}{\phi^{2/3}} - \frac{8 \cdot 3^{2/3}}{3\pi^{2/3}A^{1/3}} \cdot \frac{h^{4/3}}{\phi^{1/3}} - 1\right\}$$

which completes the proof. □

Appendix C

Proof of Theorem 26

Proof. Assume without loss of generality that $\square C$ is aligned with the coordinate axes and that $\bar{x}$ is the origin. Let $||\cdot||_{\leftrightarrow}$ denote the "horizontal norm", i.e. if $x = (x^1, x^2) \in \mathbb{R}^2$, then $||x||_{\leftrightarrow} = |x^1|$, and note that clearly $||x||_{\leftrightarrow} \leq ||x||$. Let B_r denote a "ball" of radius r about the origin $\bar{x}$ taken under the horizontal norm, so that B_r is simply the "slab" between two vertical lines at a distance of $2r$ apart from each other. Once again, we consider the lower bound for $\mathrm{SN}(X)$ defined by

$$\mathrm{SNLB}_r(X) = \begin{cases} 0 & \text{if } ||x_i||_{\leftrightarrow} \leq r \\ r & \text{otherwise} \end{cases}$$

for some radius r, and we look at the related problem of minimizing $\phi\,\mathrm{SNLB}_r(X) + \mathrm{FW}(X, C)$, or equivalently

$$\phi r|X \setminus B_r| + \mathrm{FW}(X, C \setminus B_r)\,.$$

We also note now that $\mathrm{length}(\partial B_r \cap C) \leq \mathrm{length}(\partial B_r \cap \square C) = 2h$ so that $Ap \leq 2hr$ or equivalently $r \geq {}^{Ap}/_{2h}$, where p denotes the fraction of area of C that is contained in

B_r. Following the same line of reasoning as in the proof of Lemma 22, it is easy to see that

$$\mathrm{FW}(X, C \setminus B_r) \geq \frac{A^2(1-p)^2}{4h(k^{'}+1)}$$

where $k^{'} = |X \setminus B_r|$. This is because, if we take the Fermat-Weber value of the points X under the horizontal norm (and we assume as before that B_r contains infinitely many points from X), then we again see that the Fermat-Weber value $\mathrm{FW}(X, R)$ is minimal – over all possible regions R having area $A^{'} = A(1-p)$ – when R consists of $k^{'}$ horizontal "balls" of radius ϵ (i.e. horizontal slabs of width 2ϵ) plus a neighborhood of radius ϵ about B_r (i.e. a horizontal slab of width $2(r+\epsilon)$), where ϵ is chosen such that these $k^{'}$ balls and the neighborhood have area $A^{'}$, i.e. $\epsilon = {}^{A(1-p)}/_{2h(k^{'}+1)}$. The Fermat-Weber value of such a region R, under the horizontal norm, is precisely

$$(k^{'}+1)\epsilon^2 h = \frac{A^2(1-p)^2}{4h(k^{'}+1)}$$

as desired.

We now consider the problem of choosing $k^{'}$ to minimize the sum of these lower bounds, i.e.

$$\phi\,\mathrm{SNLB}_r(X) + \mathrm{FW}(X, C) \geq \phi k^{'} \cdot \frac{Ap}{2h} + \frac{A^2(1-p)^2}{4h(k^{'}+1)}\,,$$

which completes the proof because the above expression is minimized precisely at

$$k^{'} = \max\left\{ \frac{\sqrt{A}(1-p)}{\sqrt{2p\phi}} - 1\,,\, 0 \right\}.$$

□

Appendix D

Proof of Theorem 28

In order to obtain an upper bound on the output of Algorithm 2, we consider the infinite-dimensional optimization problem of choosing the worst-case convex region C that solves the problem

$$\begin{aligned} \underset{C}{\text{maximize}}\, \mathrm{FW}(C) \qquad & s.t. \\ C &\subseteq B \\ \mathrm{Area}(C) &= A \\ C &\ni (0,0) \\ C &\text{ is convex.} \end{aligned}$$

By relaxing the convexity constraint with star convexity about the origin, the problem becomes equivalent to problem (3.1); we can use it to determine an upper bound on $\mathrm{FW}(C)$.

Following Lemma 9 we see that the worst-case star-convex region C^* takes the form shown in Figure 3.2. If $A \geq wh - \frac{h}{2}\sqrt{w^2 - h^2}$, then the optimal solution consists of two

components (rather than 4). The bound given in Theorem 28 is precisely the Fermat-Weber value $\iint_{C^*} ||x||\, dA$ obtained by analytic integration. We can prove Remark 29 by taking the Fermat-Weber values of C^* under the ℓ_1 and ℓ_∞ norms instead (which have a much simpler closed form) and observing that

$$\iint_{C^*} ||x||_1\, dA \sim \frac{2}{3}Aw - \frac{1}{12}w^2h - \frac{1}{3}\cdot\frac{A^2}{h}$$

and

$$\iint_{C^*} ||x||_\infty\, dA \sim \frac{2}{3}Aw - \frac{1}{12}w^2h - \frac{1}{3}\cdot\frac{A^2}{h}$$

from which (4.23) holds by the squeeze theorem.